SELECTIVE ANTIBODY REMOVAL FROM BLOOD, PLASMA AND BUFFER USING HOLLOW FIBER-BASED SPECIFIC ANTIBODY FILTERS

by

Mariah Sydney Hout

B.S., University of Pittsburgh, 1995

M.S., University of Pittsburgh, 1997

Submitted to the Graduate Faculty of

the School of Engineering in partial fulfillment

of the requirements for the degree of

Doctor of Philosophy

University of Pittsburgh

2003

UNIVERSITY OF PITTSBURGH

SCHOOL OF ENGINEERING

This dissertation was presented

by

Mariah Sydney Hout

It was defended on

April 21, 2003

and approved by

Alan J. Russell, Ph.D., Professor, Department of Surgery, Director, McGowan Institute for Regenerative Medicine

William R. Wagner, Ph.D., Associate Professor, Departments of Surgery, Bioengineering, and Chemical Engineering

Adriana Zeevi, Ph.D., Professor, Departments of Pathology and Surgery, Co-Director, Tissue Typing Laboratory, University of Pittsburgh Medical Center

Dissertation Director: William J. Federspiel, Ph.D., Associate Professor, Departments of Chemical Engineering, Surgery, and Bioengineering

ABSTRACT

SELECTIVE ANTIBODY REMOVAL FROM BLOOD, PLASMA AND BUFFER USING HOLLOW FIBER-BASED SPECIFIC ANTIBODY FILTERS

Mariah Sydney Hout, Ph.D.

University of Pittsburgh, 2003

Therapeutic antibody removal is performed to facilitate ABO-incompatible kidney transplants and heart and kidney xenotransplants, and to treat Goodpasture syndrome, myasthenia gravis, hemophilia with inhibitors, and thrombocytopenic purpura. Antibody removal is achieved non-selectively, via plasma exchange, or semi-selectively, via plasma perfusion through immunoadsorption columns containing immobilized protein A. We are developing hollow fiber-based specific antibody filters (SAFs) that selectively remove antibodies of a given specificity directly from whole blood, without separation of the plasma and cellular blood components and with minimal removal of plasma proteins other than the targeted antibodies. The working unit of the SAF is a hollow fiber dialysis membrane with antigens, specific for targeted antibodies, immobilized on the inner fiber wall. Several thousand SAF fibers are connected in parallel to produce a filter similar in construction to a hollow fiber hemodialyzer. A principal goal of our research is to identify the primary mechanisms that control antibody transport within the SAF, and to use this information to guide the choice of design and operational parameters that maximize the SAF-based antibody removal rate. We approached this goal by formulating a simple mathematical model of SAF-based antibody removal and performing *in vitro* antibody removal experiments to test key predictions of the model. Our model revealed three antibody

transport regimes, defined by the magnitude of the Damköhler number *Da* (antibody-binding rate/antibody diffusion rate): reaction-limited ($Da \leq 0.1$), intermediate ($0.1 < Da < 10$), and diffusion-limited ($Da \geq 10$). For a given SAF geometry, blood flow rate, and antibody diffusivity, the highest antibody removal rate was predicted for diffusion-limited antibody transport. We performed *in vitro* antibody removal experiments in which SAFs containing immobilized bovine albumin (BSA) were used to remove anti-BSA antibodies from buffer. The measured anti-BSA removal rates were consistent with antibody transport in the intermediate regime. We concluded that initial SAF development work should focus on achieving diffusion-limited antibody transport by maximizing the SAF antibody-binding capacity. If diffusion-limited antibody transport is achieved, the antibody removal rate can be raised further by increasing the number and length of the SAF fibers and by increasing the blood flow rate through the SAF.

ACKNOWLEDGEMENTS

Before describing my research I would like to thank some of the many people who have helped and befriended me during my time in graduate school. First, I give my sincere thanks to my advisor Bill Federspiel, who trained me and mentored me for the past 7 years. Thank you for the wonderful research opportunities I was given in your lab. I am very proud of the work I did with you, both in terms of the work's scientific merit and in terms of its humanitarian merit. Thank you for teaching me the value of attention to detail as well as the value of seeing the big picture. Thank you for teaching me to use experiments and mathematics to simplify and understand complex scientific phenomena. Thank you for keeping the lab well-funded, and for teaching me to write grant applications so that I will be able to fund my own research. Thank you for giving me the opportunity to present my research at international conferences, and for teaching me to communicate with other researchers through publishing manuscripts. Finally, thank you for sending me to beautiful places like Bend, Oregon and Los Angeles and San Diego, California, all in the name of science!

I would also like to thank Alan Russell, William Wagner, and Adriana Zeevi, who served on my committee for the past 4 years. Each of you generously donated your expertise and your time to help me to perform this research and to complete my education. In my career, I will be very proud if I am able to help students and other researchers as you have helped me.

I am very grateful for the financial support I received from the National Institutes of Health (Training Grant, awarded to the University of Pittsburgh), the University of Pittsburgh

Provost's Development Fund, and Advanced Extravascular Systems. I also appreciate the technical training I received from Terry Schaack, Duke Bristow, and Keith LeJeune, the scientists at Advanced Extravascular Systems.

Thank you to everyone who graciously donated blood for my research, including those who donated to the Central Blood Bank of Pittsburgh and who don't know that they helped me.

I would like to thank Robert Kormos, Harvey Borovetz, John Pristas, and Steve Winowich for giving me the opportunity to participate in the Clinical Artificial Heart Program for 3 years. The experience I gained by assisting medical device patients and their families is invaluable. Additionally, the experience of seeing desperately ill people recover and go home to their families is one I hold close to my heart.

I would like to thank my past and present lab-mates: Laura Lund, Brian Frankowski, Tamara Tulou, Joe Golob, Mike Lann, Heide Eash, Monica Garcia, Kristie Henchir, Rob Svitek, Brendan Mack, Matt Baun, Tim Nolan, and Heather Jones. You have been a second family to me over the years and I will miss seeing you every day. You are all kind and loving as well as intelligent, talented, inventive, creative, and resourceful. You have been friends to me in good and bad times. If I always work with people like you, I will be blessed.

I would like to thank Marina Kameneva for patiently answering my questions on blood rheology and blood flow, and for being a good friend to me.

Without the help of Eileen Doheny, Carole Brown, Laurie Madeya, and Monica Green, I would not have been able to schedule my committee meetings or my dissertation defense. Thank you all for your patience and resourcefulness.

Finally, I would like to thank my family, the people who bring joy and sunshine into my life. I could not have done this without your love and support. To my fiancé Christopher: before

we met, if I had tried to think of the perfect person to spend my life with, I would never have come up with someone as wonderful as you. Thank you for being your kind, loving, generous, compassionate, funny, and talented self. Thank you for being my friend when I've been at my best and when I've been at my worst. Thank you for sharing your life with me. To my mother: thank you for always believing in me. Thank you for teaching me to work hard and to take pride in my work. Thank you for teaching me the value of kindness, compassion and generosity. Thank you for teaching me how to treat other people. To my brothers Nate and Mike and my sister Kristina: Mom always told us to stick together and we have. Thank you for being my steadfast allies. To Karen: thank you for being my best and oldest friend.

I would like to dedicate this work to the people I love most in this world: Christopher; Mom, Nate, Mike, and Kris; Karen; Kathy, Steve, Beth, and Kim; Uncle Tom, Aunt Deb, Dave, Beth, and Noah. Every day I thank God for bringing us together.

This work was supported in part by the NIH National Institute of Diabetes and Digestive and Kidney Diseases under grant R44 DK54122, awarded to Advanced Extravascular Systems.

TABLE OF CONTENTS

1.0 INTRODUCTION 1

2.0 BACKGROUND 5

2.1 Antibody Structure and Function 5

2.2 Donor-Specific Antibodies in Allograft and Xenograft Rejection 9

2.2.1 ABO-Incompatible Transplantation With Pre-Transplant Anti-A and Anti-B Removal 13

a) ABO-Incompatible Kidney Transplantation 13

b) ABO-Incompatible Liver Transplantation 16

c) ABO-Incompatible Bone Marrow Transplantation 17

2.2.2 Xenotransplantation With Pre-Transplant Anti-α-Gal Removal 18

2.2.3 Implantation of HLA-Incompatible Allografts in Pre-Sensitized Recipients With Pre-Transplant Anti-HLA Removal 20

2.3 Self-Antigen-Binding Antibodies in Autoimmune Disease 21

2.4 Therapeutic Antibody Removal 26

2.4.1 Plasma Exchange 26

2.4.2 Protein A Columns 27

2.4.3 Anti-Human Immunoglobulin Columns 28

2.4.4 Bead-Based Selective Antibody Filters 29

2.4.5 Membrane-Based Selective Antibody Filters 32

2.5 Specific Antibody Filters (SAFs) 35

3.0 ANTI-A AND ANTI-B REMOVAL FROM HUMAN BLOOD USING SPECIFIC ANTIBODY FILTERS CONTAINING IMMOBILIZED A AND B ANTIGENS 42

3.1 Methods 45
3.1.1 Acquisition of Protein-Based A and B Antigens 45
3.1.2 SAF Fabrication 45
3.1.3 Neutr-AB® Purification 46
3.1.4 Blood Acquisition 47
3.1.5 Blood Typing 48
3.1.6 Cross-matching 48
3.1.7 Measurement of Anti-A and Anti-B Antibody Titers 49
3.1.8 Antigenic Quality Measurement 50
3.1.9 In Vitro Perfusion Loop 50
3.1.10 Initial Paired Antibody Removal Experiments 51
3.1.11 Biocompatibility Testing 52
3.1.12 SAF Capacity Experiments 52
3.2 Results 53
3.2.1 Initial Paired Antibody Removal Experiments 53
3.2.2 Biocompatibility Testing 55
3.2.3 SAF Capacity Experiment 1: Capacity of a SAF Containing Immobilized A and B Antigens 56
3.2.4 Purification of A and B Antigens (Neutr-AB®) 57
3.2.5 SAF Capacity Experiment 2: Capacity of a SAF Containing Immobilized Purified A and B Antigens 58
3.3 Discussion 60
4.0 ANTIBODY TRANSPORT MODEL 63
4.1 Model Geometry 63
4.2 Transport Formulation 64
4.3 Flow of Blood or Aqueous Buffer in SAF Fibers 66

4.4 Dimensional Analysis 70
4.5 Numerical Solution for Small c_b* 74
4.6 Analytical Solutions for Large and Small Da and Small c_b* 74
4.7 Model Predictions 76
4.7.1 Dimensionless Free Antibody Concentration Profiles 76
4.7.2 Dependence of the Dimensionless Clearance on the Damköhler Number 76
4.7.3 Dependence of Dimensionless Clearance on the Graetz Number 77
4.7.4 Dependence of Clearance on the Antibody Solution Flow Rate 78
4.8 Discussion 80
5.0 IN VITRO MEASUREMENT OF THE SAF-BASED ANTIBODY REMOVAL RATE IN A MODEL ANTIBODY/ANTIGEN SYSTEM 82
5.1 Methods 83
5.1.1 SAF Fabrication 83
5.1.2 Antibody Solution Preparation 84
5.1.3 Antibody Concentration Measurement 85
5.1.4 Adsorption Isotherm Experiments 85
5.1.5 In Vitro Perfusion System 86
5.1.6 In Vitro Antibody Removal Experiments 87
5.2 Results 89
5.2.1 Anti-BSA/Immobilized BSA Adsorption Isotherm 89
5.2.2 Outlet Anti-BSA Concentration as a Function of Throughput 90
5.2.3 Dependence of Anti-BSA Clearance on c_i 91
5.2.4 Dependence of Anti-BSA Clearance on Anti-BSA Solution Flow Rate 92
5.2.5 Dependence of Anti-BSA Clearance on Antibody-Binding Capacity 92
5.3 Discussion 93
6.0 CONCLUSIONS 97

APPENDIX A 99

FlexPDE Script for Numerical Solution of the Antibody Transport Model 99

BIBLIOGRAPHY 102

LIST OF TABLES

Table 2-1 Antibodies Mediating Allograft and Xenograft Rejection 10

Table 2-2 Antibodies Mediating Autoimmune Diseases 23

Table 2-3 Bead-Based Selective Antibody/Ligate Filters 30

Table 2-4 Membrane-Based Selective Antibody/Ligate Filters 34

Table 2-5 Characteristic Magnitudes of Parameters Relevant to SAF-Based Antibody Removal41

Table 3-1 Antibody Removal During Initial Paired Antibody Removal Experiments..... 55

Table 3-2 Complement Activation During Initial Paired Antibody Removal Experiments..... 56

Table 3-3 Standard and Purified Neutr-AB® Inhibition Concentrations 58

Table 4-1 Physical Properties of Blood and Water (*123-125*)..... 66

Table 4-2 Dimensionless Variables and Groups..... 71

LIST OF FIGURES

Figure 1-1 Schematic depicting antibody removal in the lumen of a SAF fiber. The relative dimensions of the fiber lumen and the antibodies and antigens are not to scale. 4

Figure 2-1 Basic structure of an antibody molecule. Hatching indicates the variable region of each chain. The number of interchain disulphide bonds varies with antibody class and subclass; intrachain disulphide bonds are not shown. N: amino-terminal end of the polypeptide chain. C: carboxyl-terminal end of the chain. 6

Figure 2-2 Induction of polyclonal antibody synthesis by an antigen with multiple different epitopes. The role of antigen-specific T_H-cells is not shown. The relative dimensions of the epitopes, cells, antibodies, and antigens are not to scale. 8

Figure 2-3 Schematic depicting SAF-based therapeutic antibody removal. Ab: antibody..... 35

Figure 2-4 Theoretical reduction in self-antigen-binding or donor-specific antibody concentration following SAF-based antibody removal, assuming that the removal session continues until equilibrium is reached. 40

Figure 2-5 Theoretical concentration of bound antibodies relative to the SAF antibody-binding capacity following SAF-based antibody removal, assuming that the removal session continues until equilibrium is reached. 40

Figure 3-1 Perfusion loop used for *in vitro* antibody removal experiments. 51

Figure 3-2 Anti-A and anti-B removal from 100 ml of freshly drawn type O whole human blood using a SAF with approximately 99 mg of immobilized A and B antigens (SAF-AB). Non-specific anti-A and anti-B removal using a control SAF with immobilized BSA (SAF-Ctrl) is also shown. Closed symbols: SAF-AB. Open symbols: SAF-Ctrl..... 54

Figure 3-3 Anti-A and anti-B removal from 6 100 ml samples of type O banked human blood using a SAF with approximately 100 mg of immobilized A and B antigens (SAF-AB). Zero percent titer reduction is indicated by the absence of a bar. 57

Figure 3-4 Ratio of the un-purified Neutr-AB® inhibition concentration to the purified Neutr-AB® inhibition concentration, for three different plasma samples with initial anti-A and anti-B titers of 0 and 64 (type A), 64 and 32 (type O, 1), and 32 and 32 (type O, 2). 59

Figure 3-5 Anti-A and anti-B removal from 6 150 ml samples of type O banked human blood using a SAF with approximately 40 mg of immobilized un-purified A and B antigens (SAF-AB) and a SAF with approximately 40 mg of immobilized purified A and B antigens (SAF-ABp). Zero percent titer reduction is indicated by the absence of a bar. 60

Figure 4-1 Schematic depicting blood flow through the blood compartment of a SAF. The shell compartment is filled with isotonic buffer and closed. The relative dimensions of the SAF fibers and the SAF housing are not to scale. 64

Figure 4-2 Schematic depicting antibody removal in the lumen of a single SAF fiber, with model parameters described in the preceding text. The relative dimensions of the fiber lumen and the antibodies and antigens are not to scale. 65

Figure 4-3 Reynolds numbers in the fiber lumens of 2 SAFs containing the smallest (SAF 1) and largest (SAF 2) number of fibers expected for clinical SAFs..... 69

Figure 4-4 Wall shear rates in the fibers comprising 2 SAFs containing the smallest (SAF 1) and largest (SAF 2) number of fibers expected for clinical SAFs..... 69

Figure 4-5 Graetz numbers for IgG and IgM antibodies for flow through 2 SAFs containing the smallest (SAF 1) and largest (SAF 2) number of fibers expected for clinical SAFs.. 72

Figure 4-6 Damköhler numbers for SAF-based removal of IgG and IgM antibodies, over the clinically relevant range of antibody/antigen association rate constants. 73

Figure 4-7 Dimensionless antibody concentration profiles within a SAF fiber at the fiber outlet, for Damköhler numbers between 0.1 and 100 and for diffusion-limited and reaction-limited antibody transport. The Graetz number is 12.5 and the dimensionless concentration of bound antibodies is near zero..... 77

Figure 4-8 Dependence of the dimensionless clearance (*K/Q*) on the Damköhler number (*Da*), for Graetz numbers (*Gz*) equal to 12.5, 25.1, and 50.2. Dashed lines indicate the dimensionless clearance for diffusion-limited antibody transport at each Graetz number. The dimensionless concentration of bound antibodies is near zero. 78

Figure 4-9 Dependence of the dimensionless clearance (*K/Q*), relative to the dimensionless clearance at Graetz number (*Gz*) equal to 10, on Graetz number, for Damköhler numbers of 1 and 10 and for diffusion-limited antibody transport. The dimensionless concentration of bound antibodies is near zero..... 79

Figure 4-10 Dependence of clearance (*K*) on antibody solution flow rate (*Q*), for Damköhler numbers (*Da*) of 1 and 10 and for diffusion-limited antibody transport. The SAF geometry is identical to the geometry of the SAF prototypes used for the *in vitro* experiments reported in Chapter 5.0. The dimensionless concentration of bound antibodies is near zero..... 80

Figure 5-1 Perfusion system for *in vitro* antibody removal experiments. 87

Figure 5-2 Anti-BSA/BSA adsorption isotherm for Hemophan® fibers with BSA immobilized on the outer surfaces of the fibers. Closed symbols: fibers with immobilized BSA. Open symbols: un-modified Hemophan® fibers. 89

Figure 5-3 Anti-BSA outlet concentration relative to inlet concentration (c_o/c_i) during a typical anti-BSA removal experiment. Throughput is the volume of anti-BSA solution perfused through the SAF. Closed symbols: SAF with immobilized BSA. Open symbols: control SAF with immobilized HSA. Each experiment was performed at an anti-BSA solution flow rate of 47 ml/min and an anti-BSA inlet concentration of one μg/ml. 90

Figure 5-4 Dependence of anti-BSA clearance (K) on anti-BSA inlet concentration (c_i). Each experiment was performed at an anti-BSA solution flow rate of 47 ml/min. Dashed lines indicate the predicted clearances for Damköhler number (Da) equal to 1, 3, and 5, and for diffusion-limited antibody transport. 91

Figure 5-5 Dependence of anti-BSA clearance (K) on anti-BSA solution flow rate (Q). Simulated dependences of clearance on flow rate, for Damköhler number (Da) equal to 1, 3, and 5, and for diffusion-limited antibody transport, are also shown. 92

Figure 5-6 Dependence of anti-BSA clearance (K) on antigen composition. Each experiment was performed at an anti-BSA solution flow rate of 47 ml/min. Dashed lines indicate the predicted clearances for Damköhler number (Da) equal to 1, 3, and 5, and for diffusion-limited antibody transport. 93

1.0 INTRODUCTION

Antibodies are specialized glycoproteins that mediate humoral immunity by binding specifically to the antigens that induced their synthesis, either neutralizing the microorganisms bearing the antigens or initiating their destruction by phagocytosis, complement-mediated lysis, or antibody-dependent cell-mediated cytotoxicity (*1*). Though normally beneficial, antibodies may be harmful if they bind to antigens on self-cells or self-tissues (self-antigens). The healthy immune system has self-tolerance mechanisms that delete self-reactive lymphocytes or regulate their activity; when these mechanisms fail due to an autoimmune disease, self-antigen-binding antibodies may be produced. Additionally, organ transplant recipients may experience damage to the transplanted donor organ by antibodies that bind to non-self antigens on cells within the donor organ (donor-specific antibodies). Donor-specific antibodies are produced as part of the healthy immune system's response to the non-self antigens within the donor organ, and are not indicative of an immune system disorder.

Therapeutic removal of self-antigen-binding antibodies is performed to treat autoimmune diseases like Goodpasture syndrome (*2*), myasthenia gravis (*3*), hemophilia with inhibitors (*4*), and idiopathic thrombocytopenic purpura (*5*), while therapeutic removal of donor-specific antibodies is performed to facilitate ABO-incompatible kidney transplants (*6*) and heart (*7*) and kidney (*8*) xenotransplants (pig-to-baboon). Antibody removal is usually achieved non-selectively, via plasma exchange, or semi-selectively, via plasma perfusion through immunoadsorption columns containing immobilized protein A or anti-human immunoglobulin

(*9-13*). Most complications of plasma exchange are related to the replacement fluid; replacement with albumin solution may cause deficiency syndromes since beneficial antibodies and clotting factors are not replenished, while replacement with donor plasma may trigger hypersensitivity reactions or allow infectious disease transmission (*9*). Patients treated using protein A or anti-human immunoglobulin immunoadsorption columns benefit from selective IgG or IgM removal and require little to no replacement fluid (*10-13*). However, only a small fraction of the total antibody population (often only antibodies of one specificity) need be removed to effect the treatments listed above, and antibody removal platforms with even greater selectivity are desired.

We are developing hollow fiber-based specific antibody filters (SAFs) that selectively remove antibodies of a given specificity directly from whole blood, without separation of the plasma and cellular blood components and with minimal removal of plasma proteins other than the targeted antibodies (*14,15*). The working unit of the SAF is a hollow fiber dialysis membrane with antigens, specific for targeted self-antigen-binding or donor-specific antibodies, immobilized on the inner fiber wall (**Figure 1-1**). Several thousand SAF fibers are connected in parallel to produce a filter similar in construction to a hollow fiber hemodialyzer. During SAF-based antibody removal blood flows through the fiber lumens, and the targeted antibodies bind to the immobilized antigens and become trapped within the SAF. Hydrophilic cellulose-based SAF fibers are used to minimize non-specific protein adsorption within the SAF, and hence the levels of non-targeted antibodies and other plasma proteins are relatively unchanged following SAF-based antibody removal.

Several studies, including two conducted by our own group (*14,15*), have shown that SAFs and similar filters can selectively remove antibodies and other substances from blood, plasma, and buffer (*16-19*). However, SAF-based antibody removal must be reasonably fast as

well as selective if the platform is to be clinically valuable. A principal goal of our research is to identify the primary mechanisms that control antibody transport within the SAF, and to use this information to guide the choice of design and operational parameters that maximize the SAF-based antibody removal rate. We approached this goal by performing studies with the following **specific aims**:

1. Show "proof of concept" by using SAF prototypes with immobilized A and B blood group antigens to remove anti-A and anti-B antibodies from type A and O whole human blood samples.
2. Develop a mathematical antibody transport model that describes antibody diffusion, convection, and reversible binding within the SAF fibers. Use the model to predict the magnitude of the SAF-based antibody removal rate, and to identify the removal rate-controlling antibody transport mechanisms, for clinically relevant SAF geometries, blood flow rates, antibody diffusivities, and antibody-binding rates.
3. Identify an appropriate model antibody/antigen system for use during quantitative *in vitro* antibody removal experiments. Fabricate SAF prototypes with the model antigens immobilized on the lumenal surfaces of the hollow fibers.
4. Perform *in vitro* antibody removal experiments in which SAF prototypes with immobilized model antigens are used to remove model antibodies from aqueous buffer. Test key predictions of the mathematical antibody transport model, including the dependence of the antibody removal rate on the buffer flow rate and the SAF antibody-binding capacity.

5. Use the information gained from the combined mathematical and experimental studies to suggest design, development, and operational approaches that can be taken to maximize the antibody removal rates achieved by SAFs developed for clinical use.

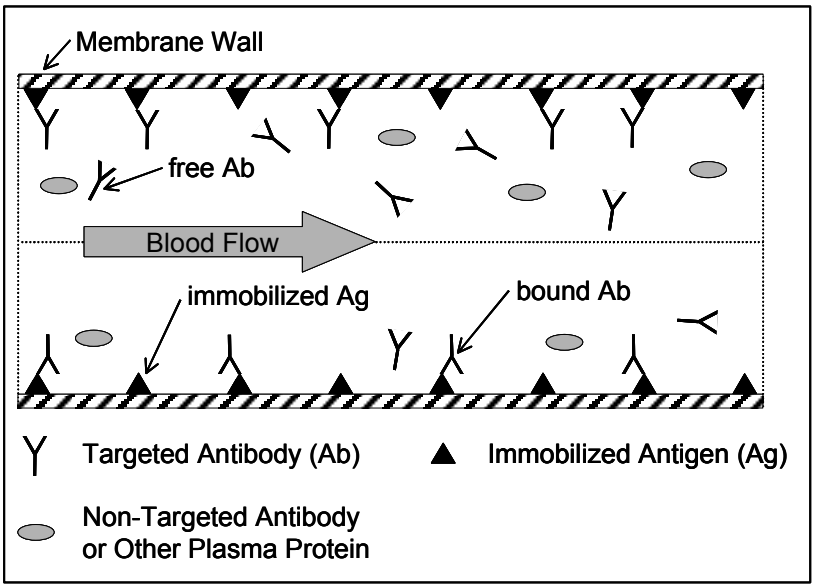

Figure 1-1 Schematic depicting antibody removal in the lumen of a SAF fiber. The relative dimensions of the fiber lumen and the antibodies and antigens are not to scale.

2.0 BACKGROUND

2.1 Antibody Structure and Function

Antibodies have distinct structural features that allow them to bind to antigens and to initiate the destruction of antigens and antigen-bearing microorganisms (*1*). Each antibody molecule consists of one or more copies of a characteristic Y-shaped unit formed by four polypeptide chains, two identical light chains and two identical heavy chains. The stem of the Y is comprised of the carboxyl-terminal parts of the two heavy chains, and each arm is comprised of the amino-terminal part of a heavy chain and an entire light chain (**Figure 2-1**). One antigen-binding site is located near the tip of each arm, and moieties that dictate the antibody's effector functions are located on the stem. Brief digestion of an antibody molecule by papain breaks the arms from the stem; the arms are referred to as Fab fragments, since they have antigen-binding activity, while the stem is referred to as an Fc fragment, since the stem fragments crystallize during cold storage.

Each light chain and heavy chain has a variable region, in which the amino acid sequence varies for antibodies of different antigen-binding specificities, and a constant region, in which the amino acid sequence is conserved for all antibodies of a given class and subclass, bearing light chains of a given subtype (**Figure 2-1**) (*1*). The variable region consists of the first 100-110 amino acids of the chain (beginning with the amino-terminal residue), and the constant region consists of the remaining 110 amino acids (light chains) or 330 or 440 amino acids (heavy chains). At the tip of each arm, an antigen-binding site is formed by three hypervariable regions

within the variable region of the light chain and three within the variable region of the heavy chain. The hypervariable regions constitute 15-20% of the variable region, and relatively invariant framework sequences constitute the rest.

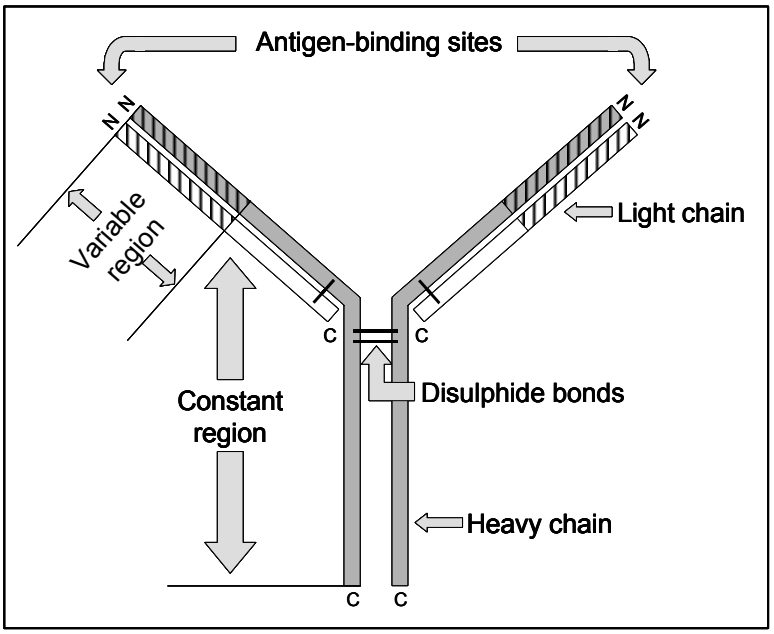

Figure 2-1 Basic structure of an antibody molecule. Hatching indicates the variable region of each chain. The number of interchain disulphide bonds varies with antibody class and subclass; intrachain disulphide bonds are not shown. N: amino-terminal end of the polypeptide chain. C: carboxyl-terminal end of the chain.

Humans have five antibody classes, and each class has its own arsenal of effector functions (*1*). The class of a given antibody molecule is determined by the amino acid sequence of its heavy chain constant region; the five classes, IgG, IgM, IgA, IgE, and IgD, have heavy chains named γ, μ, α, ε, and δ, respectively. IgG, IgE, and IgD antibodies exist as monomers of the Y-shaped unit shown in **Figure 2-1**, while IgM antibodies exist mostly as pentamers and IgA antibodies exist as monomers in blood but as dimers in external secretions. When bound to antigens, both IgG and IgM antibodies activate complement by binding to C1 molecules via C1-

binding sites on the Fc regions of the antibodies. Stable C1/antibody binding requires that each C1 molecule bind to at least two Fc regions, and hence IgM antibodies are more potent complement activators than IgG antibodies since one IgM antibody molecule provides five Fc regions in close proximity. IgG antibodies also acts as opsonins by binding to Fcγ receptors on phagocytes, and confer fetal and neonatal immunity by crossing the placenta. Dimeric IgA is the predominant antibody class in external secretions like breast milk, saliva, tears, and mucus, and in these secretions IgA antibodies crosslink large antigens like viruses and bacteria. Crosslinking prevents viruses and bacteria from attaching to mucosal cells, and the large antibody/antigen complexes formed become trapped in mucus and are eliminated. IgE antibodies mediate hypersensitivity reactions by binding to Fcε receptors on the membranes of mast cells and basophils, causing the cells to degranulate and release histamine. IgD antibodies, along with monomeric IgM antibodies, are present in membrane-bound form on mature B-cells. The effector functions of soluble IgD antibodies have not yet been identified.

Antibodies bind to distinct sites on antigens called epitopes, and hence antibodies are specific for epitopes and not for entire antigen molecules (*1*). Antibody/antigen binding depends on multiple noncovalent bonds between the amino acids that form the antigen-binding site and those that form the epitope. Since the strength of a noncovalent bond is significant only when the interacting groups are close, strong antibody/antigen binding is achieved when antigen-binding sites and epitopes have a high degree of structural complementarity. An antigen molecule may have multiple copies of a given epitope, or may have several different epitopes that induce synthesis of antibodies with different antigen-binding sites (**Figure 2-2**). A population of antibodies in which all of the antibodies bind to the same antigen, but subpopulations bind to

structurally different epitopes on the antigen, is referred to as a polyclonal antibody population, since each subpopulation is produced by a different B-cell clone.

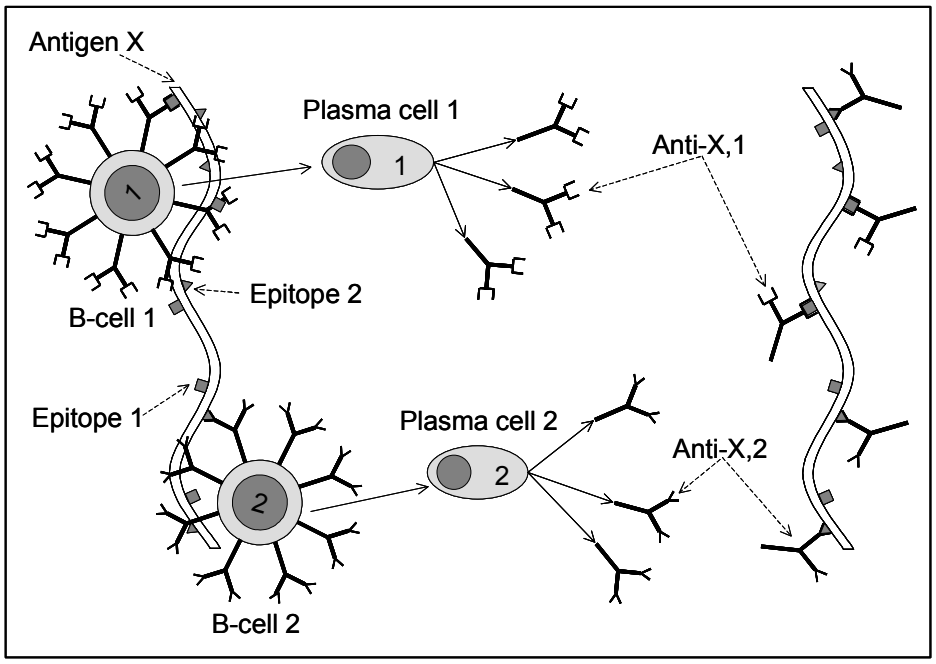

Figure 2-2 Induction of polyclonal antibody synthesis by an antigen with multiple different epitopes. The role of antigen-specific T_H-cells is not shown. The relative dimensions of the epitopes, cells, antibodies, and antigens are not to scale.

Antibodies specific for a given epitope are produced when mature B-cells, bearing membrane-bound antibodies of the same specificity, encounter the epitope-bearing antigen in the blood, lymph, or lymphoid organs (**Figure 2-2**) (*1*). Mammalian immune systems can produce B-cells of an estimated 10^8 different specificities, and hence a large number of potential antigens can be recognized; most of this diversity is accomplished during B-cell maturation, by random rearrangement of the gene segments encoding the variable regions of the light and heavy chains that comprise the membrane-bound antibodies. Binding of antigen to membrane-bound antibodies causes B-cells to proliferate and then differentiate into memory B-cells and plasma cells (antibody-producing cells). Plasma cells begin secreting antibodies about 5-7 days after

mature B-cells are stimulated with antigen, and continue secreting antibodies for 1-2 weeks before dying. Memory B-cells live much longer and may confer lifelong immunity to a given antigen or antigen-bearing microorganism.

2.2 Donor-Specific Antibodies in Allograft and Xenograft Rejection

Donor-specific antibodies mediate hyperacute rejection of ABO-incompatible allografts, discordant xenografts, and HLA-incompatible allografts implanted in pre-sensitized recipients (*20,21*). Hyperacute rejection occurs when the transplant recipient has pre-formed antibodies that bind to antigens on the graft's endothelial cells (donor-specific antibodies) (*22*). Upon initiation of blood flow through the graft, antibody/antigen complexes form rapidly and activate the complement system via the classical pathway. Endothelial cells are injured when neutrophils, attracted by C5a, infiltrate the graft and release lytic enzymes. Formation of the membrane attack complex (MAC) may cause additional endothelial cell injury, especially in xenografts whose complement regulatory proteins may be incapable of blocking MAC formation by human complement components. Platelets adhere to the injured endothelium, aggregate, and stimulate thrombin formation. Blood clots form within the graft capillaries and prevent adequate perfusion of the graft, causing necrosis of graft cells. Graft function may occur temporarily and decline rapidly, or the graft may never function. This reaction typically occurs within 24 hours of transplantation (*1,20,23*).

Anti-A and anti-B antibodies mediate hyperacute rejection of ABO-incompatible allografts; these antibodies bind to A and B blood group antigens found on the surfaces of red blood cells, lymphocytes, endothelial cells, and platelets (**Table 2-1**) (*24*). The A and B antigens are glycoproteins and glycolipids bearing immunodominant carbohydrate epitopes characterized by the terminal trisaccharides GalNAcα1-3[Fucα1-2]Galβ- (A antigen) and Galα1-3[Fucα1-

2]Galβ- (B antigen) (*25*). An individual's blood type is determined by the identities of the blood group antigens expressed on his or her tissues; thus type A individuals express A antigens, type B individuals express B antigens, type AB individuals express both A and B antigens, and type O individuals express neither A nor B antigens. Humans older then 6 months of age continually produce antibodies that bind to the blood group antigens that are not expressed on their own tissues (*26*); thus grafts from type A donors are ABO-incompatible with type B and O recipients (who produce anti-A antibodies), grafts from type B donors are ABO-incompatible with type A and O recipients (who produce anti-B antibodies), and grafts from type AB donors are ABO-incompatible with type A, B and O recipients (who produce either anti-B or anti-A antibodies, or both). Anti-A and anti-B antibody production in humans occurs in response to intestinal bacteria bearing the A and B epitopes, and does not require exposure to ABO-incompatible red blood cells or other tissues (*26*).

Table 2-1 Antibodies Mediating Allograft and Xenograft Rejection

Graft Type	Antigens	Antibodies	Rejection Type	Antibody Production Stimulant
ABO-incompatible allograft	A B	Anti-A Anti-B	Hyperacute Acute Chronic	Intestinal bacteria
Discordant xenograft	α-Gal	Anti-α-Gal	Hyperacute Acute	Intestinal bacteria
HLA-incompatible allograft	HLA	Anti-HLA	Hyperacute Acute Chronic	Non-self HLA (via blood transfusion, pregnancy, or previous transplant)

Anti-α-Gal antibodies mediate hyperacute rejection of discordant xenografts (grafts from New World monkeys or non-primate mammals implanted in humans, chimpanzees, or baboons); these antibodies bind to α-Gal antigens found on the surfaces of endothelial cells, epithelial cells, fibroblasts, smooth muscle cells, and red blood cells in New World monkeys and non-primate

mammals (**Table 2-1**) (*21*). The α-Gal antigens are glycoproteins and glycolipids bearing immunodominant carbohydrate epitopes characterized by the terminal disaccharide Galα1-3Galβ- (α-Gal). Humans, chimpanzees and baboons do not express α-Gal antigens and hence produce anti-α-Gal antibodies (*27,28*). Anti-α-Gal antibody production in humans, chimpanzees, and baboons occurs in response to intestinal bacteria bearing α-Gal epitopes, and does not require exposure to cells or tissues from New World monkeys or non-primate mammals (*29*).

Anti-HLA antibodies mediate hyperacute rejection of HLA-incompatible allografts implanted in pre-sensitized recipients; these antibodies bind to HLA antigens found on the surfaces of most nucleated cells (class I HLA antigens) or on the surfaces of macrophages, dendritic cells, B-cells, and activated endothelial cells (class II HLA antigens) (**Table 2-1**) (*20*). HLA antigens are trans-membrane glycoproteins that present peptides from processed endogenous and exogenous antigens to T_H-cells and T_C-cells (*30*). In humans, the major class I HLA antigens are named HLA-A, HLA-B, and HLA-C, and the major class II HLA antigens are named HLA-DR, HLA-DQ, and HLA-DP. The genes that code for the production of HLA antigens are highly polymorphic; over 59 different HLA-A alleles, 111 different HLA-B alleles, and 37 different HLA-C alleles have been identified (*1*). Individuals exposed to non-self HLA antigens via blood transfusion, pregnancy, or a prior transplant may produce antibodies that bind to those HLA antigens, thus becoming pre-sensitized. If such an individual receives a graft bearing the same non-self HLA antigens, the pre-formed anti-HLA antibodies may mediate hyperacute rejection of the graft.

Grafts implanted in patients without pre-formed donor-specific antibodies may stimulate production of donor-specific antibodies after the transplant (*1,23*). These grafts may undergo acute rejection, which occurs within days or weeks of transplantation, and/or chronic rejection,

which occurs within months or years of transplantation. Acute rejection is mediated by both donor-specific T-cells and donor-specific antibodies (*22,31*). During acute rejection, donor-specific T_C-cells mediate graft cell apoptosis via the perforin/granzyme pathway, and donor-specific T_H-cells produce IFN-γ, which activates macrophages that release lytic enzymes, nitric oxide, and TNF-α. Donor-specific antibodies damage the graft endothelial cells and parenchymal cells via complement activation as described above, and antibody/antigen complexes involving IgG antibodies bind natural killer cells that mediate graft cell apoptosis via the perforin/granzyme pathway (antibody-dependent cell-mediated cytotoxicity) (*32-34*). Acute rejection episodes are frequently reversible by prompt and aggressive immunosuppression. Conversely, chronic rejection is often unresponsive to immunosuppression and may necessitate re-transplantation (*22*). Chronic rejection is characterized by intimal hyperplasia of the arteries of the graft, interstitial fibrosis, atrophy of the graft parenchyma, and declining graft function, and is thought to represent a pathologic tissue remodeling response to vascular trauma experienced by the graft peri-transplant and post-transplant. The production of donor-specific antibodies post-transplant correlates strongly with the incidence of chronic rejection (*35*).

As of February 2003, the United Network for Organ Sharing (UNOS) reported that 80,451 individuals were on the waiting list for organ transplantation in the United States; 53,634 individuals were waiting for kidney transplants, 16,910 individuals were waiting for liver transplants, 3,833 individuals were waiting for heart transplants, and 3,827 individuals were waiting for lung transplants (*36*). In 2001, only 23,848 organ transplants were performed, using grafts procured from 6,081 deceased donors and 6,526 living donors; 6,190 individuals died while on the waiting list (*37*). Due to this critical shortage of donor organs, many investigators are seeking to expand the conditions under which transplantation can be performed. As described

in more detail in the following sections, pre-transplant removal of anti-A and anti-B antibodies facilitates ABO-incompatible kidney (*38*) and liver (*39*) transplants, and pre-transplant removal of anti-HLA antibodies facilitates receipt of HLA-incompatible transplants by pre-sensitized recipients (*40*). Additionally, a good deal of research is devoted to the use of swine organs for transplantation in humans, and pre-transplant removal of anti-α-Gal antibodies is employed as a key step in this procedure (*21*).

2.2.1 ABO-Incompatible Transplantation With Pre-Transplant Anti-A and Anti-B Removal

a) ABO-Incompatible Kidney Transplantation

ABO-incompatibility was recognized as a major risk factor in kidney transplantation during the early development of transplantation methodology (*24*). Starzl et al reported a series of 7 ABO-incompatible kidney transplants performed at the University of Colorado Medical Center, in which two grafts were lost due to hyperacute rejection and were explanted within several hours of transplantation (*41*). Five ABO-compatible, but not ABO-identical, kidney transplants were performed by the same group of investigators (4 type O grafts to type A recipients, 1 type A graft to a type AB recipient), and all of the grafts showed good early function (*41*). Wilbrandt et al reported a series of 12 ABO-incompatible kidney transplants performed at Cleveland Clinic, in which all of the grafts were lost within 19 months and 9 of the grafts were lost within 3 months (*42*). Six of the grafts never functioned and were explanted within 17 days. Post-explant examination revealed thrombosis of the renal artery in 9 of the grafts. Cook et al reported 25 ABO-incompatible kidney transplants performed accidentally at the University of California in Los Angeles (*43*). Twenty-four of 25 grafts were lost within one year of transplantation, and eight of those grafts were lost within 2 weeks of transplantation.

Slapak et al reported the first use of plasma exchange to reverse the rejection of an ABO-incompatible kidney graft (*44*). A graft from a type A donor was accidentally implanted in a type O recipient, and the recipient experienced four episodes of rejection at 2 days, 17 days, 36 days, and 83 days post-transplant. During 3 of the rejection episodes, plasma exchange was performed daily for six consecutive days resulting in marked clinical improvement (decreased creatinine level and increased urine production). The graft was functioning at 20 months post-transplant. Slapak et al then deliberately implanted a type A kidney in a type O recipient, following two plasma exchange sessions to reduce the recipient's anti-A antibody titer (*45*). The recipient had experienced no rejection episodes at 4 months post-transplant.

Based on the experiences of Slapak and his colleagues, several groups of investigators performed ABO-incompatible kidney transplants following pre-transplant removal of anti-A and anti-B antibodies from the recipients' blood. Between 1982 and 1986, Alexandre et al performed 17 ABO-incompatible living-related donor kidney transplants at University Hospital Saint Luc in Belgium (*46*). Each recipient underwent pre-transplant plasma exchange and splenectomy, and 15 grafts were functioning at 7 to 58 months post-transplant. Bannet et al performed 6 ABO-incompatible living-related donor kidney transplants at the Albert Einstein Medical Center, using plasma perfusion through Biosynsorb A and B columns to remove anti-A and anti-B antibodies pre-transplant (*47*). (Biosynsorb A and B columns contain synthetic A and B antigens immobilized within silica beads, and are no longer commercially available (*24*).) Five grafts were functioning at 2 to 32 months post-transplant, although the anti-A and anti-B titers of each recipient returned to pre-transplant levels within two weeks of transplantation. Mendez et al used the same columns for pre-transplant anti-A and anti-B removal in a series of 6 ABO-incompatible living-related donor kidney transplants performed at St. Vincent Medical Center

(*48*). In each case, the recipient underwent 3 to 5 antibody removal sessions during which whole blood was perfused through a Biosynsorb column for 3 to 4 hours. Transplantation was performed when the anti-A and anti-B titers were lower than 4. Five of the six grafts were functioning at 1 year post-transplant.

Between 1989 and 1999, Toma et al performed 105 ABO-incompatible living donor kidney transplants at Tokyo Women's Medical University in Japan (*49*). Before transplantation, the recipients' anti-A and anti-B titers were reduced to 16 or lower via double filtration plasmapheresis and plasma perfusion through Biosynsorb A and B columns. At 1, 5, and 10 years, the patient survival rates were 92%, 92%, and 89%, respectively, and the graft survival rates were 77%, 71%, and 51%, respectively. The investigators compared the ABO-incompatible patient and graft survival rates to the survival rates obtained in 620 ABO-compatible living donor kidney transplants performed at the same center during the same time period. At 1, 5, and 10 years, the ABO-incompatible graft survival rates were significantly lower than the ABO-compatible graft survival rates. (At 1, 5, and 10 years, the ABO-compatible graft survival rates were 95%, 80%, and 62%, respectively.) However, the investigators found no significant difference between the ABO-incompatible and ABO-compatible patient survival rates. The percentage of recipients who experienced acute rejection episodes was significantly higher in the ABO-incompatible group than in the ABO-compatible group, and the graft survival rates for ABO-incompatible recipients who experienced acute rejection episodes were significantly lower than the graft survival rates for ABO-incompatible recipients who did not experience acute rejection. In most of the ABO-incompatible recipients, the post-transplant anti-A and anti-B titers either remained low during the first few months post-transplant (75% of the recipients) or rose temporarily and fell spontaneously within several months post-transplant (12% of the

recipients) (*50*). However, in 9% of the recipients the titers rose rapidly post-transplant and the grafts were lost within 2 months. In the remaining 4% of the recipients, the titers rose slowly post-transplant and the grafts were lost within 1 year. Additionally, the graft survival rates for ABO-incompatible recipients with maximum pre-antibody removal anti-A and anti-B IgG titers greater than 128 were significantly lower than the graft survival rates of recipients with maximum pre-removal titers less than 16 or between 32 and 64 (*51*). The minimum pre-transplant anti-A and anti-B IgG titers, and the maximum and minimum pre-transplant anti-A and anti-B IgM titers, did not correlate with graft survival rate.

b) ABO-Incompatible Liver Transplantation

ABO-incompatible liver transplants are sometimes performed when the recipient is in imminent danger of dying and an ABO-compatible graft is not available. Chui et al reported 7 ABO-incompatible liver transplants performed at Royal Prince Alfred Hospital in Australia between 1986 and 1996 (*52*). All of the recipients presented with fulminant hepatic failure and had class 4 UNOS status (i.e. had life expectancies of seven days without transplantation). No attempt was made to reduce the recipients' anti-A and anti-B titers pre-transplant. Two grafts were lost within 1 month and one was lost within 11 months, while 3 grafts were functioning well at 52 months. (One recipient died with a functioning graft.) Bjoro et al reported 10 ABO-incompatible liver transplants performed in the Nordic countries (Denmark, Finland, Norway, and Sweden) between 1990 and 2001, again performed without pre-transplant reduction of the recipients' anti-A and anti-B titers (*53*). The graft survival rate at 1 year was 30%, compared to a 1-year graft survival rate of 75% for 143 ABO-identical grafts transplanted at the same centers. Recently, Hanto et al reported much better results in a series of 14 ABO-incompatible liver transplants performed between 1992 and 2001 at the University of Cincinnati Medical Center

(*39*). Each recipient underwent pre-transplant plasma exchange to reduce anti-A and anti-B titers, post-transplant plasma exchange to maintain low anti-A and anti-B titers for 2 weeks post-transplant, and splenectomy. The 1 and 5-year graft survival rates were 71.4% and 61.2%, respectively, and none of the grafts were lost due to rejection (graft loss was only due to recipient death unrelated to graft rejection). At 2 weeks post-transplant, 7 recipients had anti-A or anti-B IgG titers greater then 16 but did not experience antibody-mediated rejection. The investigators speculated that these recipients were exhibiting accommodation, a phenomenon in which a graft is not rejected and continues to function despite the presence of anti-graft antibodies and complement (*54*).

c) ABO-Incompatible Bone Marrow Transplantation

In contrast to ABO-incompatible solid organ transplantation, ABO-incompatible bone marrow transplantation is performed regularly (*55*). In bone marrow transplantation, ABO-incompatibility is characterized as minor, major, or bidirectional. Minor ABO-incompatible bone marrow transplants involve the transplant of marrow from type O donors into type A, B, or AB recipients; in this situation, donor-derived antibodies and B-cells may bind to A and B antigens on recipient cells. Major ABO-incompatible bone marrow transplants involve the transplant of marrow from type A, B, or AB donors into type O recipients; in this situation, recipient-derived antibodies may bind to A and B antigens on donor cells. Finally, bidirectional ABO-incompatible bone marrow transplants involve the transplant of marrow from type A donors into type B recipients or from type B donors into type A recipients; in this situation, both of the above-described activities may take place. To facilitate minor ABO-incompatible bone marrow transplants, donor plasma is removed from the bone marrow pre-transplant via centrifugation. To facilitate major ABO-incompatible bone marrow transplants, recipients either undergo pre-

transplant plasma exchange or the donor marrow is depleted of red blood cells pre-transplant. Both of the above-described procedures are performed to facilitate bidirectional bone marrow transplants.

Stussi et al reported a series of 361 ABO-identical, 98 minor ABO-incompatible, 96 major ABO-incompatible, and 17 bidirectional ABO-incompatible bone marrow transplants performed at University Hospital of Zurich and University Hospital of Basel in Switzerland between 1980 and 1998 (*55*). The investigators found no significant differences in the incidence of moderate to severe graft-versus-host disease among the four groups. Additionally, there was no effect of ABO-incompatibility on the relapse rate or on the time to platelet and neutrophil engraftment. However, bidirectional ABO-incompatible recipients had significantly higher mortalities than the other 3 groups of recipients.

2.2.2 Xenotransplantation With Pre-Transplant Anti-α-Gal Removal

Current efforts in xenotransplantation are focused on the transplantation of swine organs into humans (*21*). Non-primates with suitably sized organs, such as pigs, are available in large numbers and do not engender the risk of lethal virus transmission associated with transplantation of non-human primate organs into humans. As discussed in section 2.2, anti-α-Gal antibodies mediate hyperacute rejection of grafts from non-primate mammals implanted in humans, chimpanzees, or baboons. (Baboons are frequently used in animal models of pig-to-human xenotransplantation.) Several groups have used plasma exchange or blood or plasma perfusion through α-Gal-containing immunoadsorption columns to remove anti-α-Gal antibodies from baboon blood or plasma. Kozlowski et al performed *in vivo* removal of baboon anti-α-Gal antibodies by perfusing whole blood or plasma through columns containing synthetic α-Gal

antigens immobilized within silica beads (*56*). Post-immunoadsorption anti-α-Gal IgM and IgG antibody levels were less than 20% of pre-immunoadsorption levels using either whole blood or plasma perfusion, but whole blood perfusion was associated with significant hemolysis and the need for post-immunoadsorption red blood cell transfusions. Taniguchi et al performed *in vivo* removal of baboon anti-α-Gal antibodies by perfusing plasma through columns containing synthetic α-Gal antigens immobilized within macroporous glass beads (*57*). Anti-pig IgM and IgG antibody levels were reduced significantly via immunoadsorption, but rebounded within 1 week of the final immunoadsorption session despite pharmacologic immunosuppression and splenectomy. Prior to pig-to-baboon kidney transplants, Kobayashi et al used double filtration plasmapheresis (DFPP) to reduce the baboons' anti-pig IgM and IgG antibody levels to below 15% of pre-DFPP levels (*58*). Hyperacute rejection of the pig kidneys was prevented, but the grafts were lost within 1 week due to severe humoral rejection. Immunohistochemical examination of the explanted grafts revealed IgM and IgG antibodies bound to the graft endothelial cells. Cooper et al perfused baboon blood through donor-specific pig kidneys to remove baboon anti-α-Gal antibodies prior to pig-to-baboon heart transplants (*7*). None of the transplanted hearts functioned for longer than 5 days.

Unfortunately, acute loss of the graft due to antibody-mediated rejection is a common outcome in pig-to-primate transplants, despite prevention of hyperacute rejection via pre-transplant anti-α-Gal removal or complement inhibition (*59*). Currently, several groups have focused on the production of transgenic pigs that do not express α-Gal antigens. Lai et al produced miniature pigs with 1 allele of the α-1,3galactosyltransferase locus knocked out (*60*), and Phelps et al produced pigs with both alleles knocked out (*61*). (The enzyme α-1,3galactosyltransferase adds the terminal Galα1-3 residues to oligosaccharide precursors to

form the α-Gal antigens (*62*).) If consistent production of healthy pigs completely lacking α-Gal antigens is achieved, organs from these pigs may be used for pig-to-primate transplantation and pre-transplant removal of anti-α-Gal may be unnecessary.

2.2.3 Implantation of HLA-Incompatible Allografts in Pre-Sensitized Recipients With Pre-Transplant Anti-HLA Removal

Pre-sensitized organ transplantation candidates may wait years for a suitable donor organ to become available. (A suitable organ would be one from a donor who does not express the HLA antigens to which the recipient's anti-HLA antibodies bind.) Pre-transplant anti-HLA removal has been used to de-sensitize these candidates and expedite transplantation. Palmer et al decreased the anti-HLA titers and panel-reactive antibody (PRA) scores in 7 kidney transplant recipients by performing plasma perfusion through immunoadsorption columns containing immobilized protein A (*63*). Each patient had a positive cross-match with his or her donor prior to immunoadsorption, and a negative cross-match post-immunoadsorption. One graft never functioned and another was lost at 1 year post-transplant, but the remaining 5 grafts were functioning at 3 to 23 months post-transplant. Ross et al performed plasma perfusion through protein A-containing immunoadsorption columns to reduce the PRA scores of 5 kidney transplant candidates whose scores had been greater than 80% for 1.75 to 5 years (*64*). One patient lost the graft at 8 weeks post-transplant, but the other 4 patients had functioning grafts at 3 to 34 months post-transplant. Most recently, surgeons at Johns Hopkins Hospital in Baltimore instituted a protocol in which plasma exchange is used to de-sensitize kidney transplant candidates who have positive cross-matches to living donors (*40*). Eighteen kidney transplant recipients underwent this procedure between 1998 and 2001, and on average 3 plasma exchange treatments were required to attain a negative cross-match between each recipient and his or her

donor. One graft was lost due to donor non-compliance, but the other 17 grafts were functioning at 1 to 44 months post-transplant.

2.3 Self-Antigen-Binding Antibodies in Autoimmune Disease

Autoimmune diseases involve antibody-mediated or cell-mediated immune responses directed against self-antigens (*1*). Autoimmune diseases are classified as organ-specific (directed against a self-antigen isolated within a single organ) or systemic (directed against one or several self-antigens distributed within multiple organs and tissues). Examples of organ-specific autoimmune diseases include myasthenia gravis, Goodpasture syndrome, and idiopathic thrombocytopenic purpura (ITP), while examples of systemic autoimmune diseases include rheumatoid arthritis (RA) and systemic lupus erythematosus (SLE) (**Table 2-2**). The American Association of Blood Banks (AABB) and the American Society for Apheresis (ASFA) have classified autoimmune diseases based on the effectiveness of therapeutic apheresis (plasma exchange or immunoadsorption) in treating the diseases (*65*). For category I diseases, such as myasthenia gravis and Goodpasture syndrome, therapeutic apheresis is standard and acceptable as a primary therapy. For category II diseases, such as hemophilia with inhibitors, ITP, and RA, therapeutic apheresis is generally accepted but is considered to be supportive to other primary treatments. For category III diseases, such as SLE and hemolytic disease of the newborn, existing evidence is insufficient to establish the efficacy of therapeutic apheresis.

Myasthenia gravis (*66*) and Goodpasture syndrome (*67*) are customarily treated using plasma exchange in addition to immunosuppression and other pharmacological treatments. Anti-acetylcholine receptor antibodies mediate myasthenia gravis; these antibodies bind to acetylcholine receptors (AchR) on the motor end plates of muscles (**Table 2-2**) (*1*). Anti-AchR/AchR binding inhibits muscle activation and induces complement-mediated destruction of

acetylcholine receptors, and myasthenia gravis patients experience varying degrees of skeletal muscle weakness involving the facial, limb, and respiratory muscles (*68*). Plasma exchange is most often used in patients experiencing myasthenic crisis, characterized by acute weakness of the respiratory muscles and often requiring mechanical ventilation (*68*). In a retrospective study of 27 myasthenic crisis patients treated with plasma exchange, over 70% of the patients were extubated within 2 weeks (*69*). Benny et al used plasma perfusion through protein-A containing immunoadsorption columns to treat 12 myasthenia gravis patients, and 9 patients demonstrated improvement in symptom scores following treatment (*3*). During each immunoadsorption procedure approximately 8.4 L of plasma was treated, and each patient underwent 2 or 3 procedures. The mean percent reduction in anti-AchR titer achieved via immunoadsorption was 68%.

Anti-glomerular basement membrane antibodies mediate Goodpasture syndrome; these antibodies bind to type IV collagen within the basement membranes (GBM) of the kidney glomeruli and the lung alveoli (**Table 2-2**) (*2,70*). Anti-GBM/GBM binding causes glomerulonephritis and lung hemorrhage. Patients with Goodpasture syndrome typically undergo daily plasma exchange treatments for several weeks using 5% albumin as the replacement fluid (*67*). Levy et al reported the long-term outcome for 71 Goodpasture syndrome patients treated using plasma exchange and immunosuppression (*71*). In patients with pre-treatment creatinine concentrations less than 500 μmol/L, the patient and renal function survival rates were 100% and 95%, respectively, at 1 year post-treatment, and 94% and 94%, respectively, at 5 years post-treatment. In patients with pre-treatment creatinine concentrations greater than 500 μmol/L, the patient and renal function survival rates were 83% and 82%, respectively, at 1 year post-treatment, and 80% and 50%, respectively, at 5 years post-treatment.

Table 2-2 Antibodies Mediating Autoimmune Diseases

Disease	Antigens/Tissues Affected	Antibodies	Antibody Removal Indicated?	AABB and ASFA Category
Myasthenia gravis	Acetylcholine receptors (AchR)	Anti-AchR	Yes	I
Goodpasture syndrome	Glomerular basement membranes (GBM)	Anti-GBM	Yes	I
Hemophilia with inhibitors	Factor VIII Facto IX	Anti-Factor VIII Anti-Factor IX	Yes	II
Idiopathic thrombocytopenic purpura	Platelets	Anti-platelet	Yes	II
Rheumatoid arthritis	IgG antibodies	Anti-IgG (rheumatoid factors)	Yes	II
Systemic lupus erythematosus	DNA Histone Red blood cells (RBC) Platelets	Anti-DNA Anti-histone Anti-RBC Anti-platelet	Possibly	III
Hemolytic disease of the newborn	A antigens B antigens	IgG anti-A IgG anti-B	Possibly	III

Hemophilia with inhibitors (*72*), ITP (*73*), and RA (*73*) are treated using plasma perfusion through protein A-containing immunoadsorption columns in addition to immunosuppression and other pharmacological treatments. The Immunosorba® protein A-containing immunoadsorption column (Fresenius HemoCare, Inc.) is FDA-approved for the treatment of hemophilia with inhibitors, and the Prosorba® protein A-containing column (Fresenius HemoCare, Inc.) is FDA-approved for the treatment of ITP and RA. Anti-Factor VIII and anti-Factor IX antibodies mediate hemophilia with inhibitors; these antibodies bind to infused Factor VIII and Factor IX in hemophilia patients and render coagulation factor replacement therapy ineffective (**Table 2-2**) (*72*). The Malmö Treatment Model for the induction of tolerance in hemophilia (with inhibitors) patients was developed in the early 1980s, and involves plasma perfusion through protein A-containing immunoadsorption columns and administration of cyclophosphamide and intravenous immunoglobulin (*74*). Freiburghaus et al reported that 16 of 23 hemophilia patients treated with this protocol achieved tolerance (defined as the elimination of anti-Factor VIII and anti-Factor IX antibodies and the normalization of the half-lives of infused Factor VIII and Factor IX) (*74*). Jansen et al used plasma perfusion through immunoadsorption columns containing immobilized anti-human immunoglobulin to treat 10 hemophilia (with inhibitors) patients (*75*). The anti-Factor VIII antibody titer was reduced by 50-97% following each immunoadsorption session. Seven patients achieved remission, defined by sustained absence of anti-Factor VIII antibodies.

Anti-platelet antibodies mediate idiopathic thrombocytopenic purpura (ITP); anti-platelet/platelet binding causes phagocytosis of platelets by macrophages bearing Fcγ receptors (**Table 2-2**). Snyder et al used plasma perfusion through Prosorba® columns to treat 72 ITP patients with pre-immunoadsorption platelet counts less than 50,000/μl (*5*). In 18 patients

platelet counts increased to greater than 100,000/μl, and in 15 patients platelet counts increased to between 50,000/μl and 100,000/μl. Christie at al used the same columns to treat 10 ITP patients, and platelet counts in 6 patients increased to twice the pre-immunoadsorption counts (*76*).

Anti-IgG antibodies of IgM isotype (rheumatoid factors) mediate rheumatoid arthritis (RA) (**Table 2-2**) (*1*). Anti-IgG/IgG complexes are deposited in the joints of RA patients, causing chronic inflammation and synovial hypertrophy. Felson et al performed a randomized, controlled, double-blind trial to evaluate the efficacy of plasma perfusion through Prosorba® columns in the treatment of refractory RA (*77*). Thirty-two percent of the Prosorba®-treated patients experienced improvement as defined by the American College of Rheumatology (ACR) response criteria, compared to only 11.4% of the control patients.

An array of self-antigen-binding antibodies of different specificities mediate systemic lupus erythematosus (SLE), and SLE patients experience diverse symptoms ranging from non-specific symptoms such as fatigue and fever to organ-specific symptoms such as arthritis, skin rash, glomerulonephritis, and pleurisy (**Table 2-2**) (*1,73*). Unfortunately, most controlled trials evaluating the efficacy of therapeutic apheresis in the treatment of SLE have shown no clinical benefit (*73*). Wei at al performed a randomized, controlled, double-blind trial to evaluate the efficacy of plasma exchange in the treatment of mild SLE (*78*). Twenty patients underwent either 6 4-L plasma exchanges or 6 control procedures over a 2-week period. Although IgG, IgM, and IgA antibody levels were reduced by the plasma exchanges, patients in the control and plasma exchange groups experienced the same degree of clinical improvement. Lewis et al performed a randomized, controlled trial comparing the efficacy of standard therapy (prednisone and cyclophosphamide) to that of standard therapy plus plasma exchange in the treatment of severe

SLE (*79*). Plasma exchange did not reduce the incidence of renal failure or death. To date, randomized, controlled trials evaluating the efficacy of immunoadsorption in SLE treatment have not been reported, but several anecdotal studies have shown promising results. Braun et al used plasma perfusion through protein A-containing Immunosorba® columns to treat 8 SLE patients who were resistant to standard therapy (*80*). Seven patients achieved remission quantified by a decrease in the SLE activity measure (SLAM), and 2 patients who had dialysis-dependent renal insufficiency pre-immunoadsorption recovered renal function post-immunoadsorption. Using the same columns, Palmer et al treated 10 patients with rapidly progressive glomerulonephritis and acute renal failure, and 9 patients regained renal function post-immunoadsorption (*81*).

2.4 Therapeutic Antibody Removal

In the United States, therapeutic antibody removal is usually achieved non-selectively, via plasma exchange, or semi-selectively, via plasma perfusion through immunoadsorption columns containing immobilized protein A (*65*). Immunoadsorption columns containing immobilized anti-human immunoglobulin are also commercially available and are used outside the United States (*82*). In addition, several groups of investigators have developed bead-based and membrane-based antibody filters that use immobilized antigens to achieve selective antibody removal. Each of these antibody removal methods will be discussed in more detail in the following sections.

2.4.1 Plasma Exchange

Plasma exchange involves withdrawal of venous blood from a patient, separation of the plasma from the cellular blood components via centrifugation or membrane filtration, and return of the cellular blood components to the patient along with albumin solution or donor plasma as

replacement fluid (*9*). Three to 4.5 L of plasma (approximately 1 to 1.5 times the total volume of plasma in an average human) is removed and exchanged with replacement fluid during a typical plasma exchange session, and sessions are generally performed 2-4 times per week. The preferred replacement fluid is 5% albumin, but donor plasma is used for patients at risk of bleeding or requiring daily plasma exchanges for several weeks. Continuous flow centrifuges operate at inlet blood flow rates of 60-110 ml/min and outlet plasma flow rates of 35-60 ml/min, and hence 3 L of plasma can be removed within 90 min (*83*). Centrifuges separate blood components according to their specific gravities, and the concentration of pathogenic antibodies in the removed plasma is approximately equal to the concentration in the plasma before plasma/cell separation. Membrane-based plasma separators operate at inlet blood flow rates of 50-200 ml/min and outlet plasma flow rates of 15-50 ml/min, and hence 3 L of plasma can be removed within 100 min (*84*). Membrane-based plasma filters separate blood components based on the ability of each component to permeate the membranes, and some proteins (especially high molecular weight proteins like IgM antibodies) may be present at lower concentrations in the removed plasma than in the plasma before plasma/cell separation (*84*).

2.4.2 Protein A Columns

Two protein A-containing immunoadsorption columns, the Prosorba® column and the Immunosorba® column, are commercially available through Fresenius HemoCare (Redmond, WA) (*85*). As discussed in section **2.3**, the columns are FDA-approved for the treatment of rheumatoid arthritis and idiopathic thrombocytopenic purpura (Prosorba®) and hemophilia with inhibitors (Immunosorba®). The Prosorba® column contains 200 mg of purified protein A immobilized within 123 g of silica beads, and one Prosorba® column can bind about 0.6 g of IgG antibodies at saturation (*12*). One treatment consists of perfusing up to 2 L of plasma

through the column at a flow rate of 10-20 ml/min. A single treatment using a Prosorba® column causes a small reduction in the concentration of IgG antibodies in the patient's blood, and the efficacy of Prosorba®-based treatment is thought to be based on the removal of immune complexes and on subtle immunomodulatory effects rather than on the removal of IgG antibodies (*10*). The recommended course of treatment for RA is one Prosorba® perfusion per week for 12 weeks, and the recommended course of treatment for ITP is 2-3 Prosorba® perfusions per week for 2-3 weeks (*86*).

The Immunosorba® column contains purified protein A immobilized within Sepharose® beads following cyanogen bromide activation of the beads, and one Immunosorba® column can bind about 1.2 g of IgG antibodies at saturation (*12*). Two Immunosorba® columns are used intermittently during each treatment; while plasma is perfused through one column, adsorbed antibodies are eluted from the other to prepare it for re-use when the first column becomes saturated. One treatment consists of perfusing up to 10 L of plasma through the columns at a flow rate of 10-20 ml/min (*85*). A single treatment using Immunosorba® columns causes a substantial reduction in the concentration of IgG antibodies in the patient's blood, due to the "unlimited" capacity of the columns and the large volume of plasma treated (*10*). A set of 2 Immunosorba® columns can be re-used up to 20 times by the same patient (*10*).

2.4.3 Anti-Human Immunoglobulin Columns

Ig-Therasorb®, an immunoadsorption column containing immobilized anti-human immunoglobulin, is commercially available through PlasmaSelect (Teterow, Germany) (*82*). The anti-human immunoglobulin is obtained by immunizing sheep with human antibodies, and Ig-Therasorb® columns bind human IgG (all subclasses), IgM, and IgA antibodies. Each column contains anti-human immunoglobulin immobilized within 150 ml of Sepharose® beads, and one

Ig-Therasorb® column can bind approximately 4 g of IgG antibodies at saturation (*12*). Like the Immunosorba® system, the Ig-Therasorb® system employs 2 columns that are used intermittently during each treatment. One treatment consists of perfusing up to 8 L of plasma through the columns at a flow rate of 20-25 ml/min (*75*).

2.4.4 Bead-Based Selective Antibody Filters

Several groups of investigators have developed bead-based antibody filters that use immobilized antigens to achieve selective antibody removal (**Table 2-3**). As discussed in section **2.2.1**, Biosynsorb columns (no longer available), containing synthetic A and B antigens immobilized within silica beads, were developed for the removal of anti-A and anti-B antibodies from plasma and were used to facilitate ABO-incompatible kidney transplants (*48,49,87*). Each column contained 75 g of silica beads with 0.7 μmol of synthetic A or B antigens immobilized within each gram of beads (*88*). A thin coating of porous polystyrene was applied to the beads to allow whole blood perfusion of the columns (*88*). For the same application, Rieben at al developed columns called BioSorbent A and BioSorbent B, containing synthetic A and B antigens immobilized within macroporous glass beads (*89*). As a preliminary step toward the development of columns for selective anti-HLA removal, DeVito et al immobilized human HLA-A2 antigens within Sepharose® beads and showed that incubation of the beads with plasma significantly reduced anti-HLA-A2 titers in plasma samples from 3 individuals (*90*). Human HLA-A2 antigens were isolated from human spleen cells and purified using immobilized monoclonal anti-HLA-A2 antibodies, but the authors surmised that obtaining large quantities of HLA antigen variants in the future may be simpler due to advances in recombinant DNA technology.

Table 2-3 Bead-Based Selective Antibody/Ligate Filters

Immobilized Antigen/Ligand	Removed Antibody/Ligate	Matrix	Blood/Plasma Compatible	References
A B	Anti-A Anti-B	Silica beads	Blood Plasma	(*48,49,87*)
A	Anti-A	Macroporous glass beads	Plasma	(*89*)
HLA	Anti-HLA	Sepharose®	Plasma	(*90*)
α-Gal	Anti-α-Gal	Sepharose®	Plasma	(*91*)
α-Gal	Anti-α-Gal	Macroporous glass beads	Plasma	(*57*)
α-Gal	Anti-α-Gal	Silica beads	Blood Plasma	(*8*)
AchR	Anti-AchR	Not reported	Plasma	(*92*)
Heparinase	Heparin	Agarose	Blood	(*93*)
Anti-β_2-microglobulin	β_2-microglobulin	Agarose	Blood	(*94*)

Several groups have focused on developing bead-based filters for selective anti-α-Gal removal. Gerber at al immobilized synthetic α-Gal disaccharide and/or trisaccharide antigens within Sepharose® beads via polyacrylamide spacers, and found that beads containing a mixture of immobilized disaccharides and trisaccharides achieved the best removal of anti-α-Gal from human plasma (*91*). Taniguchi et al immobilized synthetic α-Gal disaccharide antigens within macroporous glass beads via polyacrylamide spacers, and used columns containing these beads to remove anti-pig antibodies from baboon plasma *in vivo* (*57*). Xu et al immobilized 2 different synthetic α-Gal trisaccharides within silica beads, and found that beads containing trisaccharide type 2 (Galα1-3Galβ1-4GlcNAc) removed more anti-α-Gal from human plasma than beads containing trisaccharide type 6 (Galα1-3Galβ1-4Glc) (*8*).

Takamori et al synthesized part of the α-subunit of the human acetylcholine receptor (AchR) and immobilized the synthetic peptide within beads (matrix material not reported) for the selective removal of anti-AchR antibodies from human plasma (*92*). Treatment of myasthenia gravis patients using plasma perfusion through AchR peptide-containing columns reduced the patients' anti-AchR antibody titers and caused clinical improvement in the patients.

Ameer et al developed a novel device for blood purification that allows both plasma/cell separation and bead-based plasma treatment to occur within a single device (*93-95*). The vortex-flow plasmapheretic reactor (VFPR) consists of a solid rotating inner cylinder inside a hollow stationary outer cylinder, and blood flows through the annular compartment between the two cylinders. A microporous membrane divides the annular compartment into an inner cell compartment and an outer plasma compartment. Blood enters the VFPR and plasma flows across the membrane into the plasma compartment, which contains either heparinase or anti-β_2-microglobulin immobilized within agarose beads. After flowing through the plasma

compartment, the treated plasma is recombined with the cellular blood components and returned to the patient. The rotating inner cylinder creates Taylor vortices that fluidize the beads. The heparinase-containing VFPR is intended for heparin neutralization, and the anti-β_2-microglobulin-containing VFPR is intended for selective removal of β_2-microglobulin.

2.4.5 Membrane-Based Selective Antibody Filters

Several groups of investigators have developed membrane-based antibody filters that use immobilized antigens to achieve selective antibody removal (**Table 2-4**). Our own group immobilized A and B antigens on the inner fiber walls of cellulose hollow fiber dialysis membranes to produce filters for anti-A and anti-B removal (*14*). Filters with 0.9 m^2 of blood contacting surface area significantly reduced the anti-A and anti-B titers of up to 900 ml of type O whole human blood. Karoor et al immobilized synthetic α-Gal trisaccharide antigens on the inner fiber walls of cellulose hollow fiber dialysis membranes, and within the pores of polysulfone and nylon hollow fiber microfiltration membranes, to produce filters for anti-α-Gal removal (*96*). Nylon microfiltration membranes containing α-Gal antigens immobilized via spacer molecules had an anti-α-Gal IgM-binding capacity of 89 mg of IgM per ml of membrane or about 2.1 μg of IgM per cm^2 of internal surface area. Singh et al immobilized insulin on the inner fiber walls of cellulose hollow fiber dialysis membranes to produce filters for anti-insulin removal, and removed up to 98% of anti-insulin antibodies from 200 ml samples of human plasma (the surface area of the filters was not reported) (*16*). Larue at al immobilized human IgG and human serum albumin (HSA) on the inner fiber walls of cellulose hollow fiber dialysis membranes to produce filters for anti-IgG and anti-HSA removal (*17*). To demonstrate the selectivity of antibody removal by the filters, the filters were used to remove anti-IgG and anti-

HSA antibodies from a dog immunized with human IgG and HSA. The IgG-containing filter, used first, caused the anti-IgG titer to fall from 128 to 2 but caused no reduction in the anti-HSA titer. The HSA-containing filter, used second, caused the anti-HSA titer to fall from 256 to 2.

To produce filters for IgG removal, Klein et al immobilized protein A within the pores of polysulfone hollow fiber membranes after coating the membranes with hydroxyethylcellulose (HEC) (*97*). At saturation, the membranes bound 16 mg of IgG per ml of membrane or about 1.3 μg of IgG per cm^2 of internal surface area. Similarly, Charcosset et al immobilized protein A within the pores of polysulfone/HEC hollow fiber membranes (*98*). The membranes bound 8.8 mg of IgG per ml of membrane or about 0.5 μg of IgG per cm^2 of internal surface area.

Two groups have developed heparin filters comprised of hollow fiber dialysis membranes with heparin-binding ligands immobilized on the inner fiber walls: Yang et al used immobilized protamine to remove heparin from canine blood during *ex vivo* studies (*18*), and Ma et al used immobilized poly(L-lysine) to remove heparin from phosphate-buffered saline and bovine blood (*19*). The heparin-binding capacity of the poly(L-lysine)-containing dialysis membranes was 0.54 $\mu g/cm^2$.

Soltys et al immobilized anti-low-density lipoprotein (LDL) antibodies within the pores of microporous polyvinylidene diflouride flat sheet membranes to produce filters for LDL removal (*99*). The LDL-binding capacity of the membranes was 2.0 mg of LDL per ml of membrane or about 0.18 μg of LDL per cm^2 of internal surface area.

Table 2-4 Membrane-Based Selective Antibody/Ligate Filters

Immobilized Antigen/Ligand	Removed Antibody/Ligate	Membrane Material/Type	Blood/Plasma Compatible	References
A B	Anti-A Anti-B	Cellulose/Dialysis	Blood	(*14,15*)
α-Gal	Anti-α-Gal	Cellulose/Dialysis Polysulfone/ Microfiltration Nylon/ Microfiltration	Blood	(*96*)
Insulin	Anti-insulin	Cellulose/Dialysis	Blood	(*16*)
Human albumin (HSA)	Anti-HSA	Cellulose/Dialysis	Blood	(*17*)
Protein A	IgG	Polysulfone/ Microfiltration	Not reported	(*97*)
Protein A	IgG	Polysulfone/ Microfiltration	Not reported	(*98*)
Protamine	Heparin	Cellulose/Dialysis	Blood	(*18*)
Poly(L-lysine)	Heparin	Poly(ethylene-vinyl alcohol)	Blood	(*19*)
Anti-low-density lipoprotein (LDL)	LDL	Polyvinylidene diflouride	Plasma	(*99*)

2.5 Specific Antibody Filters (SAFs)

The specific antibody filters (SAFs) under development in our laboratory are comprised of hollow fiber dialysis membranes with antigens, specific for targeted antibodies, immobilized on the inner fiber walls (*14,15*). Each SAF contains several thousand fibers connected in parallel, and is similar in construction to a hollow fiber hemodialyzer. For extracorporeal therapeutic antibody removal, the SAF will be incorporated within a simple perfusion loop similar to the loops used for hemodialysis (**Figure 2-3)**. Blood will be withdrawn from the patient, perfused through the SAF, and returned to the patient. As blood flows through the fiber lumens, the targeted antibodies will bind to the immobilized antigens and become trapped within the SAF. Separation of the plasma from the cellular blood components will not be required. The parameters relevant to SAF-based antibody removal, and their characteristic magnitudes, are listed in **Table 2-5**.

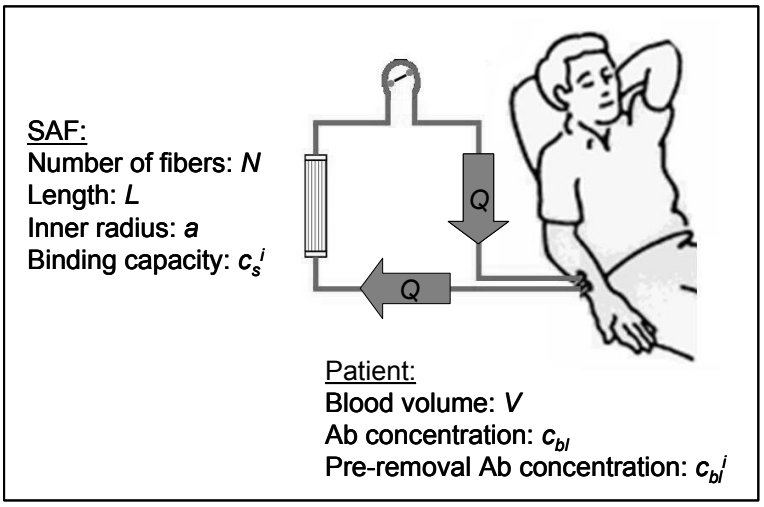

Figure 2-3 Schematic depicting SAF-based therapeutic antibody removal. Ab: antibody.

The clinical usefulness of SAF-based antibody removal will be assessed based on the post-removal concentration of self-antigen-binding or donor-specific antibodies in the patient's blood (compared to the pre-removal concentration) and the length of time required to accomplish the concentration reduction, assuming that the SAF is appropriately biocompatible and non-toxic. As discussed in Chapter 1.0, the primary focus of the research reported in this dissertation is to identify the primary mechanisms that control antibody transport within the SAF, and to use this information to guide the choice of design and operational parameters that maximize the SAF-based antibody removal rate (and hence minimize the length of time required for SAF-based antibody removal). In Chapters 4.0 and 5.0, we will describe the analytical and experimental studies we performed to approach these goals. To date we have not performed extensive studies aimed at maximizing the SAF antibody-binding capacity (and hence minimizing the post-removal blood antibody concentration), although we have performed a "proof of concept" study (reported in Chapter 3.0) showing that a SAF containing immobilized A and B blood group antigens can remove a significant fraction of the anti-A and anti-B antibodies from about 1 L of whole human blood.

However, based on the expected magnitudes of the SAF antibody-binding capacity, the pre-removal concentration of pathogenic antibodies in the patient's blood, and the antibody/antigen equilibrium dissociation constant, we can estimate the post-removal blood antibody concentration for a SAF with a reasonable blood-contacting surface area. Since antibody/antigen binding is reversible, during a SAF-based antibody removal session the concentration of pathogenic antibodies in the patient's blood will fall, and the concentration of antibodies bound to the SAF fibers will rise, until the rate of antibody/antigen association is equal to the rate of antibody/antigen dissociation (i.e. until equilibrium is reached). The

Langmuir adsorption isotherm equation relates the bound antibody concentration at equilibrium to the blood antibody concentration at equilibrium (*107*):

$$c_b^{eq} = \frac{c_{bl}^{eq} c_s^i}{c_{bl}^{eq} + K_d} \quad \textbf{(2-1)}$$

where c_b^{eq} (μg/cm^2) is the bound antibody concentration at equilibrium, c_{bl}^{eq} (μg/ml) is the blood antibody concentration at equilibrium, c_s^i (μg/cm^2) is the antibody-binding capacity of the SAF (defined as the mass of antibodies bound to the SAF fibers at saturation per unit of blood contacting surface area), and K_d (μg/ml) is the antibody/antigen equilibrium dissociation constant. The concentration of bound antibodies at equilibrium can be expressed in terms of the pre-removal blood antibody concentration (c_{bl}^i) and the equilibrium blood antibody concentration:

$$c_b^{eq} = (c_{bl}^i - c_{bl}^{eq}) \frac{V}{SA} \quad \textbf{(2-2)}$$

where V (ml) is the patient's total blood volume and SA (cm^2) is the blood-contacting surface area of the SAF. Substituting equation **(2-2)** into equation **(2-1)**, we can solve for c_{bl}^{eq}/c_{bl}^i as a function of c_{bl}^i:

$$\left(\frac{c_{bl}^{eq}}{c_{bl}^i}\right)^2 + \left(\frac{c_{bl}^{eq}}{c_{bl}^i}\right)\left(\frac{c_s^i A}{c_{bl}^i V} + \frac{K_d}{c_{bl}^i} - 1\right) - \frac{K_d}{c_{bl}^i} = 0 \quad \textbf{(2-3)}$$

We can use equation **(2-3)** to estimate the ratio of the post-removal to the pre-removal blood antibody concentration, for a given pre-removal blood antibody concentration, SAF antibody-binding capacity, SAF surface area, and antibody/antigen equilibrium dissociation constant. To use equations **(2-1)** and **(2-3)** we must assume that the populations of antibodies and immobilized antigens are homogeneous, so that K_d is the same for every antibody/antigen pair. Clinically, the antibody population will be polyclonal and hence heterogeneous, and the

population of immobilized antigens will be heterogeneous if the immobilization technique allows multiple orientations of the immobilized antigens. We must also assume that the time required for a substantial increase in the blood antibody concentration due to antibody synthesis and antibody transport from the extravascular to the intravascular compartment is small compared to the time required to conduct the antibody removal session. This assumption has been validated by comparison of the measured percent removals of IgG, IgM, and IgA antibodies during plasma exchange to the percent removals predicted when antibody synthesis and extravascular to intravascular antibody transport are neglected (*108*).

We used equation **(2-3)** to estimate the ratio of the post-removal to the pre-removal blood antibody concentration, as a function of the pre-removal concentration, for a patient treated using a SAF with a surface area of 5 m^2 and an antibody-binding capacity of 1 $\mu g/cm^2$ (**Figure 2-4**). An equilibrium dissociation constant of 1.5 μg/ml was used based on the reported dissociation constants for antibody/antigen systems with either the antibodies or the antigens immobilized (**Table 2-5**) (*1,106,107*). We chose 1 $\mu g/cm^2$ as an order of magnitude estimate of the antibody-binding capacity of the SAF, since the approximate surface concentration of a monolayer of IgG molecules is 0.6 $\mu g/cm^2$ (*101,102*), and since several investigators have developed affinity membranes with antibody-binding capacities between 0.5 and 2 $\mu g/cm^2$ (**2.4.5**) (*96-98*). Clinically, the pre-removal blood antibody concentration will most likely lie between 0.5 and 70 μg/ml, based on the reported concentrations of anti-α-Gal antibodies in human and baboon blood (*56,96*) and anti-malaria antibodies in human blood (*104*) (**Table 2-5**).

For patients with pre-removal blood antibody concentrations less than 10 μg/ml, the estimated post-removal blood antibody concentration will be less than 30% of the pre-removal concentration, assuming that the antibody removal session continues until equilibrium is reached

(**Figure 2-4**). However, for patients with pre-removal concentrations greater than 10 μg/ml, the estimated post-removal concentration will be between 30% and 90% of the pre-removal concentration. To treat these patients, we may need to use 2 SAFs intermittently during each antibody-removal session, perfusing the patient's blood through one SAF while bound antibodies are eluted from the other to prepare it for re-use when the first SAF becomes saturated. This technique is currently used in the Immunosorba® and Ig-Therasorb® antibody removal systems (*12*), but may be more difficult to use in the SAF system since the SAF will need to be emptied of whole blood (instead of plasma) before the antibodies are eluted.

We also used equation **(2-3)** to estimate the ratio of the bound antibody concentration at equilibrium to the antibody-binding capacity of the SAF, as a function of the pre-removal blood antibody concentration (again for a patient treated using a SAF with a surface area of 5 m^2 and an antibody-binding capacity of 1 μg/cm^2, and for an antibody/antigen equilibrium dissociation constant of 1.5 μg/ml) (**Figure 2-5**). For patients with pre-removal blood antibody concentrations less than 1.5 μg/ml (i.e. less than K_d), the concentration of bound antibodies at equilibrium is small compared to the antibody-binding capacity of the SAF. For patients with pre-removal blood antibody concentrations greater than K_d, the concentration of bound antibodies at equilibrium approaches the antibody-binding capacity of the SAF. Therefore, the SAF antibody-binding capacity required to reduce the blood antibody concentration by a given percentage is not linearly proportional to the pre-removal blood antibody concentration. For example, using a 5 m^2 SAF, the capacity required to reduce the blood antibody concentration to 30% of the pre-removal concentration is 0.4 μg/cm^2 if the pre-removal concentration is 1 μg/ml, and is 1 μg/cm^2 if the pre-removal concentration is 10 μg/ml.

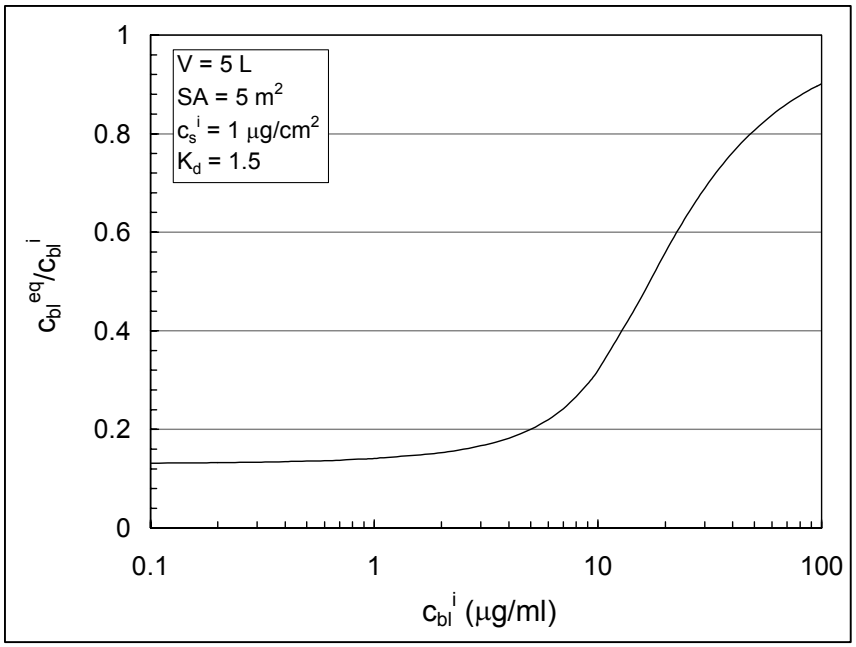

Figure 2-4 Theoretical reduction in self-antigen-binding or donor-specific antibody concentration following SAF-based antibody removal, assuming that the removal session continues until equilibrium is reached.

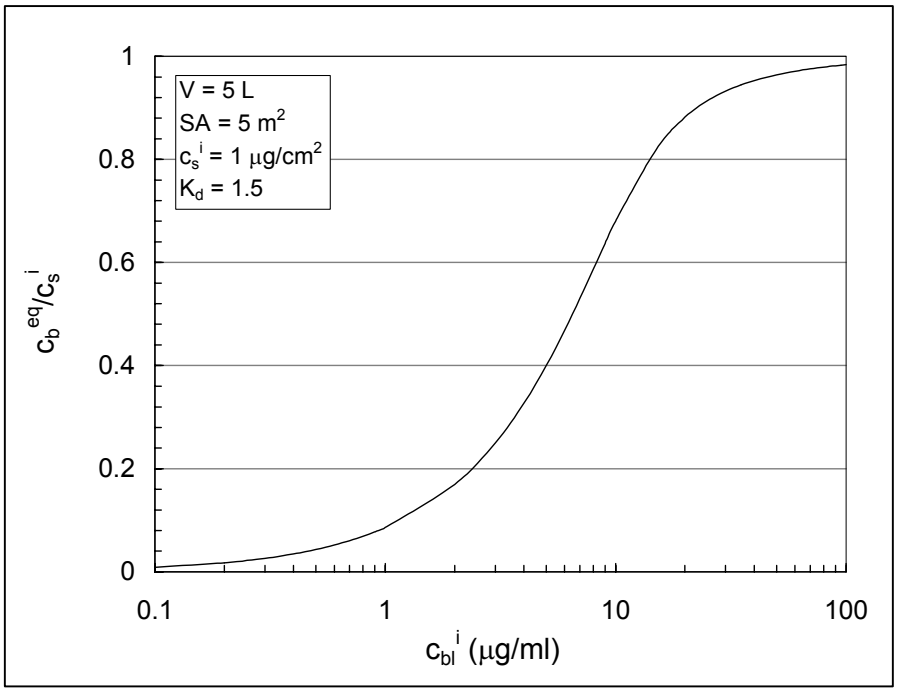

Figure 2-5 Theoretical concentration of bound antibodies relative to the SAF antibody-binding capacity following SAF-based antibody removal, assuming that the removal session continues until equilibrium is reached.

Table 2-5 Characteristic Magnitudes of Parameters Relevant to SAF-Based Antibody Removal

SAF Geometry and Binding Capacity		References
Number of fibers N	6000-32,000	(*100*)
Fiber length L (cm)	25	(*100*)
Fiber inner radius a (cm)	0.01	(*100*)
Blood-contacting surface area SA (m^2)	1-5	(*100*)
Antibody-binding capacity c_s^i (nmol/m^2 or μg/cm^2)	IgG: 40 nmol/m^2 (.6 μg/cm^2) IgM: 12 nmol/m^2 (1.1 μg/cm^2)	(*101,102*)
Patient Parameters and Blood Flow Rate		
Total blood volume V (L)	3.5-5.5	(*103*)
Concentration of donor-specific or self-antigen-binding antibodies in blood c_{bl}^i (μg/ml)	IgG: 0.5-40 IgM: 5-70	(*59,96,104*)
Blood flow rate Q (ml/min)	50-500	(*100*)
Antibody and Antibody/Antigen Parameters		
Antibody diffusivity D (cm^2/s)	IgG, water, 22 ºC: $3.9*10^{-7}$ IgM, water, 22 ºC: $1.4*10^{-7}$	(*105*)
Association rate constant k_f (L/mol*s or ml/μg*s)	10^4-10^6 L/mol*s (10^{-5}-10^{-2} ml/μg*s)	(*106,107*)
Equilibrium dissociation constant K_d (mol/L or μg/ml)	10^{-9}-10^{-7} mol/L (0.15-90 μg/ml)	(*106,107*)

3.0 ANTI-A AND ANTI-B REMOVAL FROM HUMAN BLOOD USING SPECIFIC ANTIBODY FILTERS CONTAINING IMMOBILIZED A AND B ANTIGENS

End stage renal disease (ESRD), characterized by complete and irreversible kidney failure, causes retention of metabolic wastes, water, and salts, and eventually causes death unless renal function is replaced using hemodialysis or kidney transplantation (*109*). Compared to long-term hemodialysis, kidney transplantation provides an enhanced quality of life, enhanced longevity (*110*), and lower healthcare costs, and hence ESRD patients with high probabilities of post-transplant survival (as determined by standardized pre-transplant evaluations (*111*)) are designated as candidates for living donor or cadaveric donor kidney transplantation (*111,112*). Living donor kidney transplantation is preferred to cadaveric donor transplantation because living donor grafts exhibit higher survival rates than do cadaveric donor grafts, even when the living donors are not genetically related to the transplant recipients (*113*). Thus a kidney transplant candidate with a suitable related or unrelated living donor receives the living donor kidney, provided that the donor is ABO-compatible with the candidate and the candidate does not have pre-formed antibodies that bind to the donor's HLA antigens (*111*). As discussed in Chapter 2.0, ABO-incompatible kidney transplantation is rarely performed since pre-formed anti-A and anti-B antibodies in the recipient's blood may mediate hyperacute rejection of an ABO-incompatible donor kidney (*24,38*). A kidney transplant candidate with an otherwise suitable, but ABO-incompatible, living donor does not receive the living donor kidney, but instead is listed with the United Network for Organ Sharing (UNOS), along with over 50,000 other kidney transplant candidates (*36*), and waits an average of 5 years for an ABO-compatible

cadaveric donor kidney to become available (*114*). While waiting the transplant candidate spends an average of 9-12 hours per week undergoing maintenance hemodialysis (*109*). The survival rates for ESRD patients on hemodialysis are 78% at 1 year, 63% at 2 years, and 33% at 5 years (*115*).

Based on the frequencies of ABO blood groups in the United States, an estimated 36% of potential living donor-kidney transplant candidate pairs are ABO-incompatible (*116,117*). Thus the number of kidney transplant candidates who receive living donor kidneys might be raised significantly by the development of techniques to facilitate ABO-incompatible kidney transplantation. Several groups of investigators have performed ABO-incompatible kidney transplants following pre-transplant removal of anti-A and anti-B antibodies from the recipients' blood (*46-49*). The largest series of such transplants was performed in Japan: between 1989 and 1999, Toma *et al* performed 105 ABO-incompatible living donor kidney transplants at Tokyo Women's Medical University (*49*). Before transplantation, the recipients' anti-A and anti-B titers were reduced to 16 or lower via double filtration plasmapheresis and plasma perfusion through Biosynsorb A and B columns. At 1 and 5 years post-transplant, the graft survival rates were 77% and 71%, respectively. At 3 years post-transplant, the graft survival rates for ABO-compatible living donor and cadaveric donor kidney transplants performed in the United States are 81-85% and 70%, respectively (*113*). Since the 3 to 5 year graft survival rates are similar for ABO-incompatible living donor transplants (performed according to the Toma protocol) and ABO-compatible cadaveric donor transplants, and since the survival rates for ESRD patients on hemodialysis are discouraging, a kidney transplant candidate who has an ABO-incompatible living donor may prefer to receive the ABO-incompatible living donor kidney (with treatment

according to the Toma protocol) rather than wait for an ABO-compatible cadaveric donor kidney to become available.

The methods that are currently available for extracorporeal anti-A and anti-B removal include plasma exchange and plasma perfusion through immunoadsorption columns containing immobilized protein A or anti-human immunoglobulin (*9-13*). The Biosynsorb A and B columns used by Toma et al (*49*), which contain synthetic A and B antigens and selectively remove anti-A and anti-B antibodies from plasma, are no longer commercially available (*24*). The goal of this study was to assess the feasibility of selectively removing anti-A and anti-B antibodies directly from whole human blood using specific antibody filters (SAFs) containing immobilized protein-based A and B antigens. We fabricated SAFs by immobilizing A and B antigens on the lumenal surfaces of the hollow fibers comprising commercially available hemodialyzers. Initially, we performed a series of paired antibody removal experiments to compare the anti-A and anti-B removal accomplished by SAFs containing immobilized A and B antigens to the non-specific removal accomplished by control SAFs (unmodified hemodialyzers or SAFs containing immobilized bovine serum albumin). We performed preliminary biocompatibility testing by comparing the SC5b-9 generation induced by the SAFs containing immobilized A and B antigens to the SC5b-9 generation induced by the control SAFs. We then assessed the antibody-binding capacity of a SAF containing immobilized A and B antigens by sequentially circulating 100 ml blood samples through the SAF until the titers of a newly introduced blood sample were not reduced. Finally, we purified the A and B antigens by removing a low molecular weight component that did not bind anti-A and anti-B antibodies, and assessed the antibody-binding capacity of a SAF containing immobilized purified A and B antigens.

3.1 Methods

3.1.1 Acquisition of Protein-Based A and B Antigens

The commercially available product Neutr-AB® (Dade Behring, Switzerland) was used as the source of protein-based A and B antigens. Neutr-AB® contains A antigen-bearing proteins obtained from pig intestinal mucosa, and B antigen-bearing proteins obtained from horse intestinal mucosa (*118*).

3.1.2 SAF Fabrication

Gambro (Lakewood, CO) 400 HG hemodialyzers were used as SAF modules. Each module contained approximately 7742 Hemophan® fibers of 0.02 cm nominal inner diameter and 18.5 cm length, providing a blood-contacting surface area of 0.9 m^2 (*100*). Neutr-AB® or bovine serum albumin (BSA) (Sigma Chemical Co., St. Louis, MO) was immobilized on the lumenal surfaces of the fibers using a modified version of the cyanogen bromide activation method developed by Axen *et al* (*119*). Unless otherwise noted, chemicals were obtained from Sigma Chemical Company (St. Louis, MO). During the following fiber activation steps, the blood and shell compartments of the SAF module were connected in series using tygon tubing. Both compartments of the module were first rinsed copiously with de-ionized water. To swell the fibers, 3.5 L of 0.2 N NaOH was circulated through the module for five hours, on ice, at 136 ml/min. The module was flushed with 3.5 L of 0.1 M sodium bicarbonate buffer, pH 8.5 (henceforth called bicarbonate buffer), at 225 ml/min and at 4 ˚C. An activating solution of 16 g CNBr in 200 ml of 0.2 N NaOH was circulated through both compartments at 136 ml/min, on ice, for 1.5 hours. The activating solution pH was kept above 11.0 by the addition of cold 10 N NaOH. The module was flushed with 3.5 L of de-ionized water and 3.5 L of bicarbonate buffer,

at 225 ml/min and at 4 ˚C. Excess fluid was removed from the module using filtered compressed air.

The shell compartment was then filled with bicarbonate buffer and closed. One hundred ml of a 7-mg/ml antigen solution (Neutr-AB® or BSA dissolved in bicarbonate buffer) was circulated through the blood compartment at 77 ml/min, at room temperature, overnight (at least 12 hours). Both compartments were drained, and samples were collected from the blood and shell compartments for measurement of antigen concentration. The blood and shell compartments were again connected in series and the SAF was washed three times, by circulating 500 ml of bicarbonate buffer through the SAF at 136 ml/min for one hour (each wash). Excess fluid was removed from the SAF using filtered compressed air, and the SAF was stored at 4 ˚C until use.

The mass of antigen immobilized within the SAF was calculated by subtracting the mass of antigen recovered by the washings, the mass of antigen in the antigen solution after the immobilization step, and the mass of antigen in the shell compartment after the immobilization step, from the mass of antigen initially in the antigen solution. The mass of antigen in each solution was calculated using the solution volume and the protein concentration, determined by measuring the absorbance at 280 nm with a UV/VIS spectrophotometer (Perkin Elmer, Norwalk, CT).

3.1.3 Neutr-AB® Purification

Aqueous gel filtration chromatography revealed that Neutr-AB® contained two significant protein fractions with molecular weights of approximately 35,000 and 6000 Da. One hundred and ten ml of Neutr-AB® was placed within a section of Spectra/Por® dialysis tubing with a 12,000-14,000 Da molecular weight cutoff (Thomas Scientific, Swedesboro, NJ) and

dialyzed extensively against 0.1 M sodium bicarbonate buffer, pH 8.5. The concentration of the recovered high molecular weight (purified) Neutr-AB® was 2.4 mg/ml. A 0.7-mg/ml sample of low molecular weight Neutr-AB® was recovered from the dialysate.

As described below, the antigenic quality of the purified Neutr-AB was higher than that of the un-purified Neutr-AB® (**3.1.8**, **3.2.4**). A SAF containing immobilized purified Neutr-AB® was fabricated as described above (**3.1.1**), except that the concentration of the antigen solution (purified Neutr-AB® in bicarbonate buffer) at the beginning of the immobilization step was 2.4 mg/ml instead of 7 mg/ml. As described below (**3.1.12**, **3.2.5**), the antibody-binding capacity of this SAF was compared to that of a SAF containing immobilized un-purified Neutr-AB®, also fabricated using a 2.4-mg/ml antigen solution (un-purified Neutr-AB® in bicarbonate buffer).

3.1.4 Blood Acquisition

Type O fresh blood was drawn from healthy, non-pregnant, consenting donors over age 18, with the approval of the University of Pittsburgh Institutional Review Board. Fresh blood was drawn no more than 2 hours before the initiation of the antibody removal experiment, and was anticoagulated using heparin (Elkins-Sinn, Inc., Cherry Hill, NJ) at a concentration of 10 U/ml. Overfilled bags of type O and type A banked blood were obtained from the Central Blood Bank of Pittsburgh and stored at 4°C until use. Banked blood was anticoagulated using citrate phosphate dextrose (CPD). Plasma for blood typing, titer measurement, and cross-matching was obtained by centrifugation of blood samples for 15 minutes, at 1380xG, in a bench-top centrifuge (Fisher Scientific, Pittsburgh, PA).

3.1.5 Blood Typing

Blood was typed according to the standard blood bank procedure (*120*). For each blood sample to be typed, plasma was obtained via centrifugation and 100 μl of plasma was added to each of two 12 x 75 mm disposable glass test tubes. Fifty μl of type A1 reagent red blood cells (Immucor Inc., Norcross, GA) was added to one test tube, and 50 μl of type B reagent red blood cells was added to the other test tube. The tubes were mixed gently, centrifuged for 1 minute at 1380xG, and examined for red cell agglutination. Plasma from type A blood caused agglutination of type B red cells only; plasma from type B blood caused agglutination of type A1 red cells only; plasma from type O blood caused agglutination of both type A1 and type B red cells; and plasma from type AB blood caused agglutination of neither type A1 nor type B red cells.

3.1.6 Cross-matching

For experiments requiring the use of blood samples from multiple donors, all blood samples were cross-matched according to the standard blood bank procedure (*120*). The following procedure was performed for each pair of blood samples (called sample 1 and sample 2) to be cross-matched. Plasma was obtained from each blood sample via centrifugation. A 2-4% suspension of washed red blood cells was obtained from each blood sample by washing red blood cells (obtained via centrifugation) 3 to 5 times in 0.9% NaCl, then suspending 200 μl of washed red blood cells in 4.8 ml of 0.9% NaCl. One hundred μl of plasma from sample 1 was added to one 12 x 75 mm disposable glass test tube, and 100 μl of plasma from sample 2 was added to a second test tube. Fifty μl of the 2-4% suspension of red cells from sample 1 was added to the test tube containing plasma from sample 2, and 50 μl of red cells from sample 2 was

added to the test tube containing plasma from sample 1. The tubes were mixed gently, centrifuged for 1 minute at 1380xG, and examined for red cell agglutination. If no agglutination was observed, 100 μl of antibody enhancer (LISS, Immucor Inc., Norcross, GA) was added to each tube, and the tubes were mixed gently and incubated at 37 °C for 15 minutes. The tubes were centrifuged for 1 minute at 1380xG, and examined again for red cell agglutination. If no agglutination was observed, the cells in each tube were washed 3 times with 0.9% NaCl, and the supernatant was decanted completely after the third wash. One hundred μl of anti-human globulin (Immucor Inc., Norcross, GA) was added to each tube. The tubes were mixed gently, centrifuged for 1 minute at 1380xG, and examined for red cell agglutination. If no agglutination was observed, the 2 samples had a negative cross-match and could be used safely in the same experiment. To check the validity of the cross-match, 50 μl of Coombs control cells (Immucor Inc., Norcross, GA) was added to each tube. The tubes were mixed gently, centrifuged for 1 minute at 1380xG, and examined for red cell agglutination. If the control cells failed to agglutinate, the cross-match was repeated.

3.1.7 Measurement of Anti-A and Anti-B Antibody Titers

Anti-A and anti-B antibody titers were measured using plasma serial dilutions and the standard blood bank hemagglutination assay used for blood typing (*120*). Using this method the titer was assumed to reflect the concentration of IgM anti-A and anti-B antibodies only. For each blood sample to be assayed, plasma was obtained via centrifugation and serial dilutions of the plasma were prepared in 0.9% NaCl. Each diluted sample was assayed for the ability to agglutinate type A1 or type B reagent red blood cells, as described above (**3.1.5)**. The anti-A titer was taken as the reciprocal of the largest dilution that agglutinated type A1 reagent red blood

cells, and the anti-B titer was taken as the reciprocal of the largest dilution that agglutinated type B reagent red blood cells. If an undiluted plasma sample did not agglutinate type A1 or type B reagent red blood cells, the blood sample was assigned an anti-A or anti-B titer of 0.

3.1.8 Antigenic Quality Measurement

A hemagglutination inhibition assay was used to compare the antigenic qualities of the un-purified Neutr-AB®, the purified (high molecular weight) Neutr-AB®, and the low molecular weight Neutr-AB®. The antigenic quality of each form of Neutr-AB® was quantified by determining the minimum Neutr-AB® concentration required to completely inhibit the agglutination of type A1 or type B reagent red blood cells by human plasma, after mixing equal volumes of Neutr-AB® and plasma. For the un-purified Neutr-AB®, samples with total protein concentrations between 0.01 mg/ml and 5 mg/ml were prepared using 0.9% NaCl as the diluent. For the purified Neutr-AB®, samples with total protein concentrations between 0.001 mg/ml and 0.5 mg/ml were prepared. The low molecular weight Neutr-AB® was not diluted. For each sample of Neutr-AB®, 200 μl of Neutr-AB® was added to 200 μl of plasma in a 12 x 75 mm disposable glass test tube. The tube was mixed gently and incubated at room temperature for 5 minutes. The plasma/Neutr-AB® solution was tested for the ability to agglutinate type A1 and type B reagent red blood cells, as described above (**3.1.5**). The anti-A and anti-B inhibition concentrations were taken as the minimum concentrations of Neutr-AB® required to inhibit the agglutination of type A1 and type B reagent red blood cells.

3.1.9 In Vitro Perfusion Loop

In vitro antibody removal experiments were performed using the simple perfusion loop shown in **Figure 3-1**. The loop consisted of a glass blood reservoir, a Masterflex peristaltic pump

(Cole-Parmer Instrument Company, Vernon Hills, IL), a glass bead flow meter (Cole-Parmer Instrument Company, Vernon Hills, IL), and a SAF. The components of the loop were connected using tygon tubing. The SAF was oriented horizontally as shown in **Figure 3-1**. Blood was pumped solely through the blood compartment of the SAF, and ultrafiltrate was collected from the shell compartment and returned to the reservoir. The entire loop, including both the blood and shell compartments of the SAF, was flushed with 0.9% NaCl prior to each experiment. Air was removed from the system during priming with blood.

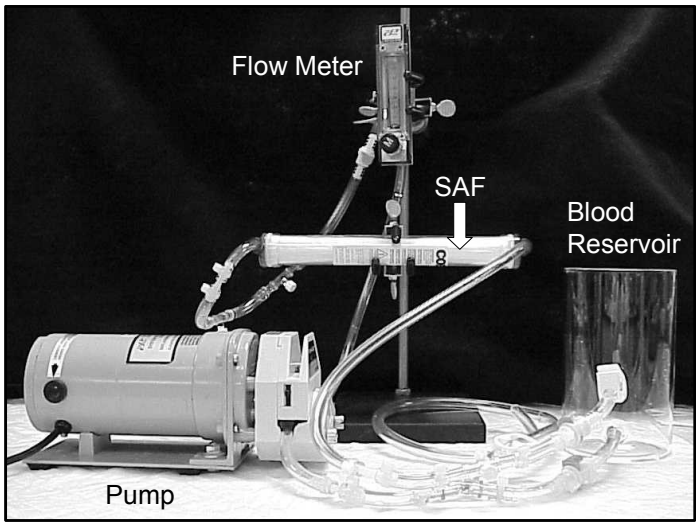

Figure 3-1 Perfusion loop used for *in vitro* antibody removal experiments.

3.1.10 Initial Paired Antibody Removal Experiments

The first series of antibody removal experiments was performed to compare the anti-A and anti-B removal accomplished by SAFs containing immobilized A and B antigens (SAF-AB) to the non-specific removal accomplished by control SAFs (unmodified hemodialyzers or SAFs containing immobilized bovine serum albumin, SAF-Ctrl). SAFs containing immobilized A and B antigens and control SAFs were tested under identical conditions. A 250 ml sample of type A

or O fresh or banked whole blood (from one donor) was obtained as described above (**3.1.4**). One hundred ml of the blood was circulated through the SAF containing immobilized A and B antigens at 100 ml/min for 30 minutes. Aliquots were taken from the reservoir every 15 minutes and the anti-A and anti-B titers were measured. One hundred ml of the blood was then circulated through the control SAF at 100 ml/min for 30 minutes, and aliquots were taken from the reservoir every 15 minutes for titer measurement. For each experiment, pre-perfusion, post-SAF-AB perfusion, and post-SAF-Ctrl perfusion plasma samples were saved to allow comparison of SAF-AB- and SAF-Ctrl-induced complement activation.

3.1.11 Biocompatibility Testing

Following each of the initial antibody removal experiments described above (**3.1.10**), pre-perfusion, post-SAF-AB perfusion, and post-SAF-Ctrl perfusion plasma samples were assayed for complement activation product SC5b-9 concentration using commercially available immunoassay kits (Quidel Corporation, San Diego, CA). The assays were performed in the Biomaterials and Tissue Engineering Laboratory, directed by William Wagner, in the McGowan Institute for Regenerative Medicine at the University of Pittsburgh.

3.1.12 SAF Capacity Experiments

The second series of antibody removal experiments was performed to estimate the antibody-binding capacities of SAFs containing immobilized A and B antigens (SAF-AB) or immobilized purified A and B antigens (SAF-ABp). SAFs containing immobilized A and B antigens and control SAFs (SAF-Ctrl) were tested under identical conditions. Up to 3 L of type O banked whole blood (from up to 6 different donors) was obtained as described above (**3.1.4**), and all of the blood samples used in each experiment were cross-matched prior to the experiment

as described above (**3.1.6**). Blood from each donor was split so that half could be circulated through the SAF-AB and half could be circulated through the SAF-Ctrl. (When testing the SAFs containing immobilized purified A and B antigens, blood from each donor was split into thirds so that 1/3 could be circulated through the SAF-AB, 1/3 could be circulated through the SAF-ABp, and 1/3 could be circulated through the SAF-Ctrl). Capacity experiments were performed by sequentially circulating multiple 100 or 150 ml samples of blood through the SAF at a flow rate of 100 ml/min. When the anti-A and anti-B titers of a given blood sample dropped to 2 or below, the entire flow loop was drained, including both the blood and shell compartments of the SAF, and a new blood sample was circulated through the SAF. The SAF was not washed between successive blood samples to avoid measurement of an artificially high capacity caused by removal of some of the bound antibodies during the washing. This procedure was repeated until the titer of a newly introduced blood sample was not reduced. The capacity of the SAF was taken as the volume of blood processed before titer reduction ceased.

3.2 Results

3.2.1 Initial Paired Antibody Removal Experiments

Anti-A and anti-B antibodies were successfully removed from 100 ml of freshly drawn type O whole human blood by a SAF containing approximately 99 mg of immobilized A and B antigens (SAF-AB) (**Figure 3-2**). After 30 minutes, the SAF-AB reduced the anti-A titer from 8 to 1 and the anti-B titer from 16 to 1. Anti-A and anti-B antibodies were not measurably removed from 100 ml of blood (from the same donor) by a control SAF containing immobilized bovine serum albumin (BSA). After 30 minutes, the control SAF had not measurably reduced the anti-A titer or the anti-B titer.

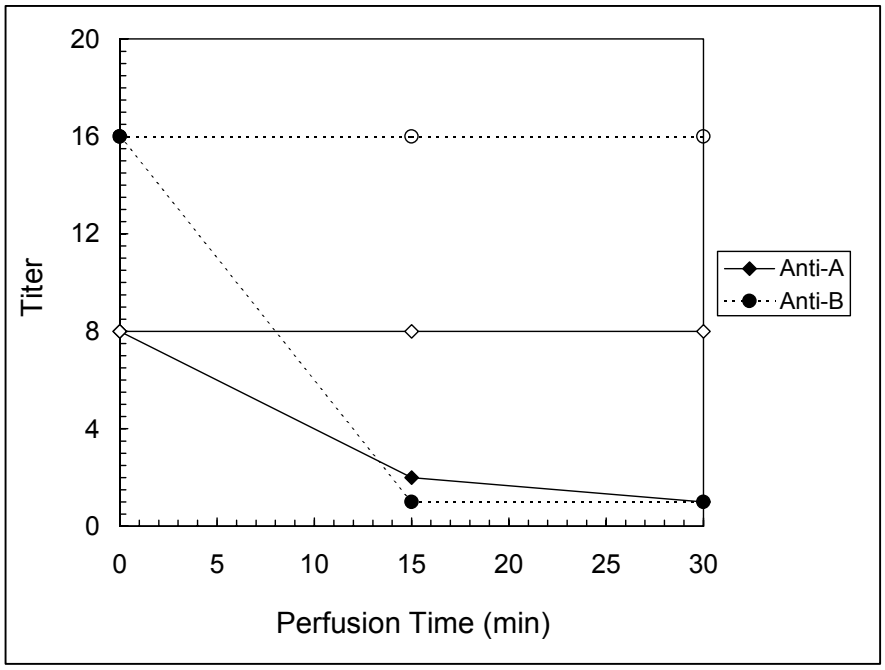

Figure 3-2 Anti-A and anti-B removal from 100 ml of freshly drawn type O whole human blood using a SAF with approximately 99 mg of immobilized A and B antigens (SAF-AB). Non-specific anti-A and anti-B removal using a control SAF with immobilized BSA (SAF-Ctrl) is also shown. Closed symbols: SAF-AB. Open symbols: SAF-Ctrl.

Six paired antibody removal experiments were performed using blood from 6 different donors, and in each experiment the SAF-AB accomplished a larger anti-A and anti-B titer reduction than did the SAF-Ctrl (**Table 3-1**). The mass of A and B antigens immobilized within each SAF-AB ranged from 69 to 99 mg, with a mean of 86 mg. The SAF-ABs accomplished a mean anti-A titer reduction of 70% and a mean anti-B titer reduction of 94%, while the SAF-Ctrls accomplished a mean anti-A titer reduction of 0% and a mean anti-B titer reduction of 33%. Using the paired t-test, the percent anti-A titer reduction and anti-B titer reduction accomplished by the SAF-ABs was statistically greater than the percent reduction accomplished by the SAF-Ctrls ($p < 0.005$).

Table 3-1 Antibody Removal During Initial Paired Antibody Removal Experiments

Trial	Blood Source	Control Filter	Initial Anti-A Titer	Initial Anti-B Titer	Final Anti-A Titer (SAF-AB)	Final Anti-B Titer (SAF-AB)	Final Anti-A Titer (SAF-Ctrl)	Final Anti-B Titer (SAF-Ctrl)
1	Fresh type O	SAF-BSA	8	16	1	1	8	16
2	Fresh type O	SAF-BSA	16	8	8	2	16	4
3	Bank type A	SAF-BSA	N/A	8	N/A	0	N/A	4
4	Fresh type O	Dialyzer	16	8	2	0	16	4
5	Fresh type O	Dialyzer	8	8	4	0	8	8
6	Bank type O	Dialyzer	16	16	4	1	16	8

3.2.2 Biocompatibility Testing

In each paired antibody removal experiment, the SC5b-9 concentration increased following both SAF-AB perfusion and SAF-Ctrl perfusion (**Table 3-2**). (SC5b-9 concentration data from trial six were not obtained due to a technical error.) The SAF-ABs induced a mean increase in SC5b-9 concentration of 500%, while the SAF-Ctrls induced a mean increase in SC5b-9 concentration of 800%. Using the paired t-test, the percent increase in SC5b-9 concentration induced by the SAF-ABs was not statistically different from the percent increase induced by the SAF-Ctrls ($p > 0.1$).

Table 3-2 Complement Activation During Initial Paired Antibody Removal Experiments

Trial	Initial SC5b-9 Concentration (ng/ml)	Final SC5b-9 Concentration (ng/ml) (SAF-AB)	Final SC5b-9 Concentration (ng/ml) (SAF-Ctrl)
1	26.4	80.7	84.1
2	14.2	39.6	26.2
3	15.5	38.0	107.8
4	1.2	14.5	22.2
5	10.9	100.7	152.3

3.2.3 SAF Capacity Experiment 1: Capacity of a SAF Containing Immobilized A and B Antigens

Anti-A and anti-B antibodies were successfully removed from 4 100 ml samples of type O banked human blood by a SAF containing approximately 100 mg of immobilized A and B antigens (**Figure 3-3**). The anti-A titers of the first three blood samples were reduced from 64 to 1 (98%), 64 to 1 (98%), and 64 to 2 (97%), respectively. The anti-A titer of the fourth sample was reduced from 16 to 4 (75%), and the anti-A titers of the fifth and sixth samples were not measurable reduced. The anti-B titers of the first four samples were reduced from 8 to zero (100%), and the anti-B titers of the fifth and sixth samples were reduced from 8 to 2 (75%) and 8 to 1 (88%), respectively. Anti-A and anti-B antibodies were not measurably removed from 6 100 ml samples of type O banked human blood (from the same donors) by a control SAF containing immobilized BSA. The anti-A and anti-B titers of each sample were not measurably reduced (data not shown).

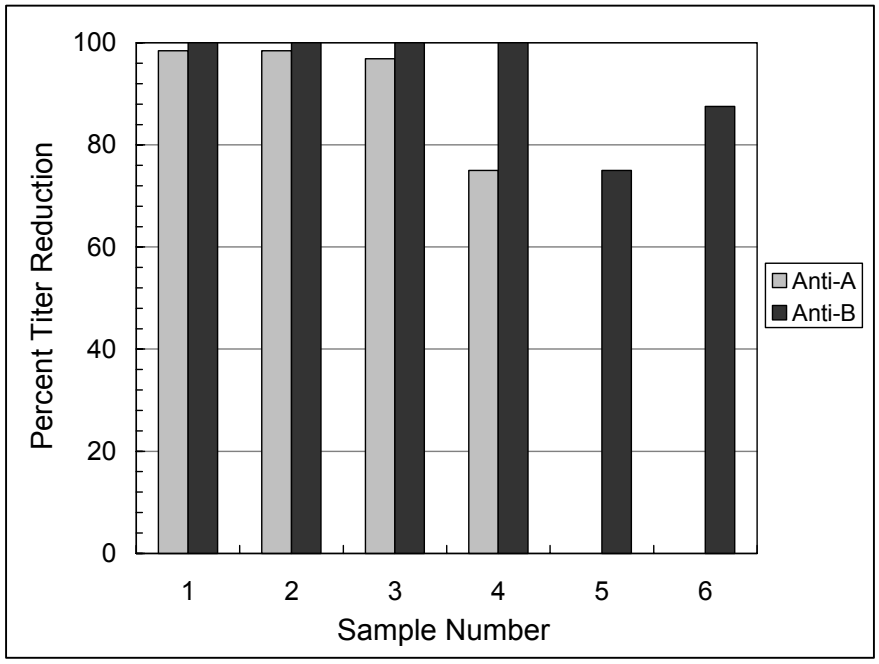

Figure 3-3 Anti-A and anti-B removal from 6 100 ml samples of type O banked human blood using a SAF with approximately 100 mg of immobilized A and B antigens (SAF-AB). Zero percent titer reduction is indicated by the absence of a bar.

3.2.4 Purification of A and B Antigens (Neutr-AB®)

The concentration of un-purified Neutr-AB® required to inhibit the agglutination of type A1 and type B reagent red blood cells by human plasma varied from 0.05 to 4 mg/ml, depending on the plasma sample used to perform the hemagglutination inhibition assay (**3.1.8**) (**Table 3-3**). The concentration of purified Neutr-AB® required to inhibit agglutination by the same plasma samples varied from 0.01 to 0.25 mg/ml. The assay was performed using 3 different plasma samples, with initial anti-A and anti-B titers of 0 and 64 (type A), 64 and 32 (type O, 1), and 32 and 32 (type O, 2). Neither the un-purified Neutr-AB® inhibition concentration nor the purified Neutr-AB® inhibition concentration increased with increasing initial anti-A or anti-B titer. The sample-to-sample variation in the inhibition concentration was likely due to sample-to-sample variation in the affinities of the anti-A and anti-B antibodies for Neutr-AB®, or sample-to-

sample variation the concentration of IgG anti-A and anti-B antibodies. At a concentration of 0.7 mg/ml, the low molecular weight Neutr-AB® was unable to inhibit the agglutination of type A1 or type B red cells by any of the tested plasma samples.

Table 3-3 Standard and Purified Neutr-AB® Inhibition Concentrations

	Un-purified Neutr-AB®		Purified (High MW) Neutr-AB®		Low MW Neutr-AB®	
Plasma Sample	Anti-A Inhibition Conc. (mg/ml)	Anti-B Inhibition Conc. (mg/ml)	Anti-A Inhibition Conc. (mg/ml)	Anti-B Inhibition Conc. (mg/ml)	Anti-A Inhibition Conc. (mg/ml)	Anti-B Inhibition Conc. (mg/ml)
A	N/A	0.3	N/A	0.025	N/A	> 0.7
O, 1	0.2	0.05	0.025	0.01	> 0.7	> 0.7
O, 2	0.75	4	0.05	0.25	> 0.7	> 0.7

For each plasma sample used, the un-purified Neutr-AB® inhibition concentration was higher than the purified Neutr-AB® inhibition concentration (**Figure 3-4**). The un-purified Neutr-AB® anti-A inhibition concentration was between 8 and 15 times the purified Neutr-AB® anti-A inhibition concentration, and the un-purified Neutr-AB® anti-B inhibition concentration was between 5 and 16 times the purified Neutr-AB® anti-A inhibition concentration.

3.2.5 SAF Capacity Experiment 2: Capacity of a SAF Containing Immobilized Purified A and B Antigens

Anti-A and anti-B antibodies were successfully removed from 6 150 ml samples of type O banked human blood by a SAF containing approximately 40 mg of immobilized purified A and B antigens (purified Neutr-AB®) (**Figure 3-5**). The anti-A titers of the first through sixth blood samples were reduced from 32 to 1 (97%), 32 to 2 (94%), 32 to 2 (94%), 16 to 1 (94%), 16 to 2 (88%), and 8 to 2 (75%), respectively. The anti-B titers of the first through sixth blood

samples were reduced from 32 to 0 (100%), 16 to 0 (100%), and 8 to 0 (100%), 4 to 0 (100%), 4 to 0 (100%), 8 to 1 (88%), respectively. Anti-A and anti-B antibodies were successfully removed from one 150 ml sample of type O banked human blood by a SAF containing approximately 40 mg of immobilized un-purified A and B antigens (un-purified Neutr-AB®). The anti-A and anti-B titers of the first sample were reduced from 32 to 8 (75%) and 32 to 4 (88%), respectively. The anti-A and anti-B titers of the second through sixth samples were not measurably reduced. Anti-A and anti-B antibodies were not measurably removed from 6 150 ml samples of type O banked human blood (from the same donors) by a control SAF containing immobilized BSA. The anti-A and anti-B titers of each sample were not measurably reduced (data not shown).

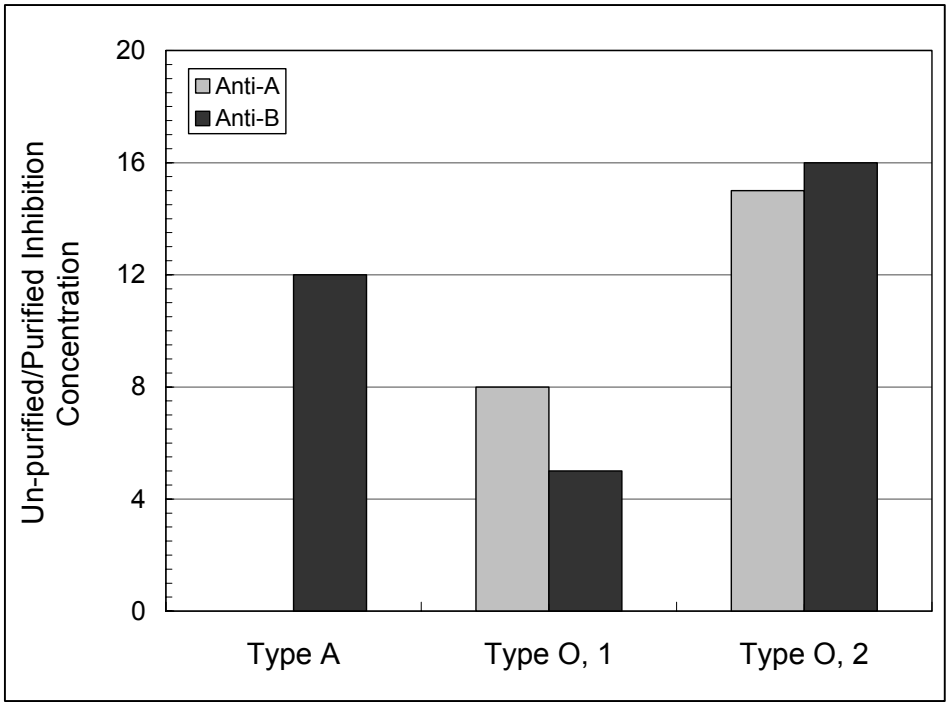

Figure 3-4 Ratio of the un-purified Neutr-AB® inhibition concentration to the purified Neutr-AB® inhibition concentration, for three different plasma samples with initial anti-A and anti-B titers of 0 and 64 (type A), 64 and 32 (type O, 1), and 32 and 32 (type O, 2).

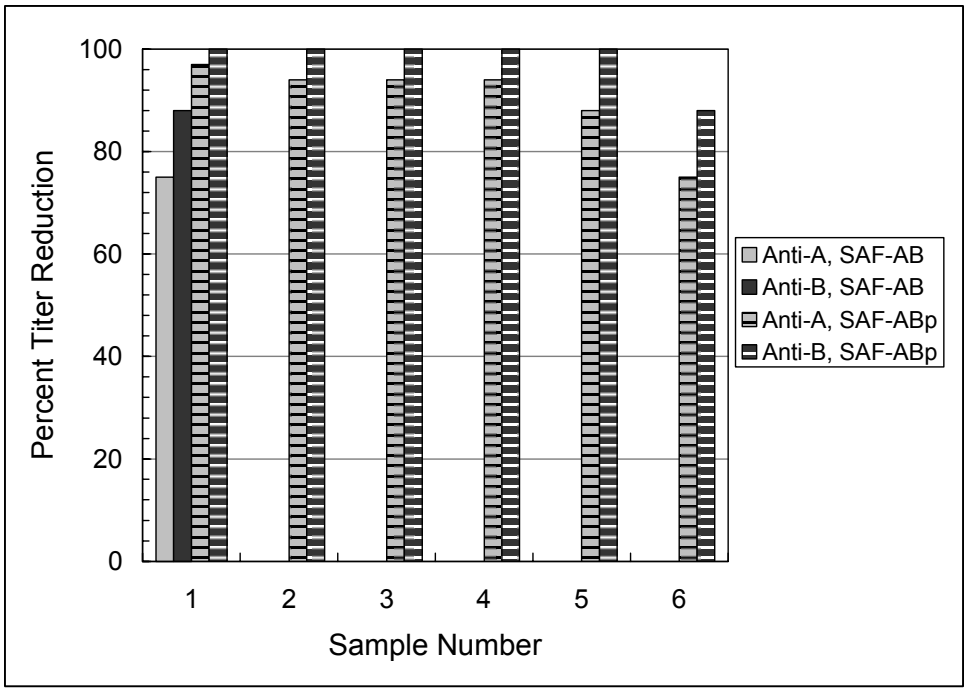

Figure 3-5 Anti-A and anti-B removal from 6 150 ml samples of type O banked human blood using a SAF with approximately 40 mg of immobilized un-purified A and B antigens (SAF-AB) and a SAF with approximately 40 mg of immobilized purified A and B antigens (SAF-ABp). Zero percent titer reduction is indicated by the absence of a bar.

3.3 Discussion

Specific antibody filters (SAFs) containing immobilized protein-based A and B antigens selectively removed anti-A and anti-B antibodies directly from whole human blood. In an initial series of six paired antibody removal experiments, the anti-A and anti-B removal accomplished by SAFs containing immobilized A and B antigens (SAF-AB) was significantly higher than the non-specific anti-A and anti-B removal accomplished by control SAFs (SAF-Ctrl). Additionally, the percent increase in SC5b-9 concentration induced by the SAF-ABs was not statistically different from the percent increase induced by the SAF-Ctrls.

A SAF containing approximately 100 mg of immobilized A and B antigens reduced the anti-A and anti-B titers of 400 ml of type O whole human blood by 75 to 100%. Assuming that

the SAF antibody-binding capacity is linearly proportional to the blood-contacting surface area, a SAF with approximately 12 times the surface area of the prototype SAF (i.e. with a blood-contacting surface area of about 11 m^2) would be required to significantly reduce the anti-A and anti-B titers of 5 L of whole human blood (the blood volume of an average adult patient). However, purifying the A and B antigens prior to immobilization improved the SAF antibody-binding capacity. A SAF containing approximately 40 mg of immobilized purified A and B antigens reduced the anti-A and anti-B titers of 900 ml of type O whole human blood by 75 to 100%, implying that a SAF with only 6 times the blood-contacting surface area of the prototype SAF (i.e. with a blood-contacting surface area of about 5.5 m^2) would be required to significantly reduce the anti-A and anti-B titers of 5 L of whole human blood.

The SAF antibody-binding capacity may possibly be further improved by using synthetic A and B antigens instead of naturally occurring protein-based A and B antigens (such as those that comprise Neutr-AB®). Synthetic antigens can be obtained at near 100% purity, and can be synthesized on spacer arms of varying lengths to allow optimization of the distance between the antigen and the membrane. Reactive groups on the spacer arms would allow oriented immobilization of the synthetic antigens, instead of the randomly oriented immobilization that occurs when protein-based antigens are immobilized via numerous available primary amines on the proteins. Finally, SAFs could be fabricated containing only A antigens or only B antigens, since the only situation in which both anti-A and anti-B removal would be necessary would be the transplant of a type AB kidney into a type O patient. Based on the frequencies of ABO blood groups in the United States, only 1% of potential living donor-kidney transplant candidate pairs would involve a type AB donor and a type O recipient (*116,117*). Based on these considerations, our continuing SAF development work will be focused on the use of synthetic A and B antigens.

During SAF-based antibody removal, antibody-antigen complexes formed on the lumenal surfaces of the SAF fibers will activate the complement system via the classical pathway, and the degree of complement activation may be greater than the degree produced during other extracorporeal therapies like hemodialysis and cardiopulmonary bypass (*121*). The preliminary biocompatibility testing we performed did not show increased complement activation by the SAFs with immobilized A and B antigens compared to the control SAFs. In our continuing studies we will perform more extensive biocompatibility testing, using both *in vitro* and *in vivo* experimental formats. However, we do not expect complement activation to be a significant problem since SAF-based antibody removal will be performed only during the peri-transplant period, and will not be performed chronically like hemodialysis. Also, Sakhrani et al used whole blood perfusion through Biosynsorb columns to remove anti-A or anti-B antibodies prior to ABO-incompatible kidney transplants (thus presumably activating the complement system via the classical pathway), and reported that the side effects were mild in most of the treated patients (*87*).

4.0 ANTIBODY TRANSPORT MODEL

As discussed in Chapter 2.0, SAF-based antibody removal must be reasonably fast as well as selective if the platform is to be clinically valuable. In this chapter, we describe the development of a mathematical antibody transport model that accounts for antibody diffusion, convection, and reversible binding within the SAF fibers. The model is used to predict the magnitude of the SAF-based antibody removal rate, and to identify the removal rate-controlling antibody transport mechanisms, for clinically relevant SAF geometries, blood flow rates, antibody diffusivities, and antibody-binding rates. In Chapter 5.0, we describe *in vitro* antibody removal experiments performed to test key predictions of the mathematical model. Since the *in vitro* experiments involve SAF-based removal of antibodies from aqueous buffer (instead of blood), in this chapter we address antibody removal from aqueous buffer as well as antibody removal from blood.

4.1 Model Geometry

The SAF is modeled as a bundle of N identical cylindrical fibers of length L (cm) and inner radius a (cm) (**Figure 4-1**). Antibody solution (blood or aqueous buffer) enters the blood compartment of the SAF at free antibody concentration c_i (μg/ml) and flow rate Q (ml/min), and is distributed evenly among the fibers so that the flow rate through each fiber lumen is Q/N. The shell compartment of the SAF (the space outside the fibers) is filled with isotonic buffer and closed. Within each fiber lumen antibodies undergo axial convection and radial diffusion, and at

the fiber wall the antibodies bind reversibly to the immobilized antigens (**Figure 4-2**). Antibody solution exits each fiber at "mixing cup" free antibody concentration c_o (μg/ml), and the SAF-based antibody removal rate is equal to the antibody solution flow rate Q multiplied by the difference between c_i and c_o.

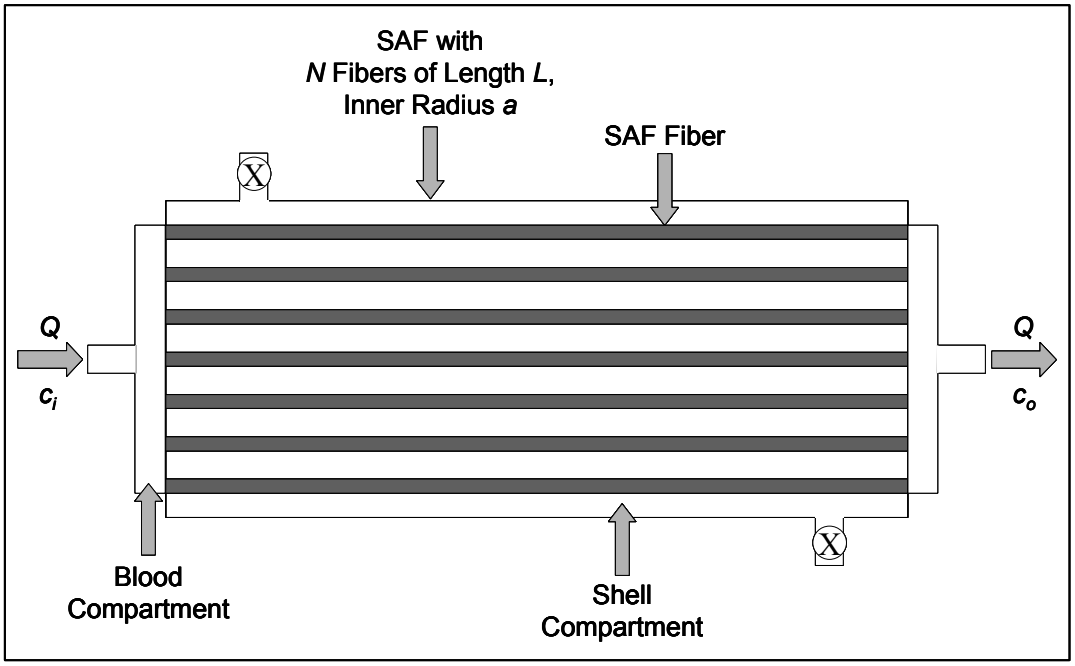

Figure 4-1 Schematic depicting blood flow through the blood compartment of a SAF. The shell compartment is filled with isotonic buffer and closed. The relative dimensions of the SAF fibers and the SAF housing are not to scale.

4.2 Transport Formulation

The quasi-steady mass conservation equation is used to describe the transport of free antibodies in the fiber lumen (*122*):

$$v_z \frac{\partial c}{\partial z} = \frac{D}{r}\frac{\partial}{\partial r}\left(r\frac{\partial c}{\partial r}\right) \qquad \textbf{(4-1)}$$

where $c(r, z)$ (μg/ml) is the concentration of free antibodies in the fiber lumen, $v_z(r)$ (cm/s) is the axial component of the antibody solution velocity, and D (cm^2/s) is the diffusion coefficient of

the antibodies in the antibody solution. Boundary conditions at the fiber wall, centerline, and inlet are required to solve equation **(4-1)** for *c(r, z)*. An expression for the antibody solution velocity profile $v_z(r)$ is also needed. As discussed further below, the boundary condition at the fiber wall involves the bound antibody concentration c_b (μg/cm^2), and thus is time-dependent since c_b increases with time. However, the quasi-steady form of the mass conservation equation is appropriate since the time scale for a substantive change in c_b is long compared to the residence time.

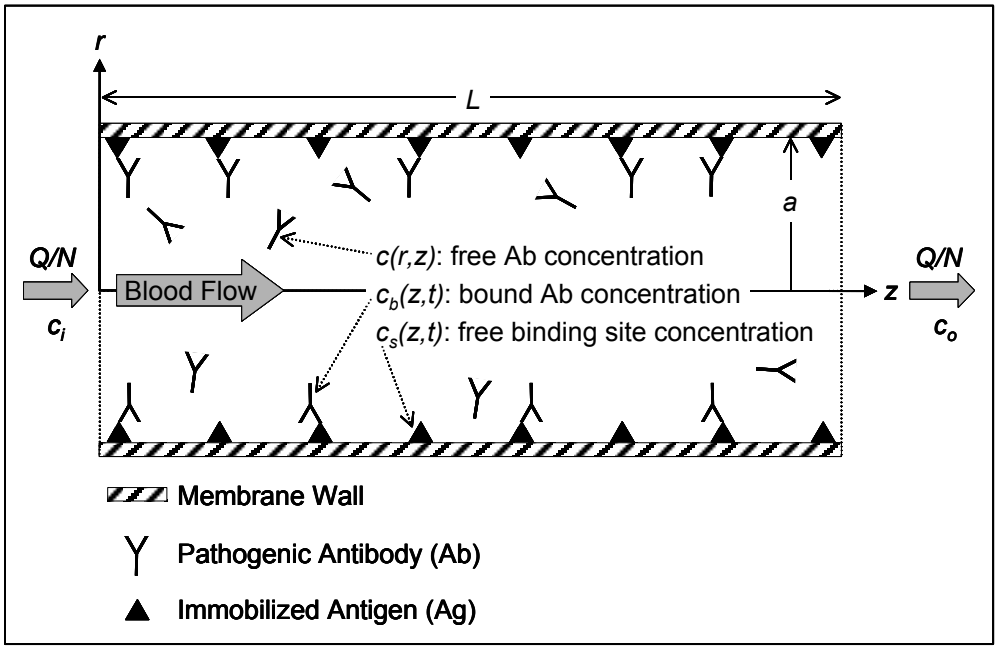

Figure 4-2 Schematic depicting antibody removal in the lumen of a single SAF fiber, with model parameters described in the preceding text. The relative dimensions of the fiber lumen and the antibodies and antigens are not to scale.

At the inner fiber wall, the radial antibody flux is equal to the antibody-binding rate per unit of fiber surface area:

$$-D\frac{\partial c}{\partial r} = k_f c\left(c_s^{\,i} - c_b\right) - k_r c_b \text{ at } r = a \qquad \textbf{(4-2)}$$

where k_f (ml/μg*s) is the intrinsic association rate constant for the antibody/antigen system, k_r (s^{-1}) is the intrinsic dissociation rate constant for the antibody/antigen system, c_b (μg/cm^2) is the bound antibody concentration, and c_s^i (μg/cm^2) is the antibody-binding capacity of the SAF. The antibody concentration profile in each fiber is symmetric with respect to radial position, and the antibody solution enters each fiber with a flat concentration profile:

$$\frac{\partial c}{\partial r} = 0 \text{ at } r = 0 \quad \textbf{(4-3)}$$

$$c = c_i \text{ at } z = 0 \quad \textbf{(4-4)}$$

Finally, $c_b(z, t)$ is determined by integrating the radial antibody flux at the fiber wall over time:

$$c_b = \int_0^t -D\frac{\partial c}{\partial r}(r = a)dt \quad \textbf{(4-5)}$$

4.3 Flow of Blood or Aqueous Buffer in SAF Fibers

The physical properties (density and viscosity) of blood and dilute aqueous buffer (water) are listed in **Table 4-1**.

Table 4-1 Physical Properties of Blood and Water (*123-125*)

Fluid	Density (g/ml)	Viscosity at 22 °C, cP	Viscosity 37 °C, cP
Blood (40% Hematocrit)	1.058	4.8 (at high shear rates)	3.5 (at high shear rates)
Water	1.0	1.0	0.7

The SAFs used clinically will contain between 6000 and 32,000 fibers of 25 cm length and 0.01 cm inner radius (**Table 2-5**). For water flow through a small SAF (6000 fibers), the Reynolds number in each SAF fiber lumen is below 14 when the water flow rate is below 500 ml/min (**Figure 4-3**). For water flow through a large SAF (32,000 fibers), the Reynolds number

is below 3 when the water flow rate is below 500 ml/min. Under the same conditions as those described above, the Reynolds number for blood flow is less than that for water flow since blood is more viscous (and only slightly more dense) than water (**Figure 4-3**). Hence, the flow of blood or aqueous buffer is laminar within each fiber lumen. Blood is a non-Newtonian fluid, but behaves as a Newtonian fluid for when the shear rate is greater than 100 s^{-1} (*126*). For flow through a small SAF (6000 fibers), the shear rate at the inner wall of each fiber exceeds 100 s^{-1} when the flow rate exceeds 30 ml/min, and for flow through a large SAF (32,000 fibers) the shear rate at the inner wall of each fiber exceeds 100 s^{-1} when the flow rate exceeds 150 ml/min (**Figure 4-4**). Hence blood can be considered a Newtonian fluid as it flows through the SAF provided that the flow rate is sufficiently high. For laminar flow of a Newtonian fluid in a circular tube, the entrance length, relative to the total length of the tube, can be estimated (*127,128*):

$$\frac{L_e}{L} = (1.18 + 0.112\,\mathrm{Re})\frac{a}{L} \qquad \textbf{(4-6)}$$

where L_e is the entrance length (cm) and Re is the Reynolds number. For the small SAF (6000 fibers), the entrance length is less than 0.1% of the SAF fiber length (for Re less than 14). For the large SAF (32,000 fibers), the entrance length is less than 0.06% of the SAF fiber length (for Re less than 3).

Hence the flow of blood or dilute aqueous buffer in each fiber lumen is laminar and fully developed, and the fluid velocity profile is the parabolic velocity profile characteristic of laminar, fully developed flow of a Newtonian fluid in a circular tube (*122*):

$$v_z = 2v_{avg}\left(1 - \frac{r^2}{a^2}\right) \qquad \textbf{(4-7)}$$

where v_{avg} (cm/s) is the average fluid velocity in the fiber.

During SAF-based antibody removal the net ultrafiltration rate (flow rate of buffer or plasma water from the blood compartment to the shell compartment) is zero since the shell compartment is filled with isotonic buffer and closed. However, buffer or plasma water re-circulates between the blood and shell compartments because the hydrostatic pressure in the lumen of each fiber decreases along the length of the fiber, while the hydrostatic pressure in the shell compartment is constant (and equal to the average of the inlet and outlet lumenal pressures (*129*)). This re-circulation (Starling re-circulation) has a negligible effect on the fluid flow in the fiber lumens if the ratio of the lumenal flow resistance (R_l) to the trans-membrane flow resistance (R_t) is less than one (*129*):

$$\frac{R_l}{R_t} = \frac{8\mu L}{\pi a^4} / \frac{1}{L_p} \qquad \textbf{(4-7)}$$

where μ is the blood or buffer viscosity (cP) and L_p (ml/mmHg*hr) is the hydraulic permeability of a single SAF fiber. For Hemophan® hollow fiber dialysis membranes (used in the *in vitro* experiments reported in Chapters 3.0 and 5.0), the hydraulic permeability of a single fiber of 25 cm length and 0.01 cm inner radius is $9*10^{-4}$ ml/hr*mmHg (*100*). Thus for blood flow at 37 ºC, R_l/R_t is equal to 0.04. (*In vivo* SAF-based antibody removal will occur at 37 ºC to avoid delivering cool blood to the patient.) For water flow at 22 ºC, R_l/R_t is equal to 0.01. (The *in vitro* antibody removal experiments described in Chapter 5.0 were performed at 22 ºC for simplicity.) In both cases, the Starling re-circulation has a negligible effect on the fluid flow in the fiber lumens.

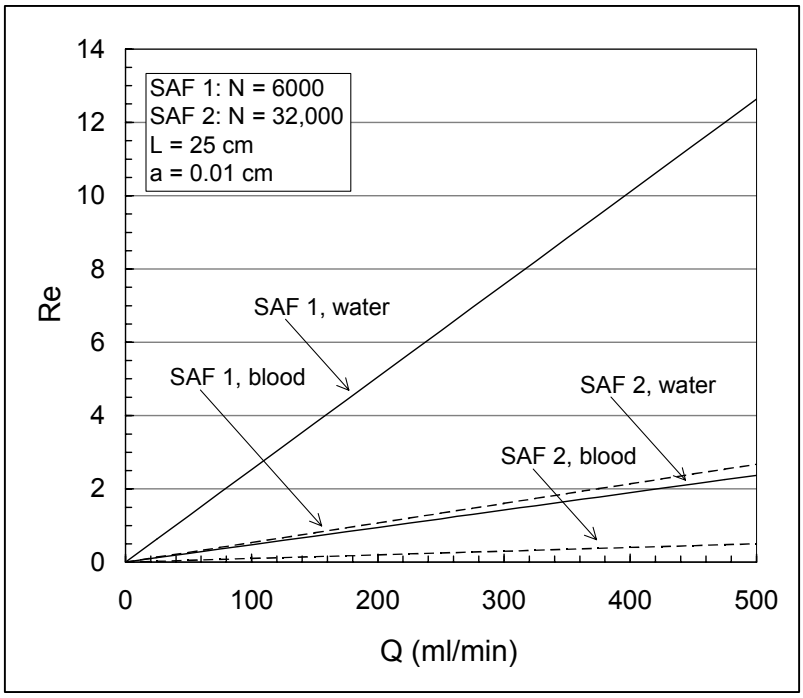

Figure 4-3 Reynolds numbers in the fiber lumens of 2 SAFs containing the smallest (SAF 1) and largest (SAF 2) number of fibers expected for clinical SAFs.

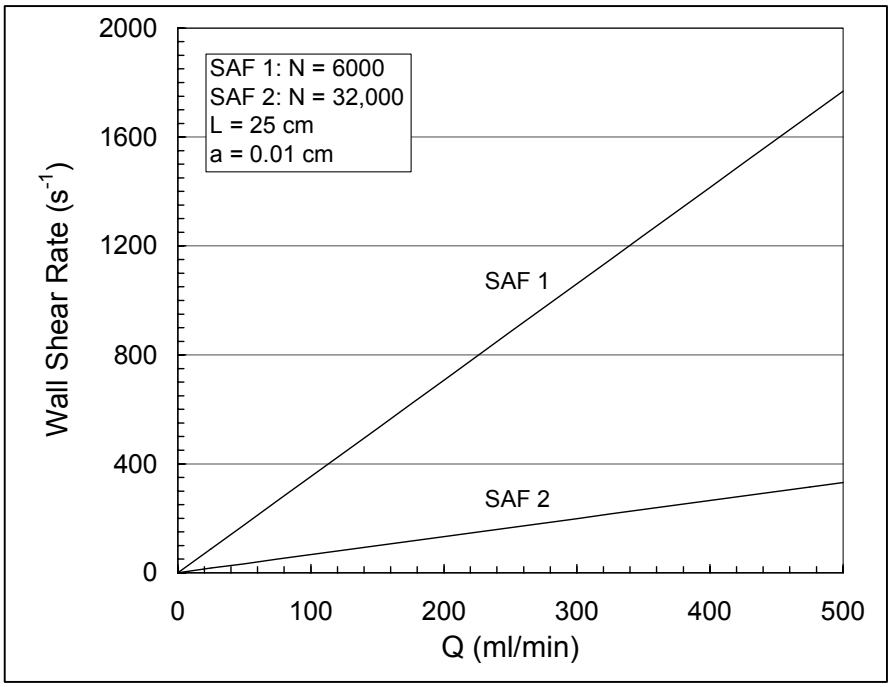

Figure 4-4 Wall shear rates in the fibers comprising 2 SAFs containing the smallest (SAF 1) and largest (SAF 2) number of fibers expected for clinical SAFs.

4.4 Dimensional Analysis

We used the dimensionless variables and groups listed in **Table 4-2** to simplify the solution and interpretation of the transport model. We normalized the radial position by the inner radius of each SAF fiber, and we normalized the axial position by the length of each fiber: $r^* = r/a$ and $z^* = z/L$. We normalized the free antibody concentration by the inlet free antibody concentration, and we normalized the bound antibody concentration by the SAF antibody-binding capacity: $c^* = c/c_i$, and $c_b^* = c_b/c_s^i$. The dimensionless form of the mass conservation equation involves the Graetz number (Gz):

$$\frac{2Gz}{\pi}\left(1 - r^{*2}\right)\frac{\partial c^*}{\partial z^*} = \frac{1}{r^*}\frac{\partial}{\partial r^*}\left(r^*\frac{\partial c^*}{\partial r^*}\right) \qquad \textbf{(4-1a)}$$

The Graetz number ($Gz = \pi a^2 v_{avg}/LD$) represents the ratio of the characteristic radial diffusion time to the residence time (*122*). As Gz approaches infinity, $\partial c^*/\partial z^*$ approaches zero since the time required for the antibodies to diffuse to the immobilized antigens is much longer than the time the antibodies spend in the SAF. Using a small SAF (6000 fibers), the Graetz number for IgG antibodies is between 7 and 143 when the antibody solution flow rate is between 25 and 500 ml/min, and the Graetz number for IgM antibodies is between 19 and 397 for the same antibody solution flow rate range (**Figure 4-5**). Using a large SAF (32,000 fibers), the Graetz number for IgG antibodies is between 1 and 26 when the antibody solution flow rate is between 25 and 500 ml/min, and the Graetz number for IgM antibodies is between 3 and 74 for the same antibody solution flow rate range. (For these calculations to apply to antibody removal from blood at 37 ºC, we must assume that the antibody diffusivity in flowing blood is equal to the antibody diffusivity in flowing water, and we must neglect the effect of temperature on antibody

diffusivity. These calculations are only strictly correct for antibody removal from aqueous buffer at 22 ºC.)

Table 4-2 Dimensionless Variables and Groups

Variable	Description
$c^* = \frac{c}{c_i}$	Free Antibody Concentration
$c_b^* = \frac{c_b}{c_s^{\,i}}$	Bound Antibody Concentration
$r^* = \frac{r}{a}$	Radial Position
$z^* = \frac{z}{L}$	Axial Position
$Gz = \frac{\pi a^2 v_{avg}}{LD}$	Graetz Number
$Da = \frac{k_f c_s^{\,i} a}{D}$	Damköhler Number

The dimensionless form of the wall boundary condition involves the Damköhler number (*Da*):

$$-\frac{1}{Da}\frac{\partial c^*}{\partial r^*} = c^* - c_b^* \left(c^* + \frac{K_d}{c_i} \right) \text{ at } r^* = 1 \qquad \textbf{(4-2a)}$$

where K_d (μg/ml) is the equilibrium dissociation constant for the antibody/antigen system. The Damköhler number ($Da = k_f c_s^{\,i} a/D$) represents the ratio of the characteristic antibody-binding rate to the characteristic radial antibody diffusion rate. As *Da* approaches infinity, antibodies that reach the fiber wall bind "instantaneously" and antibody transport in the fiber lumen is controlled by the rate of antibody diffusion (diffusion-limited). Conversely, as *Da* approaches zero, antibodies that bind to antigens are replaced "instantaneously" by diffusion of antibodies farther from the fiber wall, and antibody transport in the fiber lumen is controlled by the rate of

antibody-binding (reaction-limited). For k_f between 10^{-5} and 10^{-2} ml/μg*s (10^4 to 10^6 L/mol*s), the Damköhler number for SAF-based IgG removal is between 0.1 and 300, and the Damköhler number for SAF-based IgM removal is between 1 and 800 (**Figure 4-6**). (Again, for these calculations to apply to antibody removal from blood at 37 ºC, we must assume that the antibody diffusivity in flowing blood is equal to the antibody diffusivity in flowing water, and we must neglect the effect of temperature on antibody diffusivity. These calculations are only strictly correct for antibody removal from aqueous buffer at 22 ºC.) To make these estimates, we chose 1 μg/cm^2 as an order of magnitude estimate of the antibody-binding capacity of the SAF, since the approximate surface concentration of a monolayer of IgG molecules is 0.6 μg/cm^2 (*101,102*). We chose the antibody/antigen association rate constant range based on the reported rate constants for antibody/antigen systems with either the antibodies or the antigens immobilized (*106,107*).

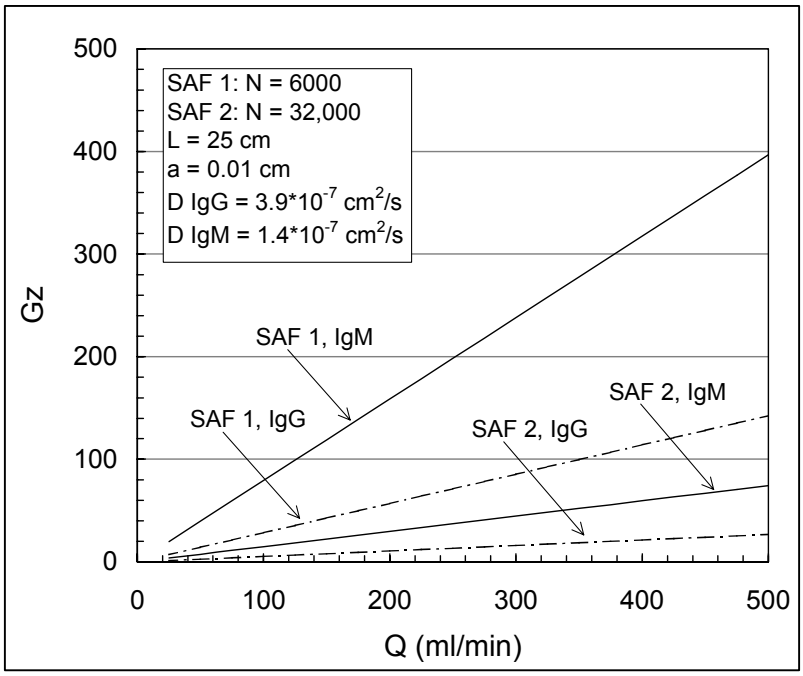

Figure 4-5 Graetz numbers for IgG and IgM antibodies for flow through 2 SAFs containing the smallest (SAF 1) and largest (SAF 2) number of fibers expected for clinical SAFs.

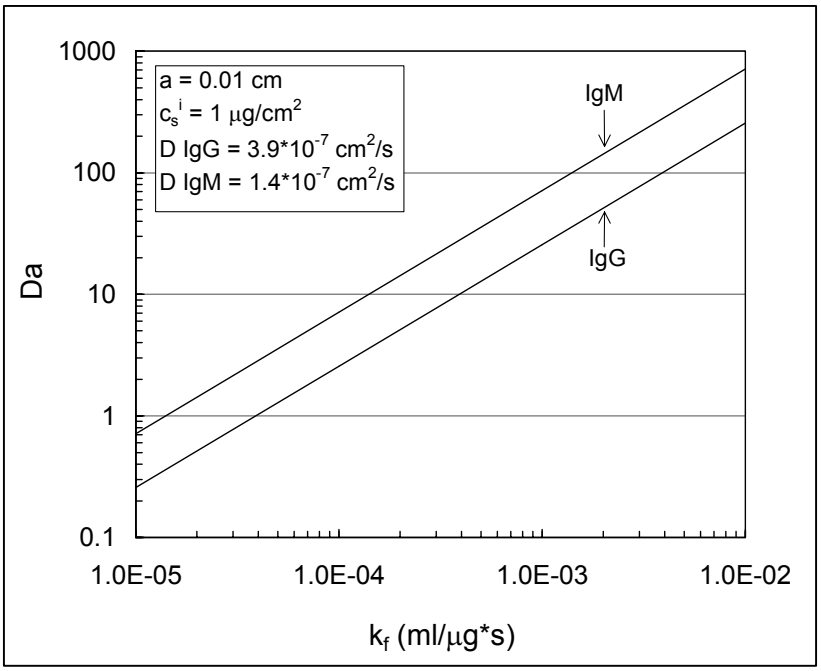

Figure 4-6 Damköhler numbers for SAF-based removal of IgG and IgM antibodies, over the clinically relevant range of antibody/antigen association rate constants.

The dimensionless forms of the centerline and inlet boundary conditions are straightforward:

$$\frac{\partial c^*}{\partial r^*} = 0 \text{ at } r^* = 0 \qquad \textbf{(4-3a)}$$

$$c^* = 1 \text{ at } z^* = 0 \qquad \textbf{(4-4a)}$$

The equation for the dimensionless bound antibody concentration involves the Graetz number and the ratio of the mass of free antibodies in one fiber volume ($V_f c_i$) to the mass of antibody-binding sites on the wall of one fiber ($SA_f c_s^{\,i}$);

$$c_b^* = \frac{2\pi}{Gz}\frac{V_f c_i}{SA_f c_s^{\,i}}\int_0^{t^*} -\frac{\partial c^*}{\partial r^*}(r^* = 1)dt^* \qquad \textbf{(4-5a)}$$

where V_f (ml) and SA_f (cm^2) are the lumenal volume and surface area of a single SAF fiber, respectively. Thus c_b* rises slowly with time if the mass of antibody-binding sites on the fiber is large compared to the mass of antibodies in the antibody solution. Also, c_b* rises slowly with

time if Gz is large, since $\partial c^*/\partial z^*$ is small for large Gz and most of the antibodies that enter the SAF leave without binding to antigen.

4.5 Numerical Solution for Small c_b^*

We used FlexPDE (PDE Solutions, Inc., Antioch, CA), a finite element-based partial differential equation solver, to obtain numerical solutions for $c^*(r^*, z^*)$ for any combination of Da and Gz and for c_b^* near zero (i.e. far from saturation of the SAF). We then calculated the "mixing cup" antibody concentration at the SAF outlet, c_o (μg/ml) (*122*):

$$c_o = c_i \int_0^1 c^*(1-r^{*2})r^* dr^* / \int_0^1 (1-r^{*2})r^* dr^* \qquad \textbf{(4-6)}$$

Finally we determined the antibody removal rate R (μg/min) ($R = Q(c_i - c_o)$) and the antibody clearance K (ml/min) ($K = R/c_i = Q(1 - c_o/c_i)$). The clearance represents the volume of antibody solution completely depleted of antibodies per unit time, and is a more useful indicator of SAF performance than the antibody removal rate since the clearance depends only on the percent reduction in antibody concentration accomplished by the SAF, and is independent of the actual antibody concentration levels in the blood (*130*). For c_b^* near zero (i.e. far from saturation of the SAF), the mass conservation equation and the boundary conditions are linear with respect to the free antibody concentration, and hence c_o is linearly proportional to c_i and the clearance is independent of c_i.

4.6 Analytical Solutions for Large and Small Da and Small c_b^*

We obtained analytical solutions for $c^*(r^*, z^*)$, c_o/c_i, and K for large and small Damköhler numbers and for c_b^* near zero (i.e. far from saturation of the SAF). As Da

approaches infinity, the left side of equation **(4-2a)** approaches zero and the wall boundary condition can be simplified:

$$c^* = \frac{c_b^*}{1 - c_b^*} \frac{K_d}{c_i} \text{ at } r^* = 1, Da \to \infty \qquad \textbf{(4-7)}$$

Thus for large *Da*, antibodies that reach the fiber wall bind "instantaneously" and the free antibody concentration at the fiber wall is equal to the equilibrium free concentration, calculated using the Langmuir adsorption isotherm equation (*107*). For large *Da* and for c_b^* equal to zero, $c^*(1, z^*)$ is equal to zero. With this simplified boundary condition, we calculated $c^*(r^*, z^*)$ and c_o/c_i using the infinite series Graetz solution for radial diffusion in a circular tube with constant wall concentration (*131*). The solution in this limiting case ($Da \to \infty$) was designated the diffusion-limited solution, since the antibody removal rate was determined by the diffusion rate and was independent of the binding rate. The expressions for $c^*(r^*, z^*)$ and c_o/c_i, and the needed eigenvalues, eigenfunctions, coefficients, and derivatives, are presented in Skelland (*131*).

As *Da* approaches zero, $\partial c^*/\partial r^*$ approaches zero throughout the fiber lumen (equation **(4-2a)**). In this case we treated the antibody-antigen binding as a homogeneous reaction:

$$\frac{dc^*}{dz^*} = \frac{-2\pi Da}{Gz}\left(c^* - c_b^*\left(c^* + \frac{K_d}{c_i}\right)\right) \qquad \textbf{(4-8)}$$

The solution for c_o/c_i was straightforward:

$$\frac{c_o}{c_i} = \exp\left(\frac{-2\pi Da}{Gz}\right) \text{ for } c_b^* = 0, Da \to 0 \qquad \textbf{(4-9)}$$

The solution in this limiting case ($Da \to 0$) was designated the reaction-limited solution, since the antibody removal rate was determined by the antibody-binding rate and was independent of the diffusion rate (note that *Da/Gz* is independent of *D*).

4.7 Model Predictions

4.7.1 Dimensionless Free Antibody Concentration Profiles

Figure 4-7 shows the dimensionless free antibody concentration profiles at the SAF fiber outlet for Damköhler numbers between 0.1 and 100, and for reaction-limited and diffusion-limited antibody transport. In each simulation the Graetz number is equal to 12.5 and c_b* is equal to zero. The numerically generated concentration profiles for finite *Da* approach the analytically generated diffusion-limited and reaction-limited profiles for large and small Damköhler numbers, respectively. In each profile, except the reaction-limited profile, the dimensionless antibody concentration is highest at the fiber centerline and lowest at the fiber wall due to binding of free antibodies at the wall. The diffusion-limited profile is the sharpest, with the dimensionless outlet concentration decreasing from about 0.6 at the fiber centerline to zero at the fiber wall. The profiles flatten with decreasing Damköhler number, and for reaction-limited antibody transport the dimensionless outlet concentration is about 0.95 at all radial positions (*Da* = 0.1).

4.7.2 Dependence of the Dimensionless Clearance on the Damköhler Number

Figure 4-8 shows the dependence of the dimensionless clearance (*K/Q*) on the Damköhler number, for Graetz numbers of 12.5, 25.1, and 50.2. In each simulation c_b* is equal to zero. Recall that the clearance represents the volume of antibody solution completely depleted of antibodies per unit time. Hence the dimensionless clearance represents the fraction of the antibody solution flow completely depleted of antibodies, and equals one if the antibody concentration at the SAF outlet equals zero. **Figure 4-8** reveals the approximate boundaries of three antibody transport regimes, defined by the magnitude of the Damköhler number: reaction-

limited ($Da \leq 0.1$), intermediate ($0.1 < Da < 10$), and diffusion-limited ($Da \geq 10$). The dimensionless clearance is very low (< 0.05) in the reaction-limited regime. In the intermediate regime, the dimensionless clearance is higher (up to 0.6 at Gz equal to 12.5 and Da equal to 10) and increases substantially with increasing Damköhler number. The dimensionless clearance is highest in the diffusion-limited regime and no longer increases with increasing Damköhler number. As expected, at all Damköhler numbers the dimensionless clearance decreases with increasing Graetz number.

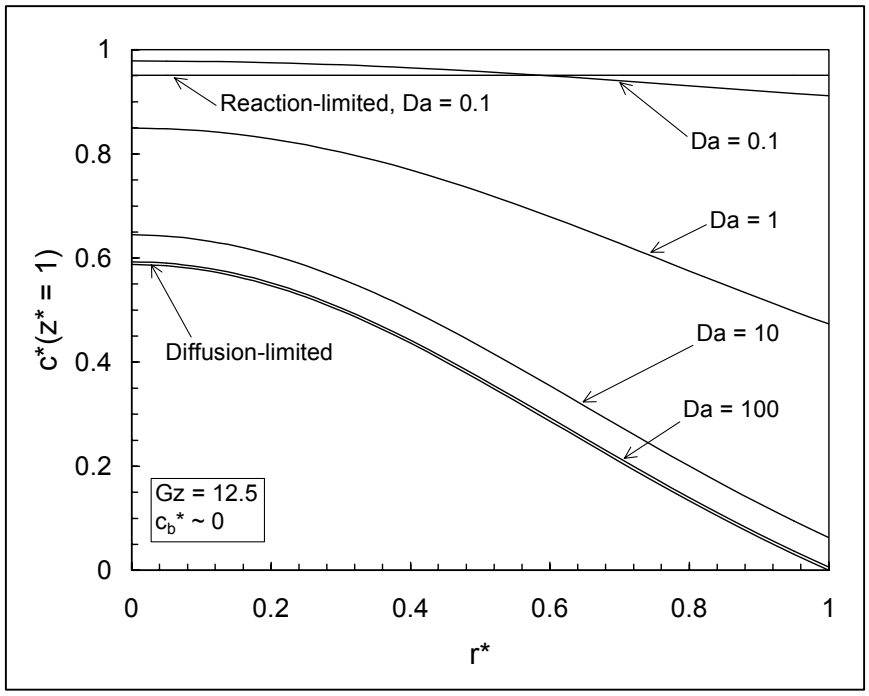

Figure 4-7 Dimensionless antibody concentration profiles within a SAF fiber at the fiber outlet, for Damköhler numbers between 0.1 and 100 and for diffusion-limited and reaction-limited antibody transport. The Graetz number is 12.5 and the dimensionless concentration of bound antibodies is near zero.

4.7.3 Dependence of Dimensionless Clearance on the Graetz Number

Figure 4-9 shows the dimensionless clearance, relative to the dimensionless clearance at Graetz number equal to 10, as a function of the Graetz number. In each simulation c_b* is equal to

zero. The dimensionless clearance is shown in normalized form to allow visual comparison of the simulations at different Damköhler numbers. As also shown in **Figure 4-8**, the dimensionless clearance decreases with increasing Graetz number at all Damköhler numbers; however, the rate at which the dimensionless clearance decreases with increasing Graetz number is slowest for diffusion-limited transport. For *Da* equal to one, increasing the Graetz number from 10 to 50 causes a 74% reduction in *K/Q*, while for diffusion-limited transport, the same increase in *Gz* causes only a 56% reduction in *K/Q*.

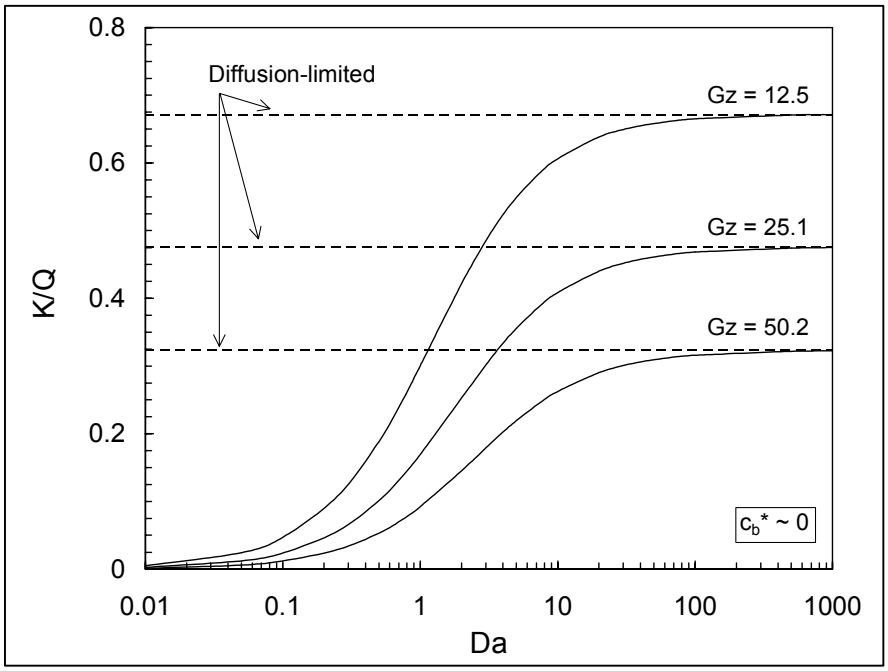

Figure 4-8 Dependence of the dimensionless clearance (*K/Q*) on the Damköhler number (*Da*), for Graetz numbers (*Gz*) equal to 12.5, 25.1, and 50.2. Dashed lines indicate the dimensionless clearance for diffusion-limited antibody transport at each Graetz number. The dimensionless concentration of bound antibodies is near zero.

4.7.4 Dependence of Clearance on the Antibody Solution Flow Rate

The increase in clearance with increasing antibody solution flow rate is greatest for diffusion-limited antibody transport (**Figure 4-10**), since the decrease in dimensionless clearance

with increasing flow rate (and Graetz number) is least for diffusion-limited transport (as explained above). For a SAF with the same geometry as the prototypes used in our *in vitro* studies (Chapter 5.0), increasing the flow rate from 50 to 100 ml/min increases the clearance from 15.0 to 17.0 ml/min (12.5%) when *Da* is equal to one, and from 33.6 to 47.6 ml/min (34%) when the transport is diffusion-limited. Therefore diffusion-limited antibody transport is doubly advantageous, producing the highest clearance at a given flow rate and the greatest increase in clearance when the flow rate is raised.

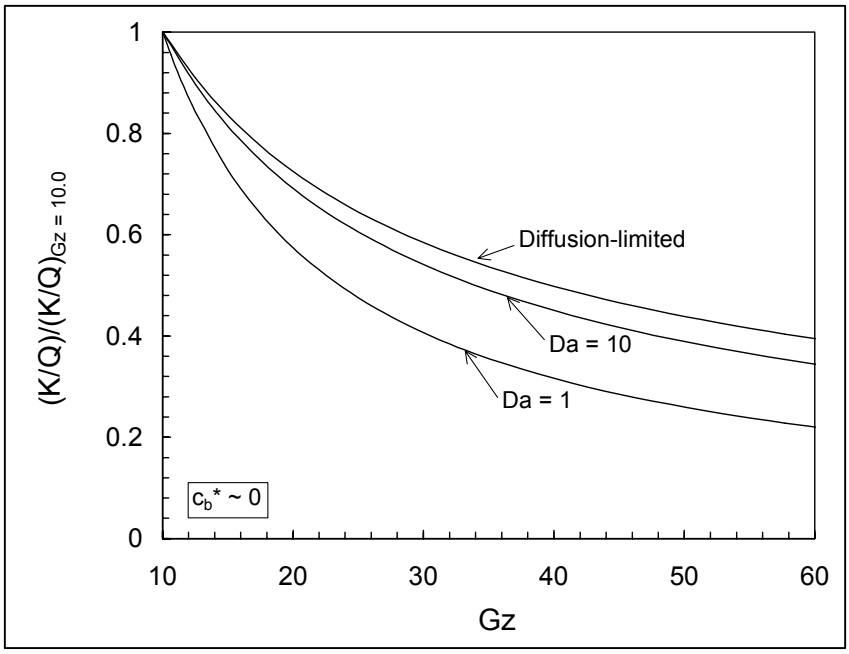

Figure 4-9 Dependence of the dimensionless clearance (*K/Q*), relative to the dimensionless clearance at Graetz number (*Gz*) equal to 10, on Graetz number, for Damköhler numbers of 1 and 10 and for diffusion-limited antibody transport. The dimensionless concentration of bound antibodies is near zero.

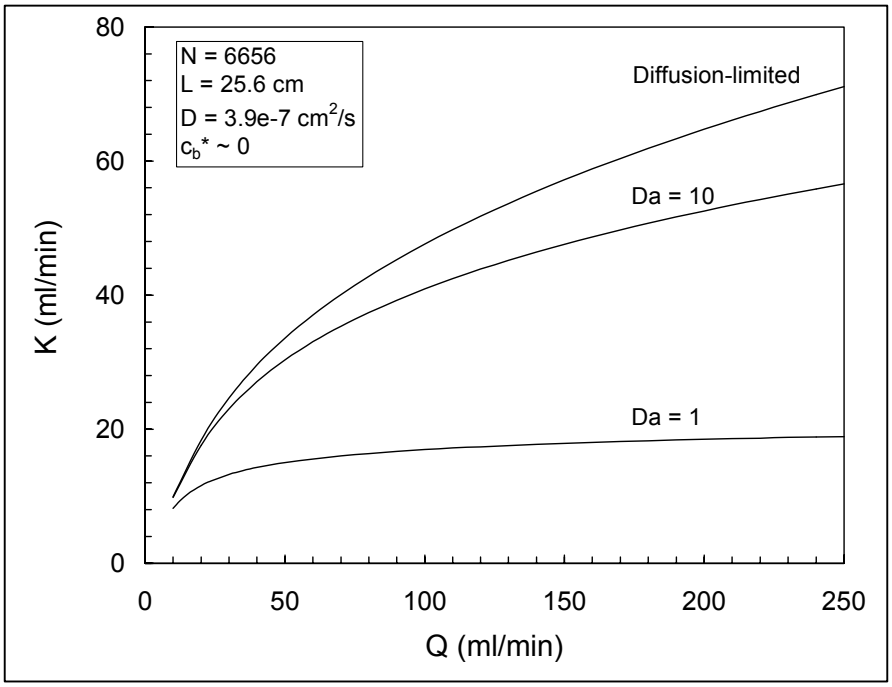

Figure 4-10 Dependence of clearance (K) on antibody solution flow rate (Q), for Damköhler numbers (Da) of 1 and 10 and for diffusion-limited antibody transport. The SAF geometry is identical to the geometry of the SAF prototypes used for the *in vitro* experiments reported in Chapter 5.0. The dimensionless concentration of bound antibodies is near zero.

4.8 Discussion

Our transport model revealed three antibody transport regimes, defined by the magnitude of the Damköhler number Da: reaction-limited ($Da \leq 0.1$), intermediate ($0.1 < Da < 10$), and diffusion-limited ($Da \geq 10$). For a given SAF geometry, blood flow rate, and antibody diffusivity, the highest antibody clearance, and hence the highest antibody removal rate, is predicted for diffusion-limited antibody transport. In each regime, the antibody clearance increases with increasing blood flow rate. However, the greatest percent increase in clearance accomplished by raising the blood flow rate occurs when the antibody transport is diffusion-limited. At a given blood flow rate, the clearance for diffusion-limited antibody transport can be increased even further by using a SAF with more fibers (i.e. decreasing the Graetz number at the

same blood flow rate). Diffusion-limited antibody transport in the SAF fibers may be achievable for medium to high affinity IgG antibodies (k_f >5*10^{-4} ml/μg*s) and IgM antibodies (k_f >2*10^{-4} ml/μg*s), if the SAF fibers have enough antibody-binding sites to obtain near monolayer coverage of bound antibodies at saturation (**Figure 4-6**).

The above insights suggest a unified approach to the design of SAF modules for clinical applications:

1. Optimize the form of the antigen (i.e. natural or synthetic, with or without a spacer molecule), and the method for immobilizing the antigen on the inner fiber walls, to obtain the highest possible antibody-binding capacity and hence to maximize the chances of achieving diffusion-limited antibody transport.
2. Use the highest possible blood flow rate, within the limits of biocompatibility and patient stability.
3. Use a SAF with the largest possible number of fibers possible, within the limits of biocompatibility and cost.

5.0 IN VITRO MEASUREMENT OF THE SAF-BASED ANTIBODY REMOVAL RATE IN A MODEL ANTIBODY/ANTIGEN SYSTEM

As discussed in Chapter 4.0, antibody transport in the SAF fibers may be primarily controlled by the rate of antibody-antigen binding (reaction-limited transport) or by the rate of radial antibody diffusion (diffusion-limited transport), or both rates may be important (intermediate transport). For a given SAF geometry, blood flow rate, and antibody diffusivity, the antibody removal rate is highest when the antibody transport is diffusion-limited. Additionally, when diffusion-limited antibody transport is achieved, the antibody removal rate is independent of the antibody-binding rate and hence is the same for any antibody/antigen system and for any patient within one antibody/antigen system. In this chapter, we describe a series of *in vitro* antibody removal experiments performed to determine whether diffusion-limited antibody transport is achieved in SAF prototypes containing immobilized protein-based antigens. The *in vitro* antibody removal experiments were performed using a model antibody/antigen system instead of a human disease-related system, to eliminate the need for a human source of antibodies and to allow all of the experiments to be performed using antibodies and antigens from single lots. We chose bovine serum albumin (BSA) as our model antigen, since BSA is a large molecular weight protein (*132*) like the ligands used in immunoadsorption columns (such as protein A and anti-human immunoglobulin), is inexpensive and non-toxic, and can be immobilized on cellulose-based SAF fibers using conventional protein immobilization methods. We used polyclonal anti-BSA antibodies as our model antibodies, and compared both the

magnitudes and the parameter-dependencies of the measured anti-BSA removal rates to the predictions of our mathematical model.

5.1 Methods

5.1.1 SAF Fabrication

Gambro (Lakewood, CO) 500 HG hemodialyzers were used as SAF modules. The modules contained approximately 6656 Hemophan® fibers of 0.02 cm nominal inner diameter and 25.6 cm length, providing a blood-contacting surface area of 1.1 m^2 (*100*). Bovine albumin (BSA) (Sigma Chemical Co., St. Louis, MO) or human albumin (HSA) (Alpine Biologics Inc., Orangeburg, NY) was immobilized on the lumenal surfaces of the fibers using a modified version of the cyanogen bromide activation method developed by Axen *et al* (*119*). Unless otherwise noted, chemicals were obtained from Sigma Chemical Company (St. Louis, MO). During the following fiber activation steps, the blood and shell compartments of the SAF module were connected in series using tygon tubing. Both compartments of the module were first rinsed copiously with de-ionized water. To swell the fibers, 3.5 L of 0.2 N NaOH was circulated through the module for four hours, on ice, at 136 ml/min. The module was flushed with 3.5 L of 0.1 M sodium bicarbonate buffer/0.5 M NaCl, pH 8.3 (henceforth called bicarbonate buffer), at 225 ml/min and at 4 ˚C. An activating solution of 25 g CNBr in 250 ml of 0.2 N NaOH was circulated through both compartments at 136 ml/min, on ice, for 1.5 hours. The activating solution pH was kept above 11.0 by the addition of cold 10 N NaOH. The module was flushed with 3.5 L of de-ionized water and 3.5 L of bicarbonate buffer, at 225 ml/min and at 4 ˚C. Excess fluid was removed from the module using filtered compressed air.

The shell compartment was then filled with bicarbonate buffer and closed. One hundred ml of 20-mg/ml antigen solution (BSA, HSA, or a mixture of BSA and HSA, dissolved in bicarbonate buffer) was circulated through the blood compartment at 77 ml/min, at room temperature, overnight (at least 12 hours). Both compartments were drained, and the mechanical integrity of the fibers and the seal separating the blood and shell compartments was verified by checking for antigen in the buffer drained from the shell compartment. The blood and shell compartments were again connected in series and the SAF was washed four times, by circulating 500 ml of bicarbonate buffer through the SAF at 136 ml/min for one hour (each wash). Un-reacted active sites on the fibers were capped by circulating 250 ml of 1 M ethanolamine, pH 8.3, through the SAF at 77 ml/min for two hours. The SAF was flushed with 3.5 L of bicarbonate buffer (at 225 ml/min), 2 L of 0.1 M glycine, pH 2.5 (at 77 ml/min), and 7 L of phosphate-buffered saline (PBS) (137 mM NaCl/2.7 mM KCl/10 mM Na_2HPO_4/1.76 mM KH_2PO_4), pH 7.4 (at 225 ml/min). Finally, 3.5 L of PBS was circulated through the SAF at 136 ml/min overnight (at least 12 hours). Excess fluid was removed from the SAF using filtered compressed air, and the SAF was stored at 4 ˚C until use.

5.1.2 Antibody Solution Preparation

Affinity purified, polyclonal sheep anti-BSA antibodies of IgG isotype were obtained from Bethyl Laboratories, Inc. (Montgomery, TX). The antibodies were supplied as a 1-mg/ml stock solution in PBS/0.1% NaN_3, and stored at 4 ˚C until use. For each antibody removal experiment, an appropriate volume of stock solution was added to PBS, pH 7.4, to obtain the desired concentration and volume of anti-BSA solution. All antibodies used were from the same lot.

5.1.3 Antibody Concentration Measurement

An in-house enzyme-linked immunosorbent assay (ELISA) (*133*) was used to measure the anti-BSA concentrations of samples collected during each experiment. Anti-BSA standards with concentrations between 2 and 40 ng/ml were prepared for construction of a reference curve. Each of the following solutions was added to the plate at 100 μl/well. Ten μg/ml BSA in 0.1 M sodium carbonate buffer, pH 9.6, was added to each well of a high-binding Costar 96-well EIA plate (Fisher Scientific, Pittsburgh, PA) and the plate was incubated at 37 ˚C for 1 hour. The plate was washed 5 times with 10 mM tris/100 mM NaCl/0.05% Tween 20, pH 7.4. The anti-BSA samples to be assayed (diluted appropriately in PBS/0.05% Tween 20, pH 7.4) and the anti-BSA standards were added to the plate in duplicate, and the plate was incubated for 1 hour at 37 ˚C and washed 5 times. Horseradish peroxidase-conjugated anti-sheep IgG antibodies (Bethyl Laboratories, Inc., Montgomery, TX), diluted to 1 μg/ml in PBS/0.05% Tween 20, pH 7.4, were added to the plate, and the plate was incubated for 1 hour at room temperature and washed 6 times. TMB peroxidase substrate (KPL, Gaithersburg, MD) was added to the plate, and the plate was incubated for 15 minutes at 37 ˚C. Finally, 1 M phosphoric acid was added to the plate, and the optical density of each well was measured at 450 nm using a microplate reader (Molecular Devices, Sunnyvale, CA). The concentration of each test sample was calculated by comparison to the reference curve.

5.1.4 Adsorption Isotherm Experiments

The adsorption isotherm for binding of anti-BSA antibodies to immobilized BSA was measured by incubating samples of Hemophan® fibers, with BSA immobilized on the outer surfaces of the fibers, in anti-BSA solutions of varying concentrations. Bovine serum albumin

(BSA) was immobilized on the outer surfaces of the fibers comprising a Gambro 500 HG hemodialyzer using a modified version of the cyanogen bromide activation method developed by Axen *et al* (*119*). The immobilization was performed as described above (**5.1.1**), except that the 20-mg/ml antigen solution was circulated through the shell compartment (instead of the blood compartment) after the fiber activation steps. The SAF was disassembled and the fibers were carefully extracted from the housing. Anti-BSA solutions at concentrations of 0.5, 1, 5, 10, 15, and 20 μg/ml were prepared using PBS/0.05% Tween 20, pH 7.4, as the diluent. For each anti-BSA solution, 3 ml was placed in a 12 x 75 mm disposable glass test tube containing 200 Hemophan®/BSA fibers of 2 cm length, and 3 ml of was placed in a second test tube containing 200 un-modified Hemophan® fibers of 2 cm length. The tubes were capped and rocked gently for 6 hours at room temperature, and the anti-BSA concentration in the supernatant of each tube was measured using the ELISA described above (**5.1.3**). The bound antibody concentration was calculated by multiplying the difference between the initial and final anti-BSA concentrations by the antibody solution volume (3 ml) divided by the fiber surface area (27 cm^2). The data was fit to the Langmuir adsorption isotherm equation (equation **(2-1)**) using a non-linear regression tool in Matlab (The Mathworks, Inc., Natick, MA), and the antibody-binding capacity (c_s^i) and the equilibrium dissociation constant (K_d) were determined.

5.1.5 In Vitro Perfusion System

In vitro antibody removal experiments were performed using the simple perfusion system shown in **Figure 5-1**. The system consisted of a glass antibody solution reservoir, a Masterflex peristaltic pump (Cole-Parmer Instrument Company, Vernon Hills, IL), a glass bead flow meter (Cole-Parmer Instrument Company), a SAF, and a sampling port at the SAF outlet. The components were connected using tygon tubing. The shell compartment of the SAF was filled

with PBS and closed, and the antibody solution was pumped solely through the blood compartment. The entire perfusion system, except the reservoir, was de-aired and primed with PBS prior to the antibody removal experiment. At the start of the experiment the reservoir was filled with anti-BSA solution and the solution was pumped through the blood compartment of the SAF at the prescribed flow rate.

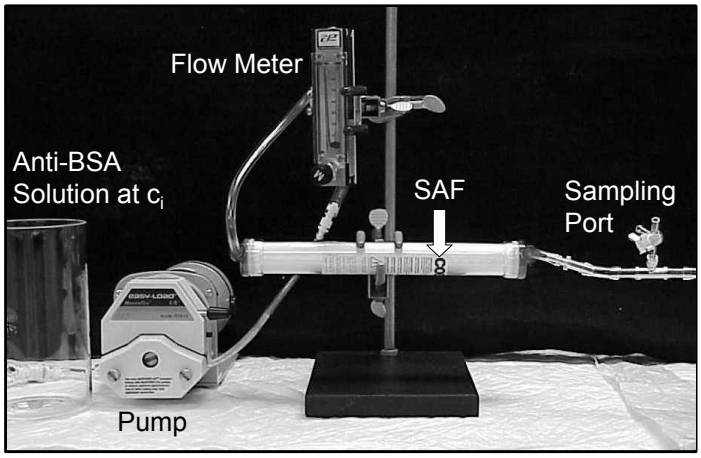

Figure 5-1 Perfusion system for *in vitro* antibody removal experiments.

5.1.6 In Vitro Antibody Removal Experiments

During each antibody removal experiment, approximately one L of antibody solution was pumped through a freshly fabricated SAF in single pass mode at constant flow rate. (A control SAF with immobilized HSA was the only SAF used in multiple anti-BSA removal experiments.) Eight 1 ml outlet samples and two inlet samples were collected and assayed for anti-BSA concentration. The clearance was calculated using the mean concentrations of both inlet samples and the second through eighth outlet samples. Negligible rise of the outlet anti-BSA concentration with time verified that c_b* remained near zero during each experiment.

The first series of experiments was performed to determine the dependence of antibody clearance on inlet anti-BSA concentration. Anti-BSA removal experiments were performed at inlet concentrations of 0.5, 1, and 2 μg/ml, at a flow rate of 47 ml/min, using SAFs with immobilized BSA. The chosen anti-BSA inlet concentrations were within the range of specific antibody concentrations reported in the literature (*56,104*). To check for non-specific anti-BSA removal, an experiment was performed using a SAF with immobilized HSA (which does not bind the anti-BSA used, data not shown), at an inlet concentration of one μg/ml and a flow rate of 47 ml/min.

The second series of experiments was performed to determine the dependence of antibody clearance on antibody solution flow rate. An anti-BSA removal experiment was performed at a flow rate of 110 ml/min and an inlet concentration of 2 μg/ml, using a SAF with immobilized BSA, and the measured clearance was compared to the previously measured clearance at 47 ml/min. Again the SAF with immobilized HSA was used to check for non-specific anti-BSA removal at 110 ml/min.

The third series of experiments was performed to determine the dependence of antibody clearance on antibody-binding capacity. To fabricate a SAF with decreased anti-BSA-binding capacity, we used an antigen solution containing 10 mg/ml BSA and 10 mg/ml HSA. Using this SAF, we measured the clearance at an inlet concentration of one μg/ml and a flow rate of 47 ml/min, and compared the measured clearance to that measured for the SAFs with immobilized BSA only.

5.2 Results

5.2.1 Anti-BSA/Immobilized BSA Adsorption Isotherm

The measured anti-BSA binding capacity of the Hemophan®/BSA fibers was 0.92 μg/cm^2, and the equilibrium dissociation constant was 3.1 μg/ml (**Figure 5-2**). The measured anti-BSA binding capacity is reasonable since the approximate surface concentration of a monolayer of IgG molecules is 0.6 μg/cm2 (*101,102*). The measured equilibrium dissociation constant is also reasonable, based on the reported dissociation constants for antibody/antigen systems with either the antibodies or the antigens immobilized (**Table 2-5**) (*1,106,107*).

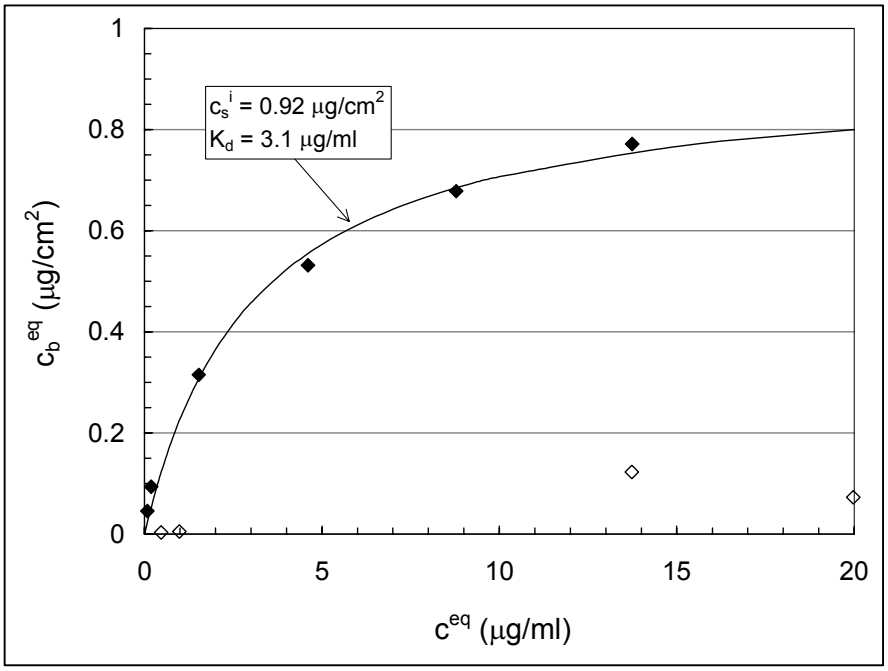

Figure 5-2 Anti-BSA/BSA adsorption isotherm for Hemophan® fibers with BSA immobilized on the outer surfaces of the fibers. Closed symbols: fibers with immobilized BSA. Open symbols: un-modified Hemophan® fibers.

5.2.2 Outlet Anti-BSA Concentration as a Function of Throughput

During each anti-BSA removal experiment, the anti-BSA concentration at the SAF outlet increased sharply with the first 200 ml of throughput (volume of antibody solution perfused through the SAF) as the priming solution was flushed from the perfusion system (**Figure 5-3**). The outlet concentration remained relatively constant for the remainder of the experiment (up to 800 ml throughput), indicating that the increase in bound anti-BSA concentration during the experiment was negligible compared to the anti-BSA-binding capacity of the SAF (i.e. c_b* was near zero throughout the experiment).

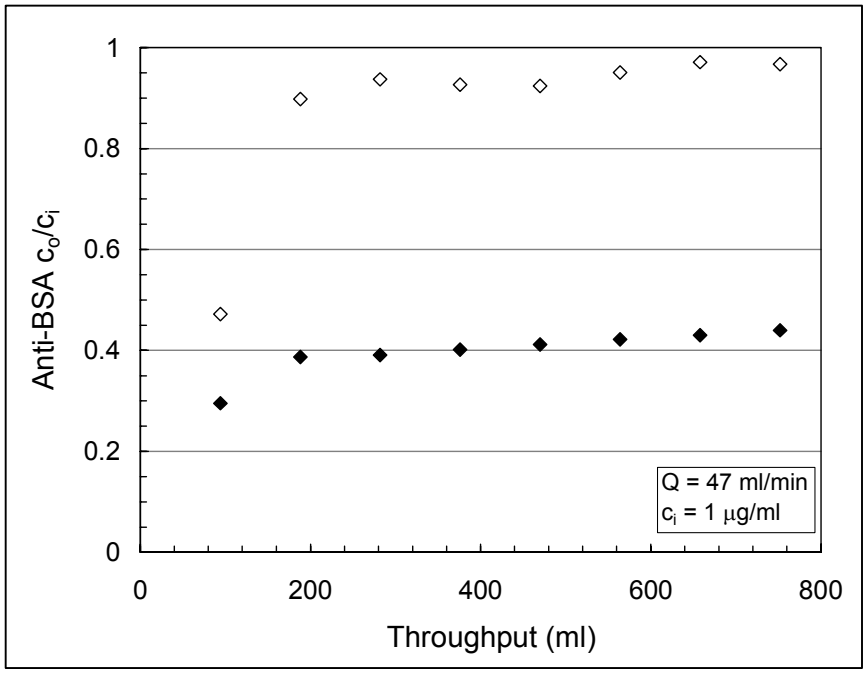

Figure 5-3 Anti-BSA outlet concentration relative to inlet concentration (c_o/c_i) during a typical anti-BSA removal experiment. Throughput is the volume of anti-BSA solution perfused through the SAF. Closed symbols: SAF with immobilized BSA. Open symbols: control SAF with immobilized HSA. Each experiment was performed at an anti-BSA solution flow rate of 47 ml/min and an anti-BSA inlet concentration of one μg/ml.

5.2.3 Dependence of Anti-BSA Clearance on c_i

As expected for c_b* approximately equal to zero, the anti-BSA clearance was independent of anti-BSA inlet concentration for inlet concentrations between 0.5 and 2 μg/ml (**Figure 5-4**). At an anti-BSA solution flow rate of 47 ml/min, the average of the clearances measured at inlet concentrations of 0.5, 1, and 2 μg/ml was 26.3 ml/min, and the non-specific clearance by the control SAF (at an inlet concentration of one μg/ml) was 2.8 ml/min. The measured clearance using the SAFs with immobilized BSA, minus the non-specific clearance, was approximately 73% of the predicted diffusion-limited clearance and was within 2% of the clearance predicted for Damköhler number equal to 3.

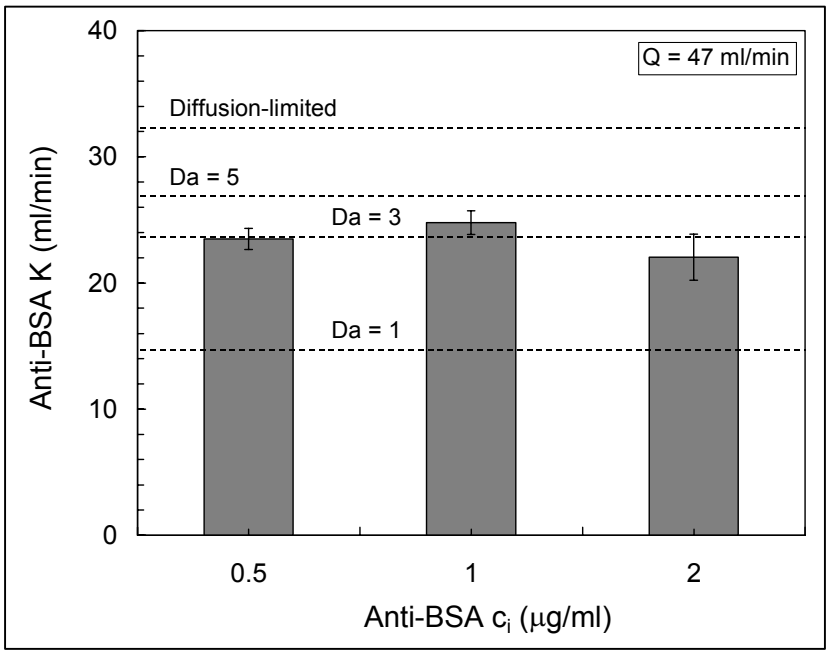

Figure 5-4 Dependence of anti-BSA clearance (K) on anti-BSA inlet concentration (c_i). Each experiment was performed at an anti-BSA solution flow rate of 47 ml/min. Dashed lines indicate the predicted clearances for Damköhler number (Da) equal to 1, 3, and 5, and for diffusion-limited antibody transport.

5.2.4 Dependence of Anti-BSA Clearance on Anti-BSA Solution Flow Rate

Anti-BSA clearance increased to 36.2 ml/min when the anti-BSA solution flow rate was raised to 110 ml/min (**Figure 5-5**). The non-specific clearance by the control SAF was 6.8 ml/min at a flow rate of 110 ml/min. The measured clearance using the SAF with immobilized BSA, minus the non-specific clearance, was approximately 60% of the predicted diffusion-limited clearance and was within 5% of the clearance predicted for Damköhler number equal to 3.

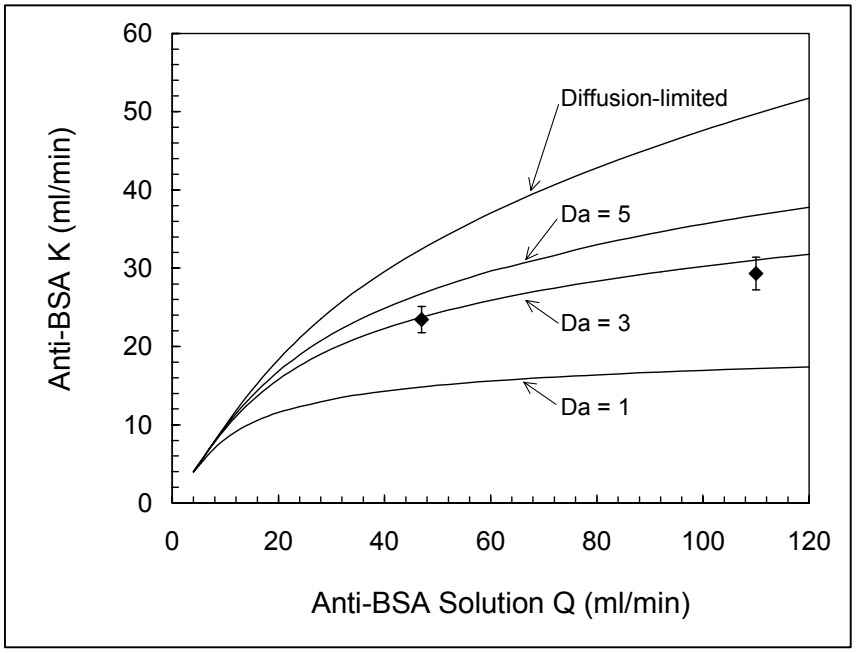

Figure 5-5 Dependence of anti-BSA clearance (*K*) on anti-BSA solution flow rate (*Q*). Simulated dependences of clearance on flow rate, for Damköhler number (*Da*) equal to 1, 3, and 5, and for diffusion-limited antibody transport, are also shown.

5.2.5 Dependence of Anti-BSA Clearance on Antibody-Binding Capacity

At an anti-BSA solution flow rate of 47 ml/min, the anti-BSA clearance decreased to 16.2 ml/min when the anti-BSA-binding capacity decreased by approximately 50% (**Figure 5-6**). The

measured anti-BSA clearance using the SAF with immobilized HSA and BSA, minus the non-specific clearance by the control SAF, was within 10% of the clearance predicted for Damköhler number equal to 1.

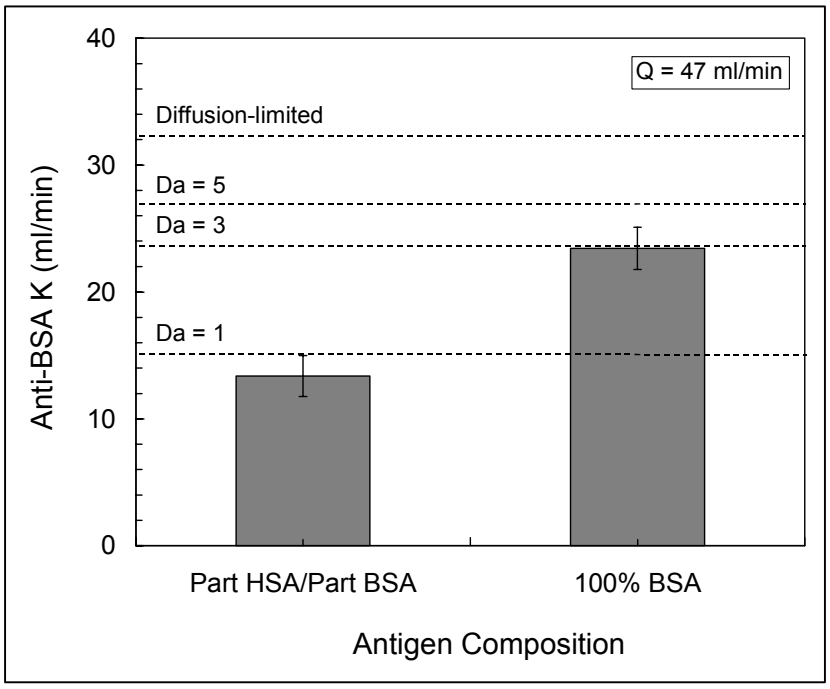

Figure 5-6 Dependence of anti-BSA clearance (K) on antigen composition. Each experiment was performed at an anti-BSA solution flow rate of 47 ml/min. Dashed lines indicate the predicted clearances for Damköhler number (*Da*) equal to 1, 3, and 5, and for diffusion-limited antibody transport.

5.3 Discussion

Transport of anti-BSA antibodies in SAF prototypes with immobilized BSA occurred in the intermediate regime, at a Damköhler number approximately equal to 3, and hence both the anti-BSA-binding rate and the radial anti-BSA diffusion rate were important determinants of the anti-BSA removal rate. At anti-BSA solution flow rates of 47 and 110 ml/min, we found close agreement between the measured anti-BSA clearances and the model-predicted clearances for Damköhler number equal to 3. Additionally, the anti-BSA clearance was highly dependent on

the anti-BSA-binding capacity of the SAF, as expected for antibody transport in the intermediate regime. Based on our initial estimates of the expected Damköhler number for SAF-based IgG removal, we expected the anti-BSA transport in the SAF prototypes to be diffusion-limited. Several factors may have contributed to the low Damköhler number achieved in our model system. In our SAF prototypes, BSA was immobilized on the fibers via accessible primary amines on the BSA. Since BSA contains 59 primary amine-containing lysine residues (*132*), of which about 30-35 are on the surface and available as immobilization points (*134*), the population of immobilized BSA was heterogeneous and a fraction of the BSA may have been unable to bind anti-BSA. Additionally, immobilization of the BSA may have reduced the intrinsic anti-BSA/BSA association rate constant and produced a low affinity antibody-antigen system. Finally, the anti-BSA population used may have had a low intrinsic affinity for BSA. Several antigens used for immunoadsorption are available in synthetic form, and can be immobilized via spacer molecules to ensure that most of the epitopes are accessible to the antibodies (*89,91*). SAFs containing these antigens may have antibody-binding capacities high enough to produce diffusion-limited transport of medium and high affinity antibodies. During development of SAFs for clinical use, equilibrium antibody-binding experiments must be performed to measure the antibody-binding capacity of the SAF fibers and ensure that the immobilization method is optimal.

Our antibody transport model can be used to determine the SAF-based antibody removal rate if the SAF geometry, blood flow rate, antibody diffusivity, and antibody-binding rate are known. The model can also be used to help assess how close a given system is to achieving diffusion-limited antibody transport. For example, if the anti-BSA/BSA system were a system of clinical relevance, we would continue the SAF prototype development with the goal of tripling

the anti-BSA-binding capacity of the SAF fibers and increasing the Damköhler number to 9. Further development to increase the Damköhler number past 9 or 10 would be unwarranted, since the model predicts little enhancement in clearance obtained by raising the Damköhler number above 10.

Our transport model does not account for the inherent heterogeneity of polyclonal antibodies. As antibody populations do not display a Gaussian distribution of affinities *in vivo* (*23*), appropriate mathematical representation of antibody heterogeneity is difficult and requires extensive knowledge of the antibody/antigen system being studied. Use of an "average" value for k_f may over-predict the clearance since the clearance depends non-linearly on k_f (i.e. the slow clearance of low affinity antibodies is not balanced by the fast clearance of high affinity antibodies).

SAF antibody clearance from flowing whole blood may be higher than clearance from plasma or buffer due to enhancement of the antibody diffusivity in flowing blood compared to the diffusivity in flowing cell-free solutions. At a shear rate of 500 s^{-1}, the IgG diffusivity in flowing human blood may be about 6 times its magnitude in stationary blood or about three times its magnitude in water (*135*). Transport of buffer-dissolved anti-BSA antibodies in our SAF prototypes with immobilized BSA occurred at a Damköhler number approximately equal to 3, and we estimate that $k_f c_s^i$ was approximately equal to $5.9*10^{-5}$ cm/s in that system (D equal to $3.9*10^{-7}$ cm^2/s). At a blood flow rate of 110 cm^3/min, using a SAF with the same geometry as the prototypes used in our *in vitro* studies and the same magnitude for $k_f c_s^i$, the predicted antibody clearance increases from 31 to 42 ml/min when the antibody diffusivity increases from $3.9*10^{-7}$ to $11.7*10^{-7}$ cm^2/s. Under the same conditions, the predicted clearance for diffusion-limited antibody transport increases from 50 to 71 ml/min. The higher percent increase in clearance for

diffusion-limited antibody transport, compared to the increase for intermediate antibody transport, reflects the greater dependence of clearance on the antibody diffusion rate in the diffusion-limited regime.

A single compartment pharmacokinetic model is typically used to describe the drop in the pathogenic antibody concentration in the patient's blood volume during an antibody removal session (*136*):

$$V\frac{dc_{bl}}{dt} = -Kc_{bl} \qquad \textbf{(5-1)}$$

where V is the blood volume (cm^3) and c_{bl} is the patient's blood antibody concentration ($\mu g/cm^3$). If the clearance is constant throughout the antibody removal session, the antibody concentration decays exponentially with time, with a time constant equal to V/K. For a clearance of 29.4 ml/min, at a blood flow rate of 110 ml/min (as achieved with our SAFs with immobilized BSA), the time constant for treatment of a 5 L blood volume is 170 minutes or 2.8 hours. For diffusion-limited transport at the same blood flow rate, the time constant is 101 minutes or 1.7 hours. In practice, the clearance will decrease as the concentration of bound antibodies becomes non-negligible compared to the capacity of the SAF (i.e. as c_b* becomes non-negligible). To limit this reduction, the SAF must contain an abundance of antibody-binding sites compared to the mass of pathogenic antibodies in the patient's blood at the beginning of the antibody removal session. Alternatively, two SAFs can be simultaneously employed during each removal session, with one SAF removing antibodies while the other is undergoing antibody elution and regeneration. This strategy is currently employed for IgG removal using the Excorim protein A columns (*3*).

6.0 CONCLUSIONS

1. Removal of anti-A and anti-B antibodies from whole human blood using SAFs containing immobilized protein-based A and B antigens is feasible, and may be preferable to the non-selective or semi-selective anti-A and anti-B removal methods that are currently available.

2. Antibody transport in the SAF fibers may be primarily controlled by the rate of antibody-antigen binding (reaction-limited transport) or by the rate of radial antibody diffusion (diffusion-limited transport), or both rates may be important (intermediate transport). For a given SAF geometry, blood flow rate, and antibody diffusivity, the antibody removal rate is highest when the antibody transport is diffusion-limited. Additionally, when diffusion-limited antibody transport is achieved, the antibody removal rate is independent of the antibody-binding rate and hence is the same for any antibody/antigen system and for any patient within one antibody/antigen system.

3. Transport of anti-BSA antibodies in SAF prototypes with immobilized BSA occurred in the intermediate regime, at a Damköhler number approximately equal to 3, and hence both the anti-BSA-binding rate and the radial anti-BSA diffusion rate were important determinants of the anti-BSA removal rate. Based on our initial estimates of the expected Damköhler number for SAF-based IgG removal, we expected the anti-BSA transport in the SAF prototypes to be diffusion-limited. Several factors may have contributed to the low Damköhler number achieved in our model system, including randomly-oriented immobilization of the BSA.

4. Initial SAF development work should focus on achieving diffusion-limited antibody transport by increasing the SAF antibody-binding capacity. If diffusion-limited transport is achieved, modifications to the SAF geometry and blood flow through the SAF can further increase the antibody removal rate.

APPENDIX A

FlexPDE Script for Numerical Solution of the Antibody Transport Model

```
{*********************************************************************
 This program simulates steady state antibody removal by a hollow fiber-based SAF.
 Blood is perfused through the SAF at constant inlet concentration and constant
 flow rate. The dimensionless outlet antibody concentration, dimensionless antibody
 clearance, and dimensional clearance are determined as functions of the Damkohler
 number and the Graetz number.
*********************************************************************}
title "Antibody Removal by SAF"
coordinates
        xcylinder(z,r)
                        { r = dimensionless radial coordinate, z = dimensionless axial coordinate }
variables
                C               { dimensionless concentration of free antibodies }
definitions
                Q = 47                  { blood flow rate, ml/min }
                a = 0.01        { SAF fiber radius, cm }
                L = 25.6        { SAF fiber length, cm }
                N = 6656        { number of SAF fibers }
```

```
        D = 3.9*10^(-7)
                        { diffusion coefficient of antibodies in blood, cm2/s}
        kfcs = 1.17*10^(-4)
                        { forward binding velocity, cm/s }
        vbar = Q/(60*N*pi*a^2)
                        { average velocity of blood in the SAF, cm/s }
        Gz = pi*vbar*a**2/(L*D)
                        { Graetz number }
            Da = kfcs*a/D
                        { Damkohler number }
            v = 2*(1-r^2)        { dimensionless velocity profile }
        Cout = surf_integral(v*c,"outlet")/surf_integral(v,"outlet")
                        { mean dimensionless concentration at SAF outlet }
            KdivQ = 1 – Cout
                    { dimensionless antibody clearance }
        K = KdivQ*Q
                        { dimensional antibody clearance, ml/min }
equations
        Gz/pi*v*dz(C) = 1/r*dr(r*dr(C))
boundaries
        Region          { define cylinder of radius = 1 centered at 0,0}
        start (1,0)     line to (1,1)

        natural(C) = Da*C
```

```
                    line to (0,1)
        value(C) = 1    line to (0,0)
        natural(C) = 0
                    line to finish
        feature start "outlet" (1,0)
                    line to (1,1)
plots               {show final solution}
        elevation(C) from (1,0) to (1,1)
        elevation(C) from (0,1) to (1,1)
        report Gz report Da report Cout report KdivQ report K
end 34287
```

BIBLIOGRAPHY

(1) Kuby, J. *Immunology*; 3rd ed.; W.H. Freeman: New York, 1997.

(2) Kluth, D. C.; Rees, A. J. Anti-Glomerular Basement Membrane Disease. *J Am Soc Nephrol* **1999**, *10*, 2446-2453.

(3) Benny, W. B.; Sutton, D. M.; Oger, J.; Bril, V.; McAteer, M. J.; Rock, G. Clinical Evaluation of a Staphylococcal Protein a Immunoadsorption System in the Treatment of Myasthenia Gravis Patients. *Transfusion* **1999**, *39*, 682-687.

(4) Knobl, P.; Derfler, K. Extracorporeal Immunoadsorption for the Treatment of Haemophilic Patients with Inhibitors to Factor Viii or Ix. *Vox Sang* **1999**, *77 Suppl 1*, 57-64.

(5) Snyder, H. W., Jr.; Cochran, S. K.; Balint, J. P., Jr.; Bertram, J. H.; Mittelman, A.; Guthrie, T. H., Jr.; Jones, F. R. Experience with Protein a-Immunoadsorption in Treatment-Resistant Adult Immune Thrombocytopenic Purpura. *Blood* **1992**, *79*, 2237-2245.

(6) Tanabe, K.; Takahashi, K.; Sonda, K.; Tokumoto, T.; Ishikawa, N.; Kawai, T.; Fuchinoue, S.; Oshima, T.; Yagisawa, T.; Nakazawa, H.; Goya, N.; Koga, S.; Kawaguchi, H.; Ito, K.; Toma, H.; Agishi, T.; Ota, K. Long-Term Results of Abo-Incompatible Living Kidney Transplantation - a Single-Center Experience. *Transplantation* **1998**, *65*, 224-228.

(7) Cooper, D. K.; Human, P. A.; Lexer, G.; Rose, A. G.; Rees, J.; Keraan, M.; Du Toit, E. Effects of Cyclosporine and Antibody Adsorption on Pig Cardiac Xenograft Survival in the Baboon. *J Heart Transplant* **1988**, *7*, 238-246.

(8) Xu, Y.; Lorf, T.; Sablinski, T.; Gianello, P.; Bailin, M.; Monroy, R.; Kozlowski, T.; Awwad, M.; Cooper, D. K. C.; Sachs, D. H. Removal of Anti-Porcine Natural Antibodies from Human and Nonhuman Primate Plasma in Vitro and in Vivo by a Gal Alpha 1-3gal Beta 1-4 Beta Glc-X Immunoaffinity Column. *Transplantation* **1998**, *65*, 172-179.

(9) Madore, F. Plasmapheresis. Technical Aspects and Indications. *Crit Care Clin* **2002**, *18*, 375-392.

(10) Matic, G.; Bosch, T.; Ramlow, W. Background and Indications for Protein a-Based Extracorporeal Immunoadsorption. *Ther Apher* **2001**, *5*, 394-403.

(11) Nydegger, U. E.; Rieben, R.; Mohacsi, P. Current Precision of Immunological Extracorporeal Plasma Treatment. *Transfus Apheresis Sci* **2001**, *24*, 39-47.

(12) Braun, N.; Bosch, T. Immunoadsorption, Current Status and Future Developments. *Expert Opin Investig Drugs* **2000**, *9*, 2017-2038.

(13) Bertram, J. H.; Jones, F. R.; Balint, J. P., Jr. Protein a Immunoadsorption. *Clin Immunother* **1996**, *6*, 211-227.

(14) Hout, M. S.; LeJeune, K. E.; Schaack, T. M.; Bristow, D. K.; Federspiel, W. J. Specific Removal of Anti-a and Anti-B Antibodies by Using Modified Dialysis Filters. *Asaio J* **2000**, *46*, 702-706.

(15) Hout, M. S.; Federspiel, W. J. Mathematical and Experimental Analyses of Antibody Transport in Hollow Fiber-Based Specific Antibody Filters. *Biotechnol Progr* **2003**, *In Review*.

(16) Singh, P.; Goldman, J.; Jackson, C. E. Preparation and in Vitro Evaluation of a New Extracorporeal Dialyzer with Immobilized Insulin. *Artif Organs* **1982**, *6*, 145-150.

(17) Larue, C.; Gueraud, V.; Rivat, C. Suitable Hollow Fibre Immunobioreactors for Specific Ex Vivo Removal of Antibodies and Antigens from Plasma. *Clin Exp Immunol* **1985**, *62*, 217-224.

(18) Yang, V. C.; Port, F. K.; Kim, J. S.; Teng, C. L.; Till, G. O.; Wakefield, T. W. The Use of Immobilized Protamine in Removing Heparin and Preventing Protamine-Induced Complications During Extracorporeal Blood Circulation. *Anesthesiology* **1991**, *75*, 288-297.

(19) Ma, X.; Mohammad, S. F.; Kim, S. W. Heparin Removal from Blood Using Poly(L-Lysine) Immobilized Hollow Fiber. *Biotechnol Bioeng* **1992**, *40*, 530-536.

(20) Platt, J. L. Antibodies in Graft Rejection. In *Transplantation Immunology*; Bach, F. H., Auchincloss, H., Eds.; Wiley-Liss, Inc.: New York, 1995, pp 113-129.

(21) Platt, J. L. The Immunological Barriers to Xenotransplantation. *Crit Rev Immunol* **1996**, *16*, 331-358.

(22) VanBuskirk, A. M.; Pidwell, D. J.; Adams, P. W.; Orosz, C. G. Transplantation Immunology. *Jama* **1997**, *278*, 1993-1999.

(23) Roitt, I. M.; Brostoff, J.; Male, D. K. *Immunology*; 4th ed.; Mosby: London ; Baltimore, 1996.

(24) Rydberg, L. Abo-Incompatibility in Solid Organ Transplantation. *Transfus Med* **2001**, *11*, 325-342.

(25) Watkins, W. M. The Abo Blood Group System: Historical Background. *Transfus Med* **2001**, *11*, 243-265.

(26) Rieben, R.; Buchs, J. P.; Fluckiger, E.; Nydegger, U. E. Antibodies to Histo-Blood Group Substances a and B: Agglutination Titers, Ig Class, and Igg Subclasses in Healthy Persons of Different Age Categories. *Transfusion* **1991**, *31*, 607-615.

(27) Galili, U.; Shohet, S. B.; Kobrin, E.; Stults, C. L.; Macher, B. A. Man, Apes, and Old World Monkeys Differ from Other Mammals in the Expression of Alpha-Galactosyl Epitopes on Nucleated Cells. *J Biol Chem* **1988**, *263*, 17755-17762.

(28) Holzknecht, Z. E.; Platt, J. L. Identification of Porcine Endothelial Cell Membrane Antigens Recognized by Human Xenoreactive Natural Antibodies. *J Immunol* **1995**, *154*, 4565-4575.

(29) Alwayn, I. P.; Basker, M.; Buhler, L.; Cooper, D. K. The Problem of Anti-Pig Antibodies in Pig-to-Primate Xenografting: Current and Novel Methods of Depletion and/or Suppression of Production of Anti-Pig Antibodies. *Xenotransplantation* **1999**, *6*, 157-168.

(30) Lechler, R. I.; Simpson, E.; Bach, F. H. Major and Minor Histocompatibility Antigens: An Introduction. In *Transplantation Immunology*; Bach, F. H., Auchincloss, H., Eds.; Wiley-Liss: New York, 1995, pp 1-34.

(31) Le Moine, A.; Goldman, M.; Abramowicz, D. Multiple Pathways to Allograft Rejection. *Transplantation* **2002**, *73*, 1373-1381.

(32) Halloran, P. F.; Schlaut, J.; Solez, K.; Srinivasa, N. S. The Significance of the Anti-Class I Response. Ii. Clinical and Pathologic Features of Renal Transplants with Anti-Class I-Like Antibody. *Transplantation* **1992**, *53*, 550-555.

(33) Lobo, P. I.; Spencer, C. E.; Stevenson, W. C.; Pruett, T. L. Evidence Demonstrating Poor Kidney Graft Survival When Acute Rejections Are Associated with Igg Donor-Specific Lymphocytotoxin. *Transplantation* **1995**, *59*, 357-360.

(34) Sumitran-Holgersson, S. Hla-Specific Alloantibodies and Renal Graft Outcome. *Nephrol Dial Transplant* **2001**, *16*, 897-904.

(35) Rose, E. A.; Smith, C. R.; Petrossian, G. A.; Barr, M. L.; Reemtsma, K. Humoral Immune Responses after Cardiac Transplantation: Correlation with Fatal Rejection and Graft Atherosclerosis. *Surgery* **1989**, *106*, 203-207; discussion 207-208.

(36) United Network for Organ Sharing, 2003. http://www.unos.org.

(37) "2002 Annual Report of the U.S. Organ Procurement and Transplantation Network and the Scientific Registry of Transplant Recipients: Transplant Data 1992-2001," University Renal Research and Education Association; United Network for Organ Sharing, 2002.

(38) Toma, H. Abo-Incompatible Renal Transplantation. *Urol Clin North Am* **1994**, *21*, 299-310.

(39) Hanto, D. W.; Fecteau, A. H.; Alonso, M. H.; Valente, J. F.; Whiting, J. F. Abo-Incompatible Liver Transplantation with No Immunological Graft Losses Using Total Plasma Exchange, Splenectomy, and Quadruple Immunosuppression: Evidence for Accommodation. *Liver Transpl* **2003**, *9*, 22-30.

(40) Sonnenday, C. J.; Ratner, L. E.; Zachary, A. A.; Burdick, J. F.; Samaniego, M. D.; Kraus, E.; Warren, D. S.; Montgomery, R. A. Preemptive Therapy with Plasmapheresis/Intravenous Immunoglobulin Allows Successful Live Donor Renal Transplantation in Patients with a Positive Cross-Match. *Transplant Proc* **2002**, *34*, 1614-1616.

(41) Starzl, T. E.; Marchioro, T. L.; Holmes, J. H. Renal Homografts in Patients with Major Donor-Recipient Blood Group Incompatibilities. *Surgery* **1964**, *55*, 195-200.

(42) Wilbrandt, R.; Tung, K. S.; Deodhar, S. D.; Nakamoto, S.; Kolff, W. J. Abo Blood Group Incompatibility in Human Renal Homotransplantation. *Am J Clin Pathol* **1969**, *51*, 15-23.

(43) Cook, D. J.; Graver, B.; Terasaki, P. I. Abo Incompatibility in Cadaver Donor Kidney Allografts. *Transplant Proc* **1987**, *19*, 4549-4552.

(44) Slapak, M.; Naik, R. B.; Lee, H. A. Renal Transplant in a Patient with Major Donor-Recipient Blood Group Incompatibility: Reversal of Acute Rejection by the Use of Modified Plasmapheresis. *Transplantation* **1981**, *31*, 4-7.

(45) Slapak, M.; Evans, P.; Trickett, L.; Harris, E. R.; Gordon, P.; Matini, A.; Mocelin, A. J. Can Abo-Incompatibility Be Used in Renal Transplantation? *Transplant Proc* **1984**, *16*, 75-79.

(46) Alexandre, G. P.; Squifflet, J. P.; De Bruyere, M.; Latinne, D.; Reding, R.; Gianello, P.; Carlier, M.; Pirson, Y. Present Experiences in a Series of 26 Abo-Incompatible Living Donor Renal Allografts. *Transplant Proc* **1987**, *19*, 4538-4542.

(47) Bannett, A. D.; McAlack, R. F.; Raja, R.; Baquero, A.; Morris, M. Experiences with Known Abo-Mismatched Renal Transplants. *Transplant Proc* **1987**, *19*, 4543-4546.

(48) Mendez, R.; Sakhrani, L.; Aswad, S.; Minasian, R.; Obispo, E.; Mendez, R. G. Successful Living-Related Abo Incompatible Renal Transplant Using the Biosynsorb Immunoadsorption Column. *Transplant Proc* **1992**, *24*, 1738-1740.

(49) Toma, H.; Tanabe, K.; Tokumoto, T. Long-Term Outcome of Abo-Incompatible Renal Transplantation. *Urol Clin North Am* **2001**, *28*, 769-780.

(50) Ishida, H.; Koyama, I.; Sawada, T.; Utsumi, K.; Murakami, T.; Sannomiya, A.; Tsuji, K.; Yoshimura, N.; Tojimbara, T.; Nakajima, I.; Tanabe, K.; Yamaguchi, Y.; Fuchinoue, S.; Takahashi, K.; Teraoka, S.; Ito, K.; Toma, H.; Agishi, T. Anti-Ab Titer Changes in

Patients with Abo Incompatibility after Living Related Kidney Transplantations: Survey of 101 Cases to Determine Whether Splenectomies Are Necessary for Successful Transplantation. *Transplantation* **2000**, *70*, 681-685.

(51) Shimmura, H.; Tanabe, K.; Ishikawa, N.; Tokumoto, T.; Takahashi, K.; Toma, H. Role of Anti-a/B Antibody Titers in Results of Abo-Incompatible Kidney Transplantation. *Transplantation* **2000**, *70*, 1331-1335.

(52) Chui, A. K.; Ling, J.; McCaughan, G. W.; Painter, D.; Shun, A.; Dorney, S. F.; Mears, D. C.; Sheil, A. G. Abo Blood Group Incompatibility in Liver Transplantation: A Single-Centre Experience. *Aust N Z J Surg* **1997**, *67*, 275-278.

(53) Bjoro, K.; Ericzon, B. G.; Kirkegaard, P.; Hockerstedt, K.; Soderdahl, G.; Olausson, M.; Foss, A.; Schmidt, L. E.; Isoniemi, H.; Brandsaeter, B.; Friman, S. Highly Urgent Liver Transplantation: Possible Impact of Donor-Recipient Abo Matching on the Outcome after Transplantation. *Transplantation* **2003**, *75*, 347-353.

(54) Bach, F. H.; Turman, M. A.; Vercellotti, G. M.; Platt, J. L.; Dalmasso, A. P. Accommodation: A Working Paradigm for Progressing toward Clinical Discordant Xenografting. *Transplant Proc* **1991**, *23*, 205-207.

(55) Stussi, G.; Muntwyler, J.; Passweg, J. R.; Seebach, L.; Schanz, U.; Gmur, J.; Gratwohl, A.; Seebach, J. D. Consequences of Abo Incompatibility in Allogeneic Hematopoietic Stem Cell Transplantation. *Bone Marrow Transplant* **2002**, *30*, 87-93.

(56) Kozlowski, T.; Ierino, F. L.; Lambrigts, D.; Foley, A.; Andrews, D.; Awwad, M.; Monroy, R.; Cosimi, A. B.; Cooper, D. K.; Sachs, D. H. Depletion of Anti-Gal(Alpha)1-3gal Antibody in Baboons by Specific Alpha-Gal Immunoaffinity Columns. *Xenotransplantation* **1998**, *5*, 122-131.

(57) Taniguchi, S.; Neethling, F. A.; Korchagina, E. Y.; Bovin, N.; Ye, Y.; Kobayashi, T.; Niekrasz, M.; Li, S.; Koren, E.; Oriol, R.; Cooper, D. K. In Vivo Immunoadsorption of Antipig Antibodies in Baboons Using a Specific Gal(Alpha)1-3gal Column. *Transplantation* **1996**, *62*, 1379-1384.

(58) Kobayashi, T.; Yokoyama, I.; Morozumi, K.; Nagasaka, T.; Hayashi, S.; Uchida, K.; Takagi, H.; Nakao, A. Comparative Study of Theefficacy of Removal of Anti-Abo and Anti-Gal Antibodies by Double Filtration Plasmapheresis. *Xenotransplantation* **2000**, *7*, 101-108.

(59) Lambrigts, D.; Sachs, D. H.; Cooper, D. K. Discordant Organ Xenotransplantation in Primates: World Experience and Current Status. *Transplantation* **1998**, *66*, 547-561.

(60) Lai, L.; Kolber-Simonds, D.; Park, K. W.; Cheong, H. T.; Greenstein, J. L.; Im, G. S.; Samuel, M.; Bonk, A.; Rieke, A.; Day, B. N.; Murphy, C. N.; Carter, D. B.; Hawley, R. J.; Prather, R. S. Production of Alpha-1,3-Galactosyltransferase Knockout Pigs by Nuclear Transfer Cloning. *Science* **2002**, *295*, 1089-1092.

(61) Phelps, C. J.; Koike, C.; Vaught, T. D.; Boone, J.; Wells, K. D.; Chen, S. H.; Ball, S.; Specht, S. M.; Polejaeva, I. A.; Monahan, J. A.; Jobst, P. M.; Sharma, S. B.; Lamborn, A. E.; Garst, A. S.; Moore, M.; Demetris, A. J.; Rudert, W. A.; Bottino, R.; Bertera, S.; Trucco, M.; Starzl, T. E.; Dai, Y.; Ayares, D. L. Production of Alpha 1,3-Galactosyltransferase-Deficient Pigs. *Science* **2003**, *299*, 411-414.

(62) Cooper, D. K.; Thall, A. D. Xenoantigens and Xenoantibodies: Their Modification. *World J Surg* **1997**, *21*, 901-906.

(63) Palmer, A.; Taube, D.; Welsh, K.; Bewick, M.; Gjorstrup, P.; Thick, M. Removal of Anti-Hla Antibodies by Extracorporeal Immunoadsorption to Enable Renal Transplantation. *Lancet* **1989**, *1*, 10-12.

(64) Ross, C. N.; Gaskin, G.; Gregor-Macgregor, S.; Patel, A. A.; Davey, N. J.; Lechler, R. I.; Williams, G.; Rees, A. J.; Pusey, C. D. Renal Transplantation Following Immunoadsorption in Highly Sensitized Recipients. *Transplantation* **1993**, *55*, 785-789.

(65) McLeod, B. C. Introduction to the Third Special Issue: Clinical Applications of Therapeutic Apheresis. *J Clin Apheresis* **2000**, *15*, 1-5.

(66) Weinstein, R. Therapeutic Apheresis in Neurological Disorders. *J Clin Apheresis* **2000**, *15*, 74-128.

(67) Winters, J. L.; Pineda, A. A.; McLeod, B. C.; Grima, K. M. Therapeutic Apheresis in Renal and Metabolic Diseases. *J Clin Apheresis* **2000**, *15*, 53-73.

(68) Qureshi, A. I.; Suri, M. F. Plasma Exchange for Treatment of Myasthenia Gravis: Pathophysiologic Basis and Clinical Experience. *Ther Apher* **2000**, *4*, 280-286.

(69) Qureshi, A. I.; Choudhry, M. A.; Akbar, M. S.; Mohammad, Y.; Chua, H. C.; Yahia, A. M.; Ulatowski, J. A.; Krendel, D. A.; Leshner, R. T. Plasma Exchange Versus Intravenous Immunoglobulin Treatment in Myasthenic Crisis. *Neurology* **1999**, *52*, 629-632.

(70) Kalluri, R. Goodpasture Syndrome. *Kidney Int* **1999**, *55*, 1120-1122.

(71) Levy, J. B.; Turner, A. N.; Rees, A. J.; Pusey, C. D. Long-Term Outcome of Anti-Glomerular Basement Membrane Antibody Disease Treated with Plasma Exchange and Immunosuppression. *Ann Intern Med* **2001**, *134*, 1033-1042.

(72) Grima, K. M. Therapeutic Apheresis in Hematological and Oncological Diseases. *J Clin Apheresis* **2000**, *15*, 28-52.

(73) Koo, A. P. Therapeutic Apheresis in Autoimmune and Rheumatic Diseases. *J Clin Apheresis* **2000**, *15*, 18-27.

(74) Freiburghaus, C.; Berntorp, E.; Ekman, M.; Gunnarsson, M.; Kjellberg, B.; Nilsson, I. M. Tolerance Induction Using the Malmo Treatment Model 1982-1995. *Haemophilia* **1999**, *5*, 32-39.

(75) Jansen, M.; Schmaldienst, S.; Banyai, S.; Quehenberger, P.; Pabinger, I.; Derfler, K.; Horl, W. H.; Knobl, P. Treatment of Coagulation Inhibitors with Extracorporeal Immunoadsorption (Ig-Therasorb). *Br J Haematol* **2001**, *112*, 91-97.

(76) Christie, D. J.; Howe, R. B.; Lennon, S. S.; Sauro, S. C. Treatment of Refractoriness to Platelet Transfusion by Protein a Column Therapy. *Transfusion* **1993**, *33*, 234-242.

(77) Felson, D. T.; LaValley, M. P.; Baldassare, A. R.; Block, J. A.; Caldwell, J. R.; Cannon, G. W.; Deal, C.; Evans, S.; Fleischmann, R.; Gendreau, R. M.; Harris, E. R.; Matteson, E. L.; Roth, S. H.; Schumacher, H. R.; Weisman, M. H.; Furst, D. E. The Prosorba Column for Treatment of Refractory Rheumatoid Arthritis: A Randomized, Double-Blind, Sham-Controlled Trial. *Arthritis Rheum* **1999**, *42*, 2153-2159.

(78) Wei, N.; Klippel, J. H.; Huston, D. P.; Hall, R. P.; Lawley, T. J.; Balow, J. E.; Steinberg, A. D.; Decker, J. L. Randomised Trial of Plasma Exchange in Mild Systemic Lupus Erythematosus. *Lancet* **1983**, *1*, 17-22.

(79) Lewis, E. J.; Hunsicker, L. G.; Lan, S. P.; Rohde, R. D.; Lachin, J. M. A Controlled Trial of Plasmapheresis Therapy in Severe Lupus Nephritis. The Lupus Nephritis Collaborative Study Group. *N Engl J Med* **1992**, *326*, 1373-1379.

(80) Braun, N.; Erley, C.; Klein, R.; Kotter, I.; Saal, J.; Risler, T. Immunoadsorption onto Protein a Induces Remission in Severe Systemic Lupus Erythematosus. *Nephrol Dial Transplant* **2000**, *15*, 1367-1372.

(81) Palmer, A.; Cairns, T.; Dische, F.; Gluck, G.; Gjorstrup, P.; Parsons, V.; Welsh, K.; Taube, D. Treatment of Rapidly Progressive Glomerulonephritis by Extracorporeal Immunoadsorption, Prednisolone and Cyclophosphamide. *Nephrol Dial Transplant* **1991**, *6*, 536-542.

(82) Plasmaselect AG, 2003. http://www.plasmaselect.com.

(83) Burgstaler, E. A.; Pineda, A. A. Therapeutic Plasma Exchange: A Paired Comparison of Fresenius As104 Vs. Cobe Spectra. *J Clin Apheresis* **2001**, *16*, 61-66.

(84) Unger, J. K.; Haltern, C.; Dohmen, B.; Rossaint, R. Maximal Flow Rates and Sieving Coefficients in Different Plasmafilters: Effects of Increased Membrane Surfaces and Effective Length under Standardized in Vitro Conditions. *J Clin Apheresis* **2002**, *17*, 190-198.

(85) Fresenius Hemocare, Inc., http://www.freseniushc.com.

(86) Prescribing Information for Prosorba Protein a Immunoadsorption Column Concord, CA.

(87) Sakhrani, L. M.; Minasian, R.; Aswad, S.; Obispo, E.; Mendez, R.; Mendez, R. G. Safety and Efficacy of Biosynsorb Immunoadsorption Column Treatment. *Transplant Proc* **1992**, *24*, 1735-1737.

(88) Mazid, M. A.; Kaplan, M. An Improved Affinity Support and Immunoadsorbent with a Synthetic Blood Group Oligosaccharide and Polymer Coating for Hemoperfusion. *J Appl Biomater* **1992**, *3*, 9-15.

(89) Rieben, R.; Korchagina, E. Y.; von Allmen, E.; Hovinga, J. K.; Lammle, B.; Jungi, T. W.; Bovin, N. V.; Nydegger, U. E. In Vitro Evaluation of the Efficacy and Biocompatibility of New, Synthetic Abo Immunoabsorbents. *Transplantation* **1995**, *60*, 425-430.

(90) DeVito, L. D.; Sollinger, H. W.; Burlingham, W. J. Adsorption of Cytotoxic Anti-Hla Antibodies with Hla Class I Immunosorbant Beads. *Transplantation* **1990**, *49*, 925-931.

(91) Gerber, B.; Tinguely, C.; Bovin, N. V.; Rieben, R.; Nydegger, U. E. Differences between Synthetic Oligosaccharide Immunoabsorbents in Depletion Capacity for Xenoreactive Anti-Galalpha1-3gal Antibodies from Human Serum. *Xenotransplantation* **2001**, *8*, 106-114.

(92) Takamori, M.; Maruta, T. Immunoadsorption in Myasthenia Gravis Based on Specific Ligands Mimicking the Immunogenic Sites of the Acetylcholine Receptor. *Ther Apher* **2001**, *5*, 340-350.

(93) Ameer, G. A.; Harmon, W.; Sasisekharan, R.; Langer, R. Investigation of a Whole Blood Fluidized Bed Taylor-Couette Flow Device for Enzymatic Heparin Neutralization. *Biotechnol Bioeng* **1999**, *62*, 602-608.

(94) Ameer, G. A.; Grovender, E. A.; Ploegh, H.; Ting, D.; Owen, W. F.; Rupnick, M.; Langer, R. A Novel Immunoadsorption Device for Removing Beta2-Microglobulin from Whole Blood. *Kidney Int* **2001**, *59*, 1544-1550.

(95) Ameer, G. A.; Raghavan, S.; Sasisekharan, R.; Harmon, W.; Cooney, C. L.; Langer, R. Regional Heparinization Via Simultaneous Separation and Reaction in a Novel Taylor-Couette Flow Device. *Biotechnol Bioeng* **1999**, *63*, 618-624.

(96) Karoor, S.; Molina, J.; Buchmann, C. R.; Colton, C.; Logan, J. S.; Henderson, L. W. Immunoaffinity Removal of Xenoreactive Antibodies Using Modified Dialysis or Microfiltration Membranes. *Biotechnol Bioeng* **2003**, *81*, 134-148.

(97) Klein, E.; Eichholz, E.; Yeager, D. H. Affinity Membranes Prepared from Hydrophilic Coatings on Microporous Polysulfone Hollow Fibers. *Journal of Membrane Science* **1994**, *90*, 69-80.

(98) Charcosset, C.; Su, Z.; Karoor, S.; Daun, G.; Colton, C. K. Protein a Immunoaffinity Hollow Fiber Membranes for Immunoglobulin G Purification: Experimental Characterization. *Biotechnol Bioeng* **1995**, *48*, 415-427.

(99) Soltys, P. J.; Etzel, M. R. Equilibrium Adsorption of Ldl and Gold Immunoconjugates to Affinity Membranes Containing Peg Spacers. *Biomaterials* **2000**, *21*, 37-48.

(100) Instructions for Use of Hemodialyzers; Gambro, Lakewood, CO.

(101) Bamford, C. H.; Al-Lamee, K. G.; Purbrick, M. D.; Wear, T. J. Studies of a Novel Membrane for Affinity Separations. *J Chromatogr* **1992**, *606*, 19-31.

(102) Waldmann-Meyer, H.; Knippel, E. A Surface Charge Density Model for Structure and Orientation of Polymer-Bound Proteins. *Journal of Colloid and Interface Science* **1992**, *148*, 508-516.

(103) Dailey, J. F. *Blood*; Medical Consulting Group: Arlington, MA, 1998.

(104) al-Yaman, F.; Genton, B.; Falk, M.; Anders, R. F.; Lewis, D.; Hii, J.; Beck, H. P.; Alpers, M. P. Humoral Response to Plasmodium Falciparum Ring-Infected Erythrocyte Surface Antigen in a Highly Endemic Area of Papua New Guinea. *Am J Trop Med Hyg* **1995**, *52*, 66-71.

(105) Yarmush, D. M.; Murphy, R. M.; Colton, C. K.; Fisch, M.; Yarmush, M. L. Quasi-Elastic Light Scattering of Antigen-Antibody Complexes. *Mol Immunol* **1988**, *25*, 17-32.

(106) Yarmush, M. L.; Patankar, D. B.; Yarmush, D. M. An Analysis of Transport Resistances in the Operation of Biacore; Implications for Kinetic Studies of Biospecific Interactions. *Mol Immunol* **1996**, *33*, 1203-1214.

(107) Chase, H. A. Affinity Separations Utilising Immobilised Monoclonal Antibodies-a New Tool for the Biochemical Engineer. *Chem Eng Sci* **1984**, *39*, 1099-1125.

(108) Kaplan, A. A. A Simple and Accurate Method for Prescribing Plasma Exchange. *ASAIO Trans* **1990**, *36*, M597-599.

(109) Gokal, R.; Hutchison, A. Dialysis Therapies for End-Stage Renal Disease. *Semin Dial* **2002**, *15*, 220-226.

(110) Wolfe, R. A.; Ashby, V. B.; Milford, E. L.; Ojo, A. O.; Ettenger, R. E.; Agodoa, L. Y.; Held, P. J.; Port, F. K. Comparison of Mortality in All Patients on Dialysis, Patients on Dialysis Awaiting Transplantation, and Recipients of a First Cadaveric Transplant. *N Engl J Med* **1999**, *341*, 1725-1730.

(111) Kasiske, B. M.; Cangro, C. B.; Hariharan, S.; Hricik, D. E.; Kerman, R. H.; Roth, D.; Rush, D. N.; Vazquez, M. A.; Weir, M. R. The Evaluation of Renal Transplant Candidates: Clinical Practice Guidelines. *American Journal of Transplantation* **2001**, *1*, s7-s95.

(112) Medscape, 2002. http://www.medscape.com.

(113) Terasaki, P. I.; Cecka, J. M.; Gjertson, D. W.; Takemoto, S. High Survival Rates of Kidney Transplants from Spousal and Living Unrelated Donors. *N Engl J Med* **1995**, *333*, 333-336.

(114) Matas, A. J.; Delmonico, F. L. Transplant Kidneys Sooner: Discard Fewer Kidneys. *Am J Transplant* **2001**, *1*, 301-304.

(115) "Usrds 2002 Annual Data Report: Atlas of End-Stage Renal Disease in the United States," National Institutes of Health, National Institute of Digestive and Kidney Diseases, 2002.

(116) Terasaki, P. I.; Gjertson, D. W.; Cecka, J. M. Paired Kidney Exchange Is Not a Solution to Abo Incompatibility. *Transplantation* **1998**, *65*, 291.

(117) Woodle, E. S.; Ross, L. F. Paired Exchanges Should Be Part of the Solution to Abo Incompatibility in Living Donor Kidney Transplantation. *Transplantation* **1998**, *66*, 406-407.

(118) Neutr-Ab Package Insert; Dade Behring, Switzerland.

(119) Axen, R.; Porath, J.; Ernback, S. Chemical Coupling of Peptides and Proteins to Polysaccharides by Means of Cyanogen Halides. *Nature* **1967**, *214*, 1302-1304.

(120) Walker, R. H.; American Association of Blood Banks. *Technical Manual*; 11th ed.; American Association of Blood Banks: Bethesda, MD, 1993.

(121) Ratner, B. D. *Biomaterials Science : An Introduction to Materials in Medicine*; Academic Press: San Diego, 1996.

(122) Welty, J. R.; Wicks, C. E.; Wilson, R. E. *Fundamentals of Momentum, Heat, and Mass Transfer*; 3rd ed.; Wiley: New York, 1984.

(123) Kameneva, M. V.; Watach, M. J.; Borovetz, H. S. Gender Difference in Rheologic Properties of Blood and Risk of Cardiovascular Diseases. *Clin Hemorheol Microcirc* **1999**, *21*, 357-363.

(124) Crc Handbook of Chemistry and Physics; CRC Press, Boca Raton, Fla.

(125) Berne, R. M. *Physiology*; 4th ed.; Mosby: St. Louis, 1998.

(126) Colton, C. K.; Lowrie, E. G. Hemodialysis: Physical Principles and Technical Considerations. In *The Kidney*; Brenner, B. M., Rector, F. C., Eds.; W.B. Saunders Company: Philadelphia, 1981, pp 2425-2489.

(127) Deen, W. M. *Analysis of Transport Phenomena*; Oxford University Press: New York, 1998.

(128) White, F. M. *Viscous Fluid Flow*; 2nd ed.; McGraw-Hill: New York, 1991.

(129) Bruining, W. J. A General Description of Flows and Pressures in Hollow Fiber Membrane Modules. *Chem Eng Sci* **1989**, *44*, 1441-1447.

(130) Sargent, J. A.; Gotch, F. A. Principles and Biophysics of Dialysis. In *Replacement of Renal Function by Dialysis*; 4th ed.; Jacobs, C., Kjellstrand, C. M., Koch, K. M., Winchester, J. F., Eds.; Kluwer Academic Publishers: Dordrecht, 1996, pp 35-102.

(131) Skelland, A. H. P. *Diffusional Mass Transfer*; Wiley: New York, 1974.

(132) Peters, T., Jr. Serum Albumin. *Adv Protein Chem* **1985**, *37*, 161-245.

(133) Crowther, J. R. *The Elisa Guidebook*; Humana Press: Totowa, N.J., 2001.

(134) Instructions for Imject Carrier Proteins Bsa, Klh, and Ova; Pierce Chemical Company, Rockford, IL.

(135) Wang, N. H. L.; Keller, K. H. Augmented Transport of Extracellular Solutes in Concentrated Erythrocyte Suspensions in Couette Flow. *Journal of Colloid and Interface Science* **1985**, *103*, 210-225.

(136) Zydney, A. L. Therapeutic Apheresis and Blood Fractionation. In *The Biomedical Engineering Handbook*; 2nd ed.; Bronzino, J. D., Ed.; CRC Press: Boca Raton, 2000, pp 132-131-132-115.